AB INITIO STUDIES OF MOLECULES

by

Henrik Mathias Eiding

Thesis

for the degree of

Master of Science

Faculty of Mathematics and Natural Sciences
University of Oslo

June 2014

Acknowledgements

First of all I would like to thank my supervisors Morten Hjorth-Jensen and Anders Malthe-Sørenssen for their encouragement, support and inspiration. Your doors have always been open, and all the discussions we have had are highly appreciated. You make it clear that your students are very important to you.

Special thanks go to Svenn-Arne Dragly and Milad H. Mobarhan, with whom I have shared office over the past two years. Thanks for all the engaging discussions we've had and all the wisdom you have shared with me. You have made the days spent at the University not only educational, but also a lot of fun.

I would also like to thank Simen Reine for his lectures on molecular integral evaluation, which have been very useful.

Last, but not least, thanks to everybody at the Computational Physics group for making these last two years a time to remember!

Collaboration details

While working on the Hartree-Fock code, I have collaborated with Svenn-Arne Dragly [1] and Milad H. Mobarhan [2], who in part have worked on similar projects. Nevertheless, all of the code in this thesis have been written by myself.

<div align="right">

Henrik Mathias Eiding
June 2014, Oslo

</div>

Contents

Chapter 1

Introduction

Multiscale physics is currently a very active field of research, and over the last few years, there has been a growing interest in the field at the Computational Physics group at the University of Oslo. The field aims to bridge the gap between the physical theories at different scales: From quantum mechanics which determines the electronic states of atoms, to classical force fields modelling the dynamics of interacting atoms and molecules, known as molecular dynamics, all the way up to continuum scale models. Of course, quantum mechanics is the most fundamental of all physical theories and should therefore be applicable to all scales. However, solving the Schrödinger equation is quite a daunting task even for constellations of relatively few atoms, and modelling millions of atoms quantum mechanically is therefore not doable in practice. Nevertheless, the overall goal of the group is to develop models on all scales which are ultimately founded on quantum mechanical first principles.

The goal of this thesis in particular has been to develop from scratch an *ab initio* computer program for calculating the electronic structure and properties of molecules. There are a variety of different methods available for this task, all with different strengths and weaknesses. In order to obtain a good compromise between accuracy and computational cost, we decided to create a Hartree-Fock solver using Gaussian basis functions, as well as an implementation of Møller-Plesset perturbation theory up to third order. The former is one of the workhorses of quantum chemistry and is able to produce often quite remarkable results considering its low computational cost. The latter is one of many so-called post-Hartree-Fock methods which aim to systematically improve the Hartree-Fock solution.

1.1 Thesis structure

The thesis consists of three main parts: Theory, Implementation, and Results and conclusion.

Part I: Theory

Part I introduces the reader to the fundamentals of many-body theory as well as the numerical methods which have been used.

- Chapter 2 gives an introduction to the theory of many-body quantum mechanics. Essential parts of this chapter are the definition of spin orbitals and the Slater determinant, which are integral components of the methods discussed later.

- Chapter 3 deals with the Hartree-Fock method. First, the general equations are derived. Thereafter, the restricted and unrestricted determinants are defined, and the equations which result from them obtained. These equations are referred to as the restricted Hartree-Fock equations (RHF) and unrestricted Hartree-Fock equations (UHF).

- Chapter 4 presents the basis functions and integration scheme which have been used. The choice of basis functions is of paramount importance as they determine the accuracy of the results as well as the computational cost of the computations. High accuracy and low computational cost are conflicting desires, and to achieve both is therefore a great challenge. A good compromise is the choice of Gaussian basis functions, for which a highly optimised integration scheme is available.

- Chapter 5 briefly discusses the main limitation of the Hartree-Fock method, namely its inability to converge to the exact solution. This motivates the introduction of more accurate methods. One such method is perturbation theory, which is the topic of chapter 6.

- Chapter 6 discusses many-body perturbation theory. Equations for the second and third order Møller-Plesset corrections are derived.

- Chapter 7 describes the Nelder-Mead minimisation method, which is a popular method in quantum chemistry for finding the equilibrium geometry of molecules.

Part II: Implementation

Part II describes how we implemented the methods of part I in the C++ programming language.

- Chapter 8 outlines the program structure and how the various routines are implemented in different classes.

- Chapter 9 elaborates on some of the classes of the previous chapter.

- Chapter 10 gives a brief description of how the code was developed in the integrated development environment Qt Creator. Furthermore, the code is validated by demonstrating that it reproduces selected results from the literature.

Part III: Results and conclusion

- Chapter 11 presents results of calculations performed on various molecular systems. Both closed and open shell molecules are considered. Special attention is payed to the correlation energy and the problem of dissociation.

- Chapter 12 summarises and concludes the thesis. Possible topics of future work are also discussed.

Part I

Theory

Chapter 2

Many-body theory

This chapter discusses the basic quantum mechanics of identical fermions. First the Hamiltonian of molecular systems is presented, and the Born-Oppenheimer approximation is introduced. Therearefter the spin orbitals and spatial orbitals are discussed. They are functions which represent the states of single particles and are used as building blocks to construct many-particle wave functions. The simplest example of such a many-particle wave function is the Hartree function, which is the product of all the spin orbitals of the system. However, the Hartree function does not satisfy the Pauli principle, which says that any fermionic many-particle wave function must be anti-symmetric with respect to particle interchange. This leads to the construction of the Slater determinant, which is the simplest example of an antisymmetric wave function comprised of spin orbitals. Next, the so-called reference energy is calculated. This is the expectation value of the Hamiltonian calculated on the basis of some chosen reference Slater determinant. It will become important later as this is a basic ansatz in the derivation of the Hartree-Fock equations. Thereafter the second quantisation formalism is briefly introduced. This is a very useful and effective notation when it comes to calculating matrix elements of operators. Furthermore, it naturally leads to a diagrammatic interpretation of the operators, which streamlines the calculation even further. This will prove to be very useful when we discuss perturbation theory in chapter 6. The chapter ends with the completeness theorem for fermionic many-particle wave functions.

The reader who wants a more thorough review of these topics is referred to Szabo and Ostlund [3], Gross *et al* [4] and Shavitt and Bartlett [5].

2.1 The Hamiltonian

Our task is to solve the time independent Schrödinger equation:

$$H|\Phi_i\rangle = \mathscr{E}_i|\Phi_i\rangle, \tag{2.1}$$

where H is the Hamiltonian, $\mathscr{E}_i$ is the energy and $|\Phi_i\rangle$ is the state of the system. We will primarily be interested in the ground state $|\Phi_0\rangle$ and ground state energy $\mathscr{E}_0$. For a molecular system consisting of N electrons with positions $\{\mathbf{r}_i\}_{i=1}^N$ and K nuclei with

posistions $\{\mathbf{R}_n\}_{n=1}^K$, the Hamiltonian is given by

$$
\begin{aligned}
H = &-\frac{1}{2}\sum_{i=1}^{N}\nabla_i^2 - \sum_{n=1}^{K}\frac{1}{2M_n}\nabla_n^2 - \sum_{i=1}^{N}\sum_{n=1}^{K}\frac{Z_n}{|\mathbf{R}_n - \mathbf{r}_i|} \\
&+ \frac{1}{2}\sum_{\substack{i,j=1 \\ i\neq j}}^{n}\frac{1}{|\mathbf{r}_i - \mathbf{r}_j|} + \frac{1}{2}\sum_{\substack{m,n=1 \\ m\neq n}}^{n}\frac{1}{|\mathbf{R}_m - \mathbf{R}_n|},
\end{aligned}
\tag{2.2}
$$

where M_n is the ratio of the mass of nucleus n and the mass of an electron, and Z_n is the charge of nucleus n. The first two terms are the kinetic energy of the electrons and the nuclei, respectively. The remaining three terms represent the Coulomb potential of the particles. The first of these is due to the attraction between the electrons and the nuclei, the next is due to the repulsion between the electrons, and the last is due to the repulsion between the nuclei. The Hamiltonian is given in atomic units.

Because the nuclei are much heavier than the electrons, they move more slowly. This means that the system can be viewed as a collection of electrons moving around in the vicinity of a number of static nuclei. Consequently, we neglect the second term of equation (2.2) and consider the last term a constant. This is the so-called *Born-Oppenheimer approximation*, first proposed by Born and Oppenheimer [6]. Adding a constant to an operator does not change its eigenstates, but only its eigenvalues (by the added constant). We therefore also leave out the final term and are left with

$$
H = -\frac{1}{2}\sum_{i=1}^{N}\nabla_i^2 - \sum_{i=1}^{N}\sum_{n=1}^{K}\frac{Z_n}{|\mathbf{R}_n - \mathbf{r}_i|} + \frac{1}{2}\sum_{\substack{i,j=1 \\ i\neq j}}^{n}\frac{1}{|\mathbf{r}_i - \mathbf{r}_j|}.
\tag{2.3}
$$

This is the Hamiltonian of the electronic system, and it is the one which we will address in this thesis. Its eigenvalues are the energies of the electrons. If we are seeking the total energies of the molecular system, we simply add the potential energy of the nuclei to the eigenvalues of the Hamiltonian.

For future reference, we split the Hamiltonian into a one-body part H_1 and a two-body part H_2:

$$
H = H_1 + H_2
\tag{2.4}
$$

where

$$
H_1 = \sum_{i=1}^{N}h(\mathbf{r}_i) = \sum_{i=1}^{N}\left[-\frac{1}{2}\nabla_i^2 - \sum_{n=1}^{K}\frac{Z_n}{|\mathbf{R}_n - \mathbf{r}_i|}\right],
\tag{2.5}
$$

$$
H_2 = \frac{1}{2}\sum_{\substack{i,j=1 \\ i\neq j}}^{N}g(\mathbf{r}_i, \mathbf{r}_j) = \frac{1}{2}\sum_{\substack{i,j=1 \\ i\neq j}}^{N}\frac{1}{|\mathbf{r}_i - \mathbf{r}_j|}.
\tag{2.6}
$$

As we will see, it is the two-body part which makes the Schrödinger equation difficult to solve.

Note that $|\Phi\rangle$ is the exact state of the system. However, most of this thesis deals with approximate states. Throughout the text, $|\Phi\rangle$ will be reserved for the exact state, while $|\Psi\rangle$ will be used for approximate states such as Hartree products and Slater determinants, which will be discussed later in this chapter.

2.2   Spatial orbitals and spin orbitals

A spatial orbital $\phi_i(\mathbf{r})$ is a wave function which describes the spatial probability distribution of an electron, meaning that $|\phi_i(\mathbf{r})|^2 d\mathbf{r}$ is the probability to find the electron in a small volume element $d\mathbf{r}$ centered at $\mathbf{r}$. We will assume that the spatial orbitals are orthonormal:

$$\langle \phi_i | \phi_j \rangle = \int d\mathbf{r}\, \phi_i(\mathbf{r})\phi_j(\mathbf{r}) = \delta_{ij}. \tag{2.7}$$

A spatial orbital does not by itself completely determine the state of an electron; there is also a spin degree of freedom. We can specify spin by multiplying the spatial orbital with a spin function:

$$\psi_i(\mathbf{x}) = \phi_i(\mathbf{r})\xi_i(s), \tag{2.8}$$

where $\mathbf{x} = (\mathbf{r}, s)$. The spin function $\xi_i(s)$ can either be $\alpha(s)$, meaning spin up, or $\beta(s)$, meaning spin down. They are defined by

$$\alpha(s) = \begin{cases} 1 & \text{if} \quad s = \uparrow \\ 0 & \text{if} \quad s = \downarrow \end{cases}, \tag{2.9}$$

and

$$\beta(s) = \begin{cases} 0 & \text{if} \quad s = \uparrow \\ 1 & \text{if} \quad s = \downarrow \end{cases}. \tag{2.10}$$

The inner product of two spin functions is defined as

$$\langle \xi_i | \xi_j \rangle = \sum_{s=\uparrow\downarrow} \xi_i(s)\xi_j(s), \tag{2.11}$$

which automatically ensures that they are orthonormal:

$$\begin{aligned}
\langle \alpha | \alpha \rangle &= \sum_{s=\uparrow\downarrow} \alpha(s)\alpha(s) = \alpha(\uparrow)\alpha(\uparrow) + \alpha(\downarrow)\alpha(\downarrow) = 1 \cdot 1 + 0 \cdot 0 = 1, \\
\langle \beta | \beta \rangle &= \sum_{s=\uparrow\downarrow} \beta(s)\beta(s) = \beta(\uparrow)\beta(\uparrow) + \beta(\downarrow)\beta(\downarrow) = 0 \cdot 0 + 1 \cdot 1 = 1, \\
\langle \alpha | \beta \rangle &= \sum_{s=\uparrow\downarrow} \alpha(s)\beta(s) = \alpha(\uparrow)\beta(\uparrow) + \alpha(\downarrow)\beta(\downarrow) = 1 \cdot 0 + 0 \cdot 1 = 0.
\end{aligned} \tag{2.12}$$

We define the inner product of two spin orbitals as

$$\langle \psi_i | \psi_j \rangle = \langle \phi_i | \phi_j \rangle \langle \xi_i | \xi_j \rangle, \tag{2.13}$$

and we will also use the notation

$$\langle \psi_i | \psi_j \rangle = \int d\mathbf{x}\, \psi_i(\mathbf{x})\psi_j(\mathbf{x}). \tag{2.14}$$

Note that since the spatial orbitals and the spin functions are orthonormal, this definition implies that the spin orbitals are so too.

A point worth mentioning here is that the inner product of two spin orbitals ψ_i and ψ_j is equal to zero if they have unequal spins no matter what their spatial orbitals are. In fact, even the integral $\langle \psi_i | a(\mathbf{r}) | \psi_j \rangle = 0$ for any operator $a(\mathbf{r})$ which is only a function of $\mathbf{r}$.

2.3 The Hartree function

If the Hamiltonian did not contain the term H_2, the Schrödinger equation would be separable and easy to solve. One possible solution is the so-called Hartree function, Ψ_H, which is defined as:

$$\Psi_H(\mathbf{x}_1, \ldots, \mathbf{x}_N) = \psi_1(\mathbf{x}_1) \cdots \psi_N(\mathbf{x}_N), \tag{2.15}$$

where $\psi_i(\mathbf{x})$ is the spin orbital which solves the single-particle Schrödinger equation

$$h(\mathbf{r})\psi_i(\mathbf{x}) = \varepsilon_i \psi_i(\mathbf{x}), \tag{2.16}$$

and $h(\mathbf{r})$ is defined in equation (2.5). This is easy to verify by direct computation:

$$\begin{aligned}
H_1 \Psi_H &= \sum_{i=1}^{N} h(\mathbf{r}_i) \psi_1(\mathbf{x}_1) \psi_2(\mathbf{x}_2) \cdots \psi_N(\mathbf{x}_N) \\
&= \Big(\sum_{i=1}^{N} \varepsilon_i \Big) \psi_1(\mathbf{x}_1) \psi_2(\mathbf{x}_2) \cdots \psi_N(\mathbf{x}_N) \\
&= \mathscr{E}_0 \, \Psi_H,
\end{aligned} \tag{2.17}$$

which means that the total energy of the system is $\mathscr{E}_0 = \sum_{i=1}^{N} \varepsilon_i$.

Unfortunately, the term H_2 must be taken into account, and this makes the Schrödinger equation considerably more difficult to solve. In fact, except for a few simple systems, no analytical solution is known, and approximative methods are needed. The Hartree-Fock method, which we discuss in the next chapter, is perhaps the most important of such methods.

2.4 The Slater determinant

For the simple case where $H = H_1$, the Hartree function, Ψ_H, in equation (2.15) solves the Schrödinger equation. However, it is still not a physically valid solution. Why? Because the solution does not reflect the fact that we are dealing with *identical* particles. To see what is wrong with the solution, let us consider a system of N identical particles in the state Φ. Suppose we want to calculate the expectation value $\langle B \rangle$ of some observable B. Since the particles are identical, $\langle B \rangle$ should not change if we were to switch the coordinates of two particles i and j, say. If P_{ij} is the operator which changes the coordinates of particles i and j, that is to say, if

$$P_{ij} \Phi(\mathbf{x}_1, \ldots, \mathbf{x}_i, \ldots, \mathbf{x}_j, \ldots, \mathbf{x}_N) = \Phi(\mathbf{x}_1, \ldots, \mathbf{x}_j, \ldots, \mathbf{x}_j, \ldots, \mathbf{x}_N), \tag{2.18}$$

then we must have

$$\langle \Phi | B | \Phi \rangle = \langle P_{ij} \Phi | B | P_{ij} \Phi \rangle = \langle \Phi | P_{ij}^\dagger B P_{ij} | \Phi \rangle. \tag{2.19}$$

Inserting this on the right hand side of the identity

$$\begin{aligned}
\langle \Phi | B | \tilde{\Phi} \rangle = \frac{1}{4} \big(&\langle \Phi + \tilde{\Phi} | B | \Phi + \tilde{\Phi} \rangle - \langle \Phi - \tilde{\Phi} | B | \Phi - \tilde{\Phi} \rangle \\
&- i \langle \Phi + i\tilde{\Phi} | B | \Phi + i\tilde{\Phi} \rangle + i \langle \Phi - i\tilde{\Phi} | B | \Phi - i\tilde{\Phi} \rangle \big),
\end{aligned} \tag{2.20}$$

where Φ and $\tilde{\Phi}$ are two arbitrary states, yields

$$\langle\Phi|B|\tilde{\Phi}\rangle = \langle\Phi|P_{ij}^\dagger B P_{ij}|\tilde{\Phi}\rangle, \tag{2.21}$$

which implies that

$$P_{ij}^\dagger B P_{ij} = B. \tag{2.22}$$

Multiplying this equation from the right by P_{ij} gives

$$P_{ij}^\dagger B = B P_{ij}, \tag{2.23}$$

since $P_{ij}^2 = I$. For the special case where $B = I$ this means that $P_{ij}^\dagger = P_{ij}$. From this we can draw the following conclusions:

1. The permutation operator is Hermitian, i.e., $P_{ij}^\dagger = P_{ij}$.

2. The permutation operator is unitary, i.e., $P_{ij}^\dagger = P_{ij}^{-1}$.

3. The permutation operator commutes with any observable B,
   i.e., $[P_{ij}, B] = 0$. This means that B and P_{ij} share a common set of eigenstates.

It is now possible to determine what the eigenvalue of P_{ij} must be. Suppose that it is some number p_{ij}. Then the eigenvalue of P_{ij}^2 is p_{ij}^2. But we know that $p_{ij}^2 = 1$ (since $P_{ij}^2 = I$). This, together with the fact that P_{ij} is Hermitian[1], implies that $p_{ij} = \pm 1$. Thus Φ is either symmetric or antisymmetric with respect to the interchange of particles i and j.

We next show that the eigenvalues of all P_{ij} are the same. This can be done by considering the following way of expressing P_{ij}

$$P_{ij} = P_{2j} P_{1i} P_{12} P_{2j} P_{1i}. \tag{2.24}$$

The eigenvalue of P_{ij} is then

$$P_{ij}|\Phi\rangle = a_{2j}^2 a_{1i}^2 a_{12}|\Phi\rangle = a_{12}|\Phi\rangle. \tag{2.25}$$

Thus all eigenvalues are the same, and the state is either symmetric or antisymmetric with respect to the exchange of any two particle coordinates. Particles with a symmetric state are called bosons, and particles with an antisymmetric state are called fermions. This thesis deals with fermions only. The fact that the wave function of fermions is antisymmetric with respect to the exchange of any two particle coordinates, is called the Pauli principle. The so-called spin-statistics theorem, proved by Pauli [7], states that bosons have spin $s \in \{0, 1, 2, \dots\}$ and that fermions have spin $s \in \{1/2, 3/2, 5/2 \dots\}$.

It is now clear why (2.15) cannot be a physically correct solution; it is neither symmetric nor antisymmetric. However, we can make it antisymmetric by applying the antisymmetrisation operator $\mathcal{A}$. It is defined by

$$\mathcal{A} = \frac{1}{N!}\sum_P (-1)^p P, \tag{2.26}$$

---

[1]Recall that the eigenvalues of a Hermitian operator are real.

where P is a permutation operator, p is the parity of the permutation, and the sum is over all permutations. The permutation operator P can always be written as

$$P = P_{ij}P_{kl} \cdots P_{qr}. \tag{2.27}$$

A solution of the Schrödinger equation, still assuming $H = H_1$, which also satisfies the antisymmetry requirement can now be written as

$$\Psi_0(\mathbf{x}_1, \ldots, \mathbf{x}_N) = \sqrt{N!}\, \mathcal{A}\, \Psi_H(\mathbf{x}_1, \ldots, \mathbf{x}_N). \tag{2.28}$$

Another common way of writing this is through the determinant

$$\Psi_0(\mathbf{x}_1, \ldots, \mathbf{x}_N) = \frac{1}{\sqrt{N!}} \begin{vmatrix} \psi_1(\mathbf{x}_1) & \ldots & \psi_N(\mathbf{x}_1) \\ \vdots & & \vdots \\ \psi_1(\mathbf{x}_N) & \ldots & \psi_N(\mathbf{x}_N) \end{vmatrix}. \tag{2.29}$$

The wave function in (2.28) and (2.29) is called a Slater determinant. From the last equation it is seen that if two spin orbitals are equal, the total wave function vanishes. This means that two identical fermions cannot occupy the same single-particle state. The total wave function also vanishes if the coordinates of two particles are the same. Hence, two fermions with equal spins cannot be located at the same point in space.

Let us illustrate these last remarks by considering a system of two particles. Assume that the electrons occupy the spin orbitals $\{\psi_i(\mathbf{x}) = \phi_i(\mathbf{r})\xi_i(s)\}_{i=1}^2$, where $\{\phi_i(\mathbf{r})\}_{i=1}^2$ are the spatial parts and $\{\xi(s)\}_{i=1}^2$ are the spin parts, and let us construct the Slater determinant from these spin orbitals. Consider now the probability density $\rho(\mathbf{x}_1, \mathbf{x}_2)$ to observe one of the particles with coordinate $\mathbf{x}_1$ and the other with coordinate $\mathbf{x}_2$:

$$\begin{aligned} \rho(\mathbf{x}_1, \mathbf{x}_2) &= \langle \Psi_0 | \Psi_0 \rangle \\ &= \frac{1}{2} |\psi_1(\mathbf{x}_1)\psi_2(\mathbf{x}_2) - \psi_2(\mathbf{x}_1)\psi_1(\mathbf{x}_2)|^2 \\ &= \frac{1}{2} \Big[|\psi_1(\mathbf{x}_1)|^2|\psi_2(\mathbf{x}_2)|^2 + |\psi_2(\mathbf{x}_1)|^2|\psi_1(\mathbf{x}_2)|^2 \\ &\quad - \psi_1^*(\mathbf{x}_1)\psi_2^*(\mathbf{x}_2)\psi_2(\mathbf{x}_1)\psi_1(\mathbf{x}_2) - \psi_2^*(\mathbf{x}_1)\psi_1^*(\mathbf{x}_2)\psi_1(\mathbf{x}_1)\psi_2(\mathbf{x}_2) \Big]. \end{aligned} \tag{2.30}$$

In order to find the probability density $\rho(\mathbf{r}_1, \mathbf{r}_2)$ to observe the particles at *spatial positions* $\mathbf{r}_1$ and $\mathbf{r}_2$, we need to integrate with respect to the spin coordinates s_1 and s_2. However, the result of this integration depends upon the specific spin configuration of the particles.

Let us first assume that the particles have the same spatial orbital, but opposite spins, i.e., that $\phi_1 = \phi_2 = \phi$ and $\xi_1 \neq \xi_2$. If we now integrate over the spin coordinates of the above equation, the last two negative terms vanish, and we are left with

$$\rho(\mathbf{r}_1, \mathbf{r}_2) = |\phi(\mathbf{r}_1)|^2|\phi(\mathbf{r}_2)|^2. \tag{2.31}$$

This expression shows explicitly that the positions of the two electrons are uncorrelated, that is to say, the probability distribution of one electron has no effect on the probability

distribution of the other. In fact, the expression above is the statistical definition of uncorrelated probability distributions.

Next, consider the case where the electrons have different spatial orbitals, but equal spins, i.e., that $\phi_1 \neq \phi_2$ and $\xi_1 = \xi_2$. Integrating over the spin coordinates then gives

$$
\begin{aligned}
\rho(\mathbf{r}_1, \mathbf{r}_2) = \frac{1}{2}\Big[&|\phi_1(\mathbf{r}_1)|^2|\phi_2(\mathbf{r}_2)|^2 + |\phi_2(\mathbf{r}_1)|^2|\phi_1(\mathbf{r}_2)|^2 \\
&- \phi_1^*(\mathbf{r}_1)\phi_2^*(\mathbf{r}_2)\phi_2(\mathbf{r}_1)\phi_1(\mathbf{r}_2) - \phi_2^*(\mathbf{r}_1)\phi_1^*(\mathbf{r}_2)\phi_1(\mathbf{r}_1)\phi_2(\mathbf{r}_2) \Big].
\end{aligned}
\tag{2.32}
$$

The positions of the two electrons are now obviously correlated. Furthermore, it is seen that the probability to find the two electrons at the same position is equal to zero. This means that there is some kind of "force" pushing the electrons away from each other. This "force" is often referred to as the exchange force. It is not a force in the classical sense and has nothing to do with the Coulomb repulsion between the electrons, but it is a statistical effect which arises due to the antisymmetry of the wave function.

This discussion illustrates a point which will become important later when we discuss Hartree-Fock theory: The exchange force, which pushes electrons apart, is only acting between electrons with equal spins.

We end this section by showing the following two important properties of the antisymmetrisation operator

$$
\mathcal{A}^2 = \mathcal{A} \tag{2.33}
$$

$$
\mathcal{A}^\dagger = \mathcal{A} \tag{2.34}
$$

The first can be shown as follows

$$
\begin{aligned}
\mathcal{A}^2 &= \frac{1}{(N!)^2} \sum_{p'} (-1)^{p'} P' \sum_p (-1)^p P \\
&= \frac{1}{(N!)^2} \Big(\sum_{p'} (-1)^{p'+p_1} P' P_1 + \cdots + \sum_{p'} (-1)^{p'+p_{N!}} P' P_{N!} \Big),
\end{aligned}
\tag{2.35}
$$

where P_I is permutation operator number I. There are a total of $N!$ different permutation operators, since the coordinates can be placed in $N!$ different orders. Since $\sum_{p'}(-1)^{p'} P'$ produces all possible permutations, the multiplication of an extra permutation $(-1)^{p_I} P_I$ does not alter the result. Hence, it follows that

$$
\begin{aligned}
\mathcal{A}^2 &= \frac{1}{(N!)^2} \underbrace{\Big(\sum_p (-1)^p P + \cdots + \sum_p (-1)^p P \Big)}_{N! \text{ times}} \\
&= \frac{1}{N!} \sum_p (-1)^p P \\
&= \mathcal{A}.
\end{aligned}
\tag{2.36}
$$

We next show the second property. Consider an arbitrary permutation operator

$$
P = P_{ij} P_{kl} \dots P_{qr}. \tag{2.37}
$$

Taking the adjoint of this gives

$$
\begin{aligned}
P^\dagger &= P_{qr}^\dagger \ldots P_{kl}^\dagger P_{ij}^\dagger \\
&= P_{qr} \ldots P_{kl} P_{ij} \\
&= P^{-1}.
\end{aligned}
\tag{2.38}
$$

Thus P and $P^\dagger$ carry out the same operations, but in inverse order. Moreover, the parity of the two operators are the same. This means that

$$
\mathcal{A}^\dagger = \frac{1}{N!} \sum_P (-1)^p P^\dagger = \frac{1}{N!} \sum_P (-1)^p P^{-1},
\tag{2.39}
$$

and since the permutations in P^{-1} are arbitrary, we may replace it with P. Ergo we conclude that $\mathcal{A}^\dagger = \mathcal{A}$.

2.5 The reference energy

Even though the Slater determinant in (2.28) and (2.29) does not solve the Schrödinger equation with the full Hamiltonian (2.4), it can nevertheless be used as an ansatz to estimate the energy. We call this energy the reference energy:

$$
E_0 = \langle \Psi_0 | H | \Psi_0 \rangle.
\tag{2.40}
$$

Inserting the Slater determinant (2.28) yields

$$
E_0 = N! \int d\mathbf{x}_1 \ldots d\mathbf{x}_N (\mathcal{A}\Psi_H(\mathbf{x}_1 \cdots \mathbf{x}_N))^* H \mathcal{A}\Psi_H(\mathbf{x}_1 \cdots \mathbf{x}_N).
\tag{2.41}
$$

By using the fact that $\mathcal{A}$ is Hermitian and commutes with H as well as the fact that $\mathcal{A}^2 = \mathcal{A}$, this can be simplified to

$$
E_0 = N! \int d\mathbf{x}_1 \ldots d\mathbf{x}_N \Psi_H^*(\mathbf{x}_1 \cdots \mathbf{x}_N) H \mathcal{A}\Psi_H(\mathbf{x}_1 \cdots \mathbf{x}_N).
\tag{2.42}
$$

The contributions from H_1 and H_2 are

$$
\langle \Psi_0 | H_1 | \Psi_0 \rangle = \sum_{i=1}^N \int d\mathbf{x}\, \psi_i^*(\mathbf{x})\, h(\mathbf{x})\, \psi_i(\mathbf{x}) = \sum_{i=1}^N \langle i|h|i \rangle
\tag{2.43}
$$

and

$$
\begin{aligned}
\langle \Psi_0 | H_2 | \Psi_0 \rangle &= \frac{1}{2} \sum_{\substack{i,j=1 \\ i \neq j}}^N \int d\mathbf{x}\, d\mathbf{x}' [\psi_i^*(\mathbf{x})\, \psi_j^*(\mathbf{x}')\, g(\mathbf{r}, \mathbf{r}') \times \\
&\qquad\qquad [\psi_i(\mathbf{x})\, \psi_j(\mathbf{x}') - \psi_j(\mathbf{x})\, \psi_i(\mathbf{x}')]
\end{aligned}
\tag{2.44}
$$

$$
\langle \Psi_0 | H_2 | \Psi_0 \rangle = \frac{1}{2} \sum_{i,j=1}^N [\langle ij|g|ij \rangle - \langle ij|g|ji \rangle],
\tag{2.45}
$$

where we have defined

$$\langle p|h|q\rangle = \int d\mathbf{x}\, \psi_p^*(\mathbf{x})\, h(\mathbf{x})\, \psi_q(\mathbf{x}), \tag{2.46}$$

$$\langle pq|g|rs\rangle = \int d\mathbf{x}\, d\mathbf{x}'[\psi_p^*(\mathbf{x})\, \psi_q^*(\mathbf{x}')\, g(\mathbf{r}, \mathbf{r}')\psi_r(\mathbf{x})\, \psi_s(\mathbf{x}'). \tag{2.47}$$

Equation (2.43) results from the fact that all permutations of the spin orbitals vanish. When calculating the contribution from H_2, however, the interchange of two coordinates $\mathbf{x}_i$ and $\mathbf{x}_j$ will give a non-zero result for the cases where $\mathbf{r}_i$ and $\mathbf{r}_j$ are the arguments of g. Note that in equation (2.45) the restriction $i \neq j$ has been removed since the two terms automatically cancel in this case. The total reference energy is thus

$$E_0 = \sum_{i=1}^{N} \langle i|h|i\rangle + \frac{1}{2} \sum_{i,j=1}^{N} [\langle ij|g|ij\rangle - \langle ij|g|ji\rangle]. \tag{2.48}$$

Although we until now have discussed the case where the orbitals are eigenfunctions of H_1 (see equation (2.5)), this is not necessary; in fact, through the remainder of the thesis we assume them to be eigenfunctions of the Hartree-Fock equations to be discussed in chapter 3.

2.6   Second quantisation

We will now briefly discuss the so-called second quantisation. Second quantisation is an alternative way to express quantum mechanical operators and Slater determinants. An attractive feature of the formalism is that it makes no reference to the number of particles of the system. Most important for us, however, is the fact that it provides a compact notation and an efficient way of manipulating operators. It will prove to be especially useful when we later discuss perturbation theory.

To begin, we assume that there exists a basis of orthonormal single-particle spin orbitals $\{\psi_i\}_{i=1}^{\infty}$. As discussed above, these functions can be chosen freely, but we will assume that they are eigefunctions of the Hartree-Fock equations. We can combine the functions in various ways to form Slater determinants, which we will write as

$$|\Psi_0\rangle = |ijk\cdots z\rangle, \tag{2.49}$$

where the indices inside the ket indicate the spin orbitals that are occupied by particles. Because (2.49) represents a Slater determinant, which is necessarily antisymmetric, changing the order of two indices introduces a minus sign. It is customary to let the indices be ordered lexicographically so that

$$i < j < k < \cdots < z. \tag{2.50}$$

The physical vacuum state, in which no single-particle states are occupied, is written $|0\rangle$.

Next, we define the creation and annihilation operators $a_p^\dagger$ and a_p, respectively. They are defined through the relations

$$a_p^\dagger |ijk\cdots z\rangle = (-1)^{\eta_p}|ijk\cdots p\cdots z\rangle,$$
$$a_p|ijk\cdots p\ldots z\rangle = (-1)^{\eta_p}|ijk\cdots z\rangle, \tag{2.51}$$

where η_p are the number of spin orbitals preceeding ψ_p, and

$$a_p^\dagger|\Psi_0\rangle = 0, \qquad \text{if } \psi_p \text{ is occupied in } |\Psi_0\rangle,$$
$$a_p|\Psi_0\rangle = 0, \qquad \text{if } \psi_p \text{ is not occupied in } |\Psi_0\rangle. \tag{2.52}$$

The fact that these operators are each others adjoints is not self evident, but can be realised by considering the quantity $\langle\Psi_0'|a_p^\dagger|\Psi_0\rangle$. Obviously, this will have the value 0 or ± 1. By letting the creation operator act on the ket we see that the answer can be nonzero only if the orbital ψ_p is unoccupied in $|\Psi_0\rangle$ and occupied in $\langle\Psi_0'|$. Also, all other occupancies must be identical. If we let the operator act on the bra instead we should get the same answer. This is only possible if a_p removes the occupancy of ψ_p. Hence, the annihilation operator is the adjoint of the creation operator and vice versa.

Note that any Slater determinant $|ijk\cdots z\rangle$ can be written as a sequence of creation operators acting on the vacuum state:

$$|ijk\ldots z\rangle = a_i^\dagger a_j^\dagger a_k^\dagger \cdots a_z^\dagger |0\rangle \tag{2.53}$$

Fundamental to the second quantisation formalism are the anti-commuation relations of the creation and annihilation operators. By considering how they operate on general Slater determinants, it is not difficult to derive the following relations

$$[a_p^\dagger,\, a_q^\dagger]_+ = 0$$
$$[a_p,\, a_q]_+ = 0 \tag{2.54}$$
$$[a_p^\dagger,\, a_q]_+ = \delta_{pq},$$

where $[A,\, B]_+ = AB + BA$.

2.6.1   The Hamiltonian in second quantisation

The creation and annihilation operators are used to construct other operators. The one- and two-particle operators (2.5) and (2.6) are in second quantisation written as

$$H_1 = \sum_{pq}\langle p|h|q\rangle a_p^\dagger a_q \tag{2.55}$$

$$H_2 = \frac{1}{2}\sum_{pqrs}\langle pq|g|rs\rangle a_p^\dagger a_q^\dagger a_s a_r. \tag{2.56}$$

The sums in equations (2.55) and (2.56) are over all single-particle states. Because $a_s^\dagger a_r^\dagger = -a_r^\dagger a_s^\dagger$, H_2 can alternatively be written as

$$H_2 = \frac{1}{4}\sum_{pqrs}\langle pq||rs\rangle a_p^\dagger a_q^\dagger a_s a_r, \tag{2.57}$$

where

$$\langle pq||rs\rangle = \langle pq|g|rs\rangle - \langle pq|g|sr\rangle, \tag{2.58}$$

is the antisymmetrised integral, and $\langle pq|g|rs\rangle$ is defined in equation (2.47).

2.6.2   Particle-hole formulation

Instead of referring all Slater determinants to the physical vacuum, it is more useful to operate with a reference Slater determinant

$$|\Psi_0\rangle = |ijk\ldots z\rangle, \tag{2.59}$$

which is called the Fermi vacuum. For a system of N particles, it is typically build up of the N lowest eigenfunctions of the Hartree-Fock equations. The spin orbitals included in the Fermi vacuum are called hole states or occupied states, and all others are called particle states or virtual states. When using creation and annihilation operators, $a_p^\dagger$ and a_p, it is common to let indices $(i,j,k,\ldots)$ indicate hole states, $(a,b,c,\ldots)$ indicate particle states and $(p,q,r,\ldots)$ indicate both hole and particle states. Thus, other Slater determinants relative to the Fermi vacuum can be created as

$$|\Psi_i^a\rangle = a_a^\dagger a_i|\Psi_0\rangle = a_a^\dagger a_i|ijk\ldots n\rangle = |ajk\ldots n\rangle \tag{2.60}$$

$$|\Psi_{ij}^{ab}\rangle = a_a^\dagger a_b^\dagger a_j a_i|\Psi_0\rangle = a_a^\dagger a_b^\dagger a_j a_i|ijk\ldots n\rangle = |abk\ldots n\rangle. \tag{2.61}$$

These states are often referred to as excited states. The first is a singly excited state and the second is a doubly excited state. Note that there are many different ways to make a singly excited state; any of the hole states can be excited to any of the particle states. Typically the single-particle basis has infinite dimensionality which means that there are infinitely many different singly excited states. The idea is illustrated in figure 2.1.

Recall that any annihilation operator acting to the right on the physical vacuum gives zero. However, this is not the case when operating on the Fermi vacuum. It is desired to retain this property also for the Fermi vacuum. In order to achieve this, we introduce the so-called pseudo creation and pseudo annihilation operators $b_p^\dagger$ and b_p, respectively. They are defined as

$$b_i^\dagger = a_i, \qquad b_i = a_i^\dagger, \tag{2.62}$$
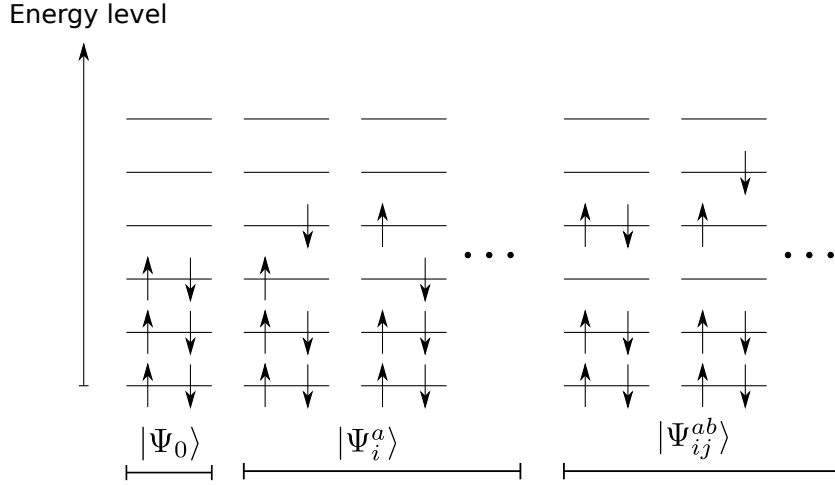
$$b_a^\dagger = a_a^\dagger, \qquad b_a = a_a. \tag{2.63}$$

From this it is clear that any pseudo annihilation operator acting on the Fermi vacuum gives zero.

Unless stated otherwise, we will always refer to the Fermi vacuum throughout this thesis.

2.6.3   Normal order, contractions and Wick's theorem

The normal ordering of a product of operators, written $\{AB\ldots Z\}$, is the rearrangement of all operators such that all pseudo creation operators are to the left of all pseudo

Figure 2.1: Illustration of how different Slater determinants can be created by exciting one or more of the electrons in the reference Slater.

annihilation operators times the factor $(-1)^\sigma$, where σ is equal to the number of interchanges made in order to obtain the rearrangement. As an example, consider the normal ordering of the product $a_a a_i a_b^\dagger a_j^\dagger$:

$$\{a_a a_i a_b^\dagger a_j^\dagger\} = \{b_a b_i^\dagger b_b^\dagger b_j\} = (-1)^2\, b_i^\dagger b_b^\dagger b_a b_j = a_i a_b^\dagger a_a a_j^\dagger \tag{2.64}$$

The normal ordering is not unique since the following is also correct:

$$\{a_a a_i a_b^\dagger a_j^\dagger\} = -a_i a_b^\dagger a_j^\dagger a_a. \tag{2.65}$$

Note also that the vacuum expectation of a normal product of operators is equal to zero.

The *contraction* of two operators A and B is defined as

$$\overbracket{AB} = AB - \{AB\}. \tag{2.66}$$

It will always be equal to zero or one. This is easily seen by considering all four possible contractions:

$$
\begin{aligned}
\overbracket{b_p b_q} &= b_p b_q - b_p b_q = 0, \\
\overbracket{b_p^\dagger b_q^\dagger} &= b_p^\dagger b_q^\dagger - b_p^\dagger b_q^\dagger = 0, \\
\overbracket{b_p^\dagger b_q} &= b_p^\dagger b_q - b_p^\dagger b_q = 0, \\
\overbracket{b_p b_q^\dagger} &= b_p b_q^\dagger - (-b_q^\dagger b_p) = [b_p, b_q^\dagger]_+ = \delta_{pq}.
\end{aligned}
\tag{2.67}
$$

Contractions can occur between operators within a normal product:

$$\{ABC\cdots \overbracket{R\cdots S}\cdots T\} = (-1)^\sigma\, \overbracket{RS}\{ABC\cdots T\}, \tag{2.68}$$

where σ is the number of interchanges needed to bring the operators R and S next to each other.

We next state *Wick's theorem* [8]: *A product of a string of pseudo creation and pseudo annihilation operators is equal to their normal product plus the sum of all possible normal products with contractions:*

$$AB\cdots Z = \{AB\cdots Z\} + \sum\{\overline{AB\cdots} Z\} + \sum\{\overline{AB\cdots} Z\} + \dots \qquad (2.69)$$

The theorem is extremely useful when calculating the vacuum expectation of operators. As explained above, all expectation values of normal products are equal to zero. Therefore, only the fully contracted terms contribute. Moreover, the vacuum expectation of a product of an odd number of creation and annihilation operators will always be equal to zero because there can be no fully contracted terms.

A corollary of Wick's theorem, often referred to as Wick's generalised theorem, will also prove to be useful. It says that a general product of pseudo creation and pseudo annihilation operators in which some strings of operators are already normal ordered, is equal to the overall normal product plus the sum of all possible normal products with contractions between operators which are not within the same original normal product:

$$\{A_1 A_2 \cdots\}\{B_1 B_2 \cdots\}\{C_1 C_2 \cdots\}\cdots$$

$$= \{A_1 A_2 \cdots B_1 B_2 \cdots C_1 C_2 \cdots\} + \sideset{}{'}\sum\{A_1 \overline{A_2 \cdots B_1 \overline{B_2 \cdots C_1}} C_2 \cdots\}, \qquad (2.70)$$

where the sum has been labeled with a prime to indicate that contractions between operators which belong to the same original normal product shall be omitted.

2.6.4   Normal ordered operators

As pointed out in the previous section, normal ordered operators are very useful when calculating vacuum expectation values. We will therefore show what the normal ordered one- and two-particle operators in (2.55) and (2.57) look like.

Let us first consider the one-particle operator. Using Wick's theorem we find that

$$\begin{aligned} a_p^\dagger a_q &= \{a_p^\dagger a_q\} + \{\overline{a_p^\dagger a_q}\} \\ &= \{a_p^\dagger a_q\} + \delta_{pq\in I}. \end{aligned} \qquad (2.71)$$

The subindex $pq \in I$ signifies that p and q must be hole states. From this we arrive at the operator:

$$H_1 = \sum_{pq}\langle p|h|q\rangle\{a_p^\dagger a_q\} + \sum_i\langle i|h|i\rangle. \qquad (2.72)$$

Wick's theorem applied on the two-particle operator gives:

$$a_p^\dagger a_q^\dagger a_s a_r = \{a_p^\dagger a_q^\dagger a_s a_r\} + \{\overline{a_p^\dagger a_q^\dagger} a_s a_r\} + \{\overline{a_p^\dagger a_q^\dagger a_s a_r}\}$$

$$+ \{a_p^\dagger \overline{a_q^\dagger a_s} a_r\} + \{a_p^\dagger \overline{a_q^\dagger a_s a_r}\} + \{\overline{a_p^\dagger a_q^\dagger a_s} a_r\}$$

$$+ \quad \{\overparen{a_p^\dagger a_q^\dagger a_s a_r}\}$$

$$a_p^\dagger a_q^\dagger a_s a_r = \{a_p^\dagger a_q^\dagger a_s a_r\} - \{a_q^\dagger a_r\}\delta_{ps\in I} + \{a_q^\dagger a_s\}\delta_{pr\in I}$$
$$+ \{a_p^\dagger a_r\}\delta_{qs\in I} - \{a_p^\dagger a_s\}\delta_{qr\in I} + \delta_{pr\in I}\delta_{qs\in I} \tag{2.73}$$
$$- \delta_{ps\in I}\delta_{qr\in I}.$$

Inserting this into equation (2.57) gives:

$$H_2 = \frac{1}{4}\sum_{pqrs}\langle pq||rs\rangle\{a_p^\dagger a_q^\dagger a_s a_r\}$$
$$+ \frac{1}{4}\sum_{pqi}\Big[-\langle ip||qi\rangle + \langle ip||iq\rangle + \langle pi||qi\rangle - \langle pi||iq\rangle\Big]\{a_p^\dagger a_q\} \tag{2.74}$$
$$+ \frac{1}{4}\sum_{ij}\Big[\langle ij||ij\rangle - \langle ij||ji\rangle\Big].$$

By using the fact that $\langle pq||rs\rangle = \langle qp||sr\rangle$ and $\langle pq||rs\rangle = -\langle pq||sr\rangle$ this can be written as

$$H_2 = \frac{1}{4}\sum_{pqrs}\langle pq||rs\rangle\{a_p^\dagger a_q^\dagger a_s a_r\} + \sum_{pqi}\langle pi||qi\rangle\{a_p^\dagger a_q\} + \frac{1}{2}\sum_{ij}\langle ij||ij\rangle \tag{2.75}$$

Thus the total Hamiltonian can be expressed as

$$H = \sum_{pq}[\langle p|h|q\rangle + \sum_i\langle pi||qi\rangle]\{a_p^\dagger a_q\} + \frac{1}{4}\sum_{pqrs}\langle pq||rs\rangle\{a_p^\dagger a_q^\dagger a_s a_r\} + E_0. \tag{2.76}$$

$$H = F + W + E_0, \tag{2.77}$$

where

$$F = \sum_{pq}[\langle p|h|q\rangle + \sum_i\langle pi||qi\rangle]\{a_p^\dagger a_q\}, \tag{2.78}$$

$$W = \frac{1}{4}\sum_{pqrs}\langle pq||rs\rangle\{a_p^\dagger a_q^\dagger a_s a_r\}, \tag{2.79}$$

are the normal ordered one- and two-body operators, respectively, and E_0 is the reference energy defined in equation (2.48). We will write the one-body operator F as

$$F = \sum_{pq}\langle p|\mathcal{F}|q\rangle\{a_p^\dagger a_q^\dagger\}, \tag{2.80}$$

where $\langle p|\mathcal{F}|q\rangle$ are the elements of the Fock operator $\mathcal{F}$.

2.6.5 Evaluation of matrix elements

Wick's generalised theorem is an effective tool for evaluating expectation values of operators. As a simple demonstration, let us evaluate the matrix element

$$\langle\Psi_i^a|F|\Psi_i^a\rangle. \tag{2.81}$$

This can be done by noting that the Slater determinants can be written as

$$|\Psi_i^a\rangle = \{a_a^\dagger a_i\}|\Psi_0\rangle. \tag{2.82}$$

Using this we get

$$\langle\Psi_i^a|F|\Psi_i^a\rangle = \sum_{pq}\langle\Psi_0|\langle p|\mathcal{F}|q\rangle\{a_i^\dagger a_a\}\{a_p^\dagger a_q\}\{a_a^\dagger a_i\}|\Psi_0\rangle$$

$$= \sum_{pq}\langle\Psi_0|\langle p|\mathcal{F}|q\rangle\{\overline{a_i^\dagger \overline{a_a}\}\{\overline{a_p^\dagger} \overline{a_q}\}\{\overline{a_a^\dagger} a_i}\}|\Psi_0\rangle$$

$$+ \sum_{pq}\langle\Psi_0|\langle p|\mathcal{F}|q\rangle\{\overline{a_i^\dagger \overline{a_a}\}\{a_p^\dagger \overline{a_q}\}\{\overline{a_a^\dagger} a_i}\}|\Psi_0\rangle$$

$$= \sum_{pq}\left[\langle p|\mathcal{F}|q\rangle\delta_{pa}\delta_{qa} - \langle p|\mathcal{F}|q\rangle\delta_{pi}\delta_{qi}\right]$$

$$= \langle a|\mathcal{F}|a\rangle - \langle i|\mathcal{F}|i\rangle. \tag{2.83}$$

A more complicated example, which will become important for us later when we discuss perturbation theory, is the vacuum expectation of W^2:

$$\langle\Psi_0|W^2|\Psi_0\rangle = \frac{1}{16}\sum_{pqrs}\sum_{tuvw}\langle pq||rs\rangle\langle tu||vw\rangle\langle\Psi_0|\{a_p^\dagger a_q^\dagger a_s a_r\}\{a_t^\dagger a_u^\dagger a_w a_v\}|\Psi_0\rangle. \tag{2.84}$$
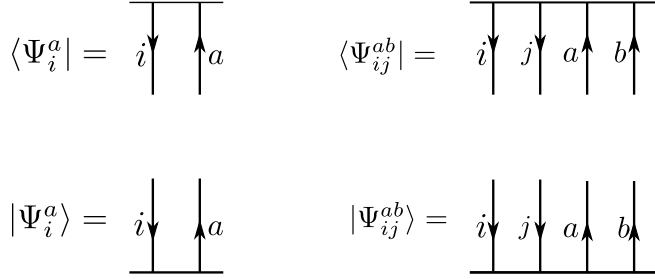
The only surviving contractions are those where the pair $a_p^\dagger, a_q^\dagger$ are contracted with a_w, a_v, in either order, and the pair a_s, a_r are contracted with $a_t^\dagger, a_u^\dagger$, in either order. Furthermore, p, q, w, v must be particle states and s, r, t, u must be hole states. Explicitly we get

$$\{a_a^\dagger a_b^\dagger a_j a_i\}\{a_k^\dagger a_l^\dagger a_d a_c\} = \{a_a^\dagger a_b^\dagger a_j a_i\}\{a_k^\dagger a_l^\dagger a_d a_c\} + \{a_a^\dagger a_b^\dagger a_j a_i\}\{a_k^\dagger a_l^\dagger a_d a_c\}$$

$$+ \{a_a^\dagger a_b^\dagger a_j a_i\}\{a_k^\dagger a_l^\dagger a_d a_c\} + \{a_a^\dagger a_b^\dagger a_j a_i\}\{a_k^\dagger a_l^\dagger a_d a_c\}$$

$$= \delta_{ac}\delta_{bd}\delta_{ik}\delta_{jl} - \delta_{ad}\delta_{bc}\delta_{ik}\delta_{jl}$$

$$- \delta_{ac}\delta_{bd}\delta_{il}\delta_{jk} + \delta_{ad}\delta_{bc}\delta_{il}\delta_{jk}.$$

Thus the resulting matrix element is

$$\langle\Psi_0|W^2|\Psi_0\rangle = \frac{1}{16}\sum_{abij}\left[\langle ab||ij\rangle\langle ij||ab\rangle - \langle ab||ij\rangle\langle ij||ba\rangle\right.$$

$$\left. - \langle ab||ij\rangle\langle ji||ab\rangle + \langle ab||ij\rangle\langle ji||ba\rangle\right] \tag{2.85}$$

$$= \frac{1}{4}\sum_{abij}|\langle ab||ij\rangle|^2.$$

More complicated matrix elements can be evaluated in the same way, but the contractions quickly become rather complicated and tedious to carry out. Diagrammatic notation, which we introduce in the next subsection, makes this process easier.

Figure 2.2: Diagrammatic representation of Slater determinants. Kets and bras have horisontal bottom and top lines, respectively.

2.7   Diagrammatic notation

In diagrammatic notation, Slater determinants are represented by vertical arrows, upward pointing meaning particle states and downward pointing meaning hole states, as shown in figure 2.2. The vacuum state is defined as the absence of vertical lines.

The diagrams for the one-particle operator F defined in equation (2.78) and (2.80), called *Goldstone diagrams*, are pictured in figure 2.3. The four diagrams correspond to the sums

$$
\begin{aligned}
F = & \sum_{ab} \langle a|\mathcal{F}|b\rangle \{a_a^\dagger a_b\} + \sum_{ij} \langle i|\mathcal{F}|j\rangle \{a_i^\dagger a_j\} \\
& + \sum_{ia} \langle a|\mathcal{F}|i\rangle \{a_a^\dagger a_i\} + \sum_{ia} \langle i|\mathcal{F}|a\rangle \{a_i^\dagger a_a\}.
\end{aligned}
\tag{2.86}
$$
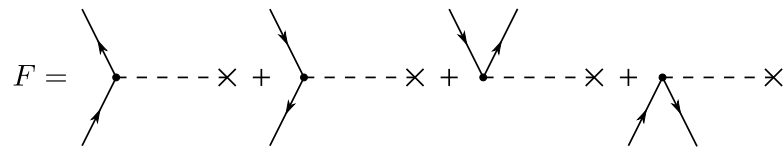
An incoming line represents a ket state and the associated annihilation operator, while an outgoing line represents a bra state and the associated creation operator.

The contractions we performed when calculating $\langle \Psi_i^a|F|\Psi_i^a\rangle$ in the previous subsection are done diagrammatically as follows. First, each of the diagrams of F are placed between the Slater determinants $\langle \Psi_i^a|$ and $|\Psi_i^a\rangle$. Thereafter, the lines are connected in all possible ways, and the resulting diagrams are drawn. However, the lines must be connected properly, that is to say, the arrows must point in the same direction. Moreover, there can be no loose lines; both ends of a line must connect either to an operator or to the bra or ket. The resulting diagrams are shown in figure 2.4. Once these have been drawn, the matrix element is determined by reading the lines going into and out of the operator according to the following rule
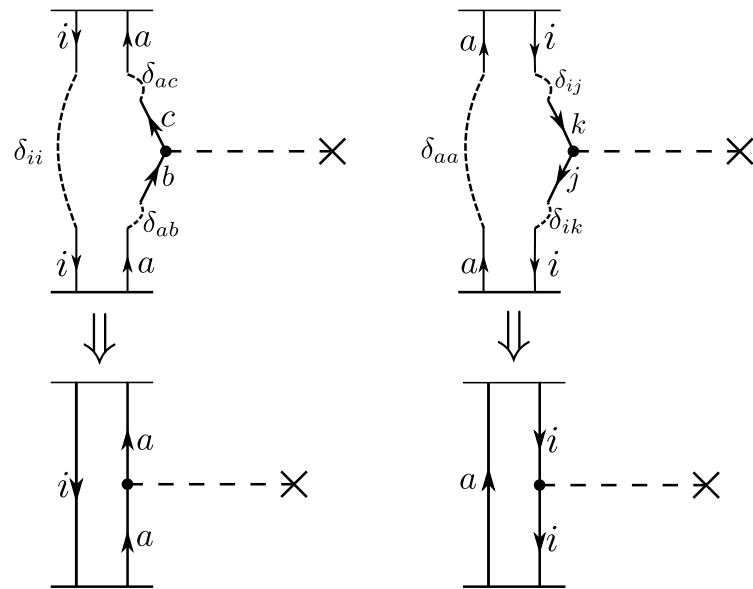
$$
\langle \text{outgoing line}|\mathcal{F}|\text{incoming line}\rangle
\tag{2.87}
$$

for each diagram, and the terms are summed. By comparing the diagrams of figure 2.4 with equation (2.83), we see that there should be a minus sign in front of the diagram to the right. The sign is determined according to the following rule. A diagram with l loops and h hole lines has the sign $(-1)^{h-l}$.
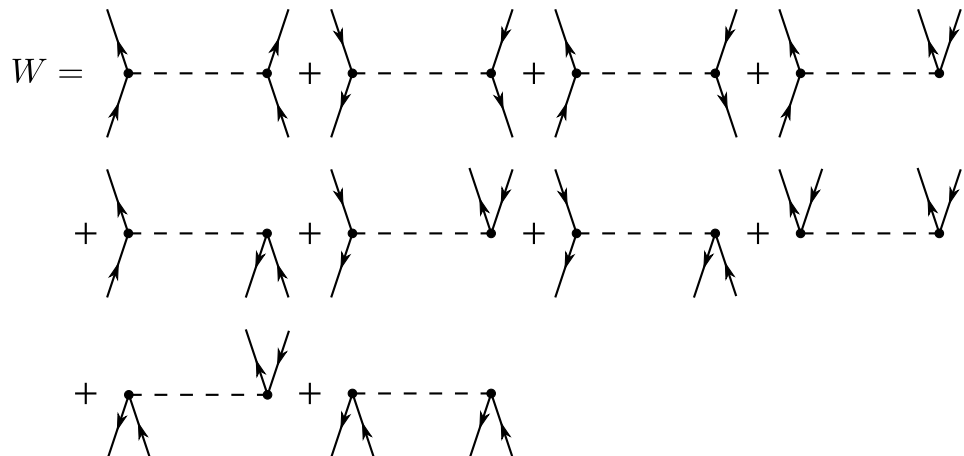
The diagrams for the two-particle operator W of equation (2.79) are shown in figure 2.5. The diagrams are called *antisymmetrised Goldstone diagrams*. The procedure for

$$F = \; \rangle \text{-----} \times \; + \; \rangle \text{-----} \times \; + \; \rangle \text{-----} \times \; + \; \rangle \text{-----} \times$$
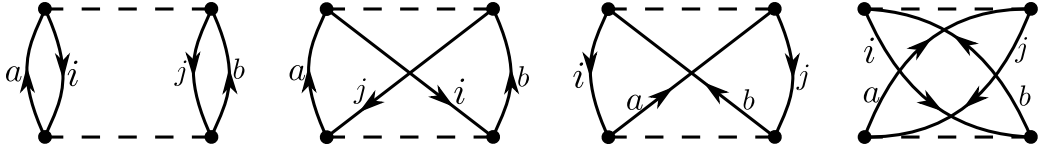
Figure 2.3: Diagrammatic representation of the one-particle operator F of equation (2.78).

Figure 2.4: Diagrammatic representation of the matrix element $\langle \Psi_i^a | F | \Psi_i^a \rangle = \langle a | \mathcal{F} | a \rangle - \langle i | \mathcal{F} | i \rangle$.

$$W = \; \rangle \text{-----} \langle \; + \; \rangle \text{-----} \langle \; + \; \rangle \text{-----} \langle \; + \; \rangle \text{-----} \rangle$$

Figure 2.5: Diagrammatic representation of the two-particle operator W of equation (2.79). Diagrams which can be constructed by reflection through a vertical centerline are not shown (although they are contributing).

Figure 2.6:   Antisymmetrised Goldstone diagrams representing the matrix element $\langle \Psi_0 | W^2 | \Psi_0 \rangle$.

calculating matrix elements involving the two-particle operator W is the same as for the one-particle operator F. As a useful demonstration we will calculate $\langle \Psi_0 | W^2 | \Psi_0 \rangle$ diagrammatically. Whenever we have more than one operator, the diagrams of the operators are placed on top of each other in the same order as they appear in the formula (the one next to the ket at the bottom and the one next to the bra at the top). Since we are calculating the expectation value of a vacuum state, the only surviving terms will be the diagrams where the upper operator is given by the tenth diagram and the lower operator is given by the eighth diagram of figure 2.5. There are a total of four different ways to connect these diagrams, as shown in figure 2.6. The resulting matrix element is given according to the following rule:

$$\langle (\text{left out})(\text{right out}) || (\text{left in})(\text{right in}) \rangle. \tag{2.88}$$
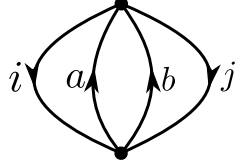
As before, the sign is given by $(-1)^{h-l}$, where h is the number of hole lines and l is the number of loops. The first and last diagrams have $h = 2$ and $l = 2$, and the second and third diagrams have $h = 2$ and $l = 1$. Hence, we get

$$
\begin{aligned}
\langle \Psi_0 | W^2 | \Psi_0 \rangle = \frac{1}{16} \sum_{ijab} \Big[& \langle ij || ab \rangle \langle ab || ij \rangle - \langle ij || ab \rangle \langle ab || ji \rangle \\
& - \langle ij || ba \rangle \langle ab || ij \rangle + \langle ij || ba \rangle \langle ab || ji \rangle \Big].
\end{aligned}
\tag{2.89}
$$

The factor of $1/16$ comes from the fact that each W operator carries a factor of $1/4$. Due to the antisymmetry property of the integrals, all of the four terms are in fact equal, and we end up with

$$\langle \Psi_0 | W^2 | \Psi_0 \rangle = \frac{1}{4} \sum_{ijab} \langle ij || ab \rangle \langle ab || ij \rangle. \tag{2.90}$$

The evaluation of $\langle \Psi_0 | W^n | \Psi_0 \rangle$ for integer values of n typically occurs in perturbation theory, and it is therefore important to be able to evaluate such matrix elements. However, because the number of different diagrams increases rapidly with n, it quickly becomes difficult to list all possible diagrams. Fortunately, it is not actually necessary to list them all; for the case of $\langle \Psi_0 | W^2 | \Psi_0 \rangle$ we would get the correct answer if we only drew one of the four diagrams in figure 2.6 and multiplied the corresponding matrix element with a factor of 4. Of course, we need some way to determine the weight factor. To do this we introduce the so-called *Hugenholtz diagrams*. The Hugenholtz diagram for the one-particle operator is identical to the Goldstone diagram. The two-particle diagram is similar, except that the horisontal dashed line corresponding to each operator

Figure 2.7: Hugenholtz diagram of the matrix element $\langle\Psi_0|W^2|\Psi_0\rangle$.

is shrinked to a point. The Hugenholtz diagram for the matrix element $\langle\Psi_0|W^2|\Psi_0\rangle$ is shown in figure 2.7. Each vertex in a diagram must have two outgoing and two incoming lines. The order of the lines makes no difference. Thus there can be only one Hugenholtz diagram for $\langle\Psi_0|W^2|\Psi_0\rangle$. The value of the matrix element, including the sign, is obtained by expanding the Hugenholtz diagram into one of the Goldstone diagrams of figure 2.6. The numerical factor in front is determined by counting the number of equivalent line pairs of the Hugenholtz diagram. Two lines are equivalent if they connect the same two vertices in the same direction. For n equivalent line pairs, the numerical factor is $(1/2)^n$. In the case of figure 2.7 there are two equivalent line pairs, which yields a numerical factor of $1/4$ in agreement with equation (2.90).

The general rules for drawing and intepreting Hugenholtz diagrams are as follows (quoted almost directly from Shavitt and Bartlett [5]):

1. Generate all distinct Hugenholtz diagrams.

2. Expand each Hugenholtz diagram into an antisymmetrised Goldstone diagram in any of the possible equivalent ways.

3. Interpret each two-body vertex in each antisymmetrised Goldstone diagram in terms of an antisymmetrised integral, with the usual

$$\langle(\text{left out})(\text{right out})||(\text{left in})(\text{right in})\rangle$$

   arrangement.
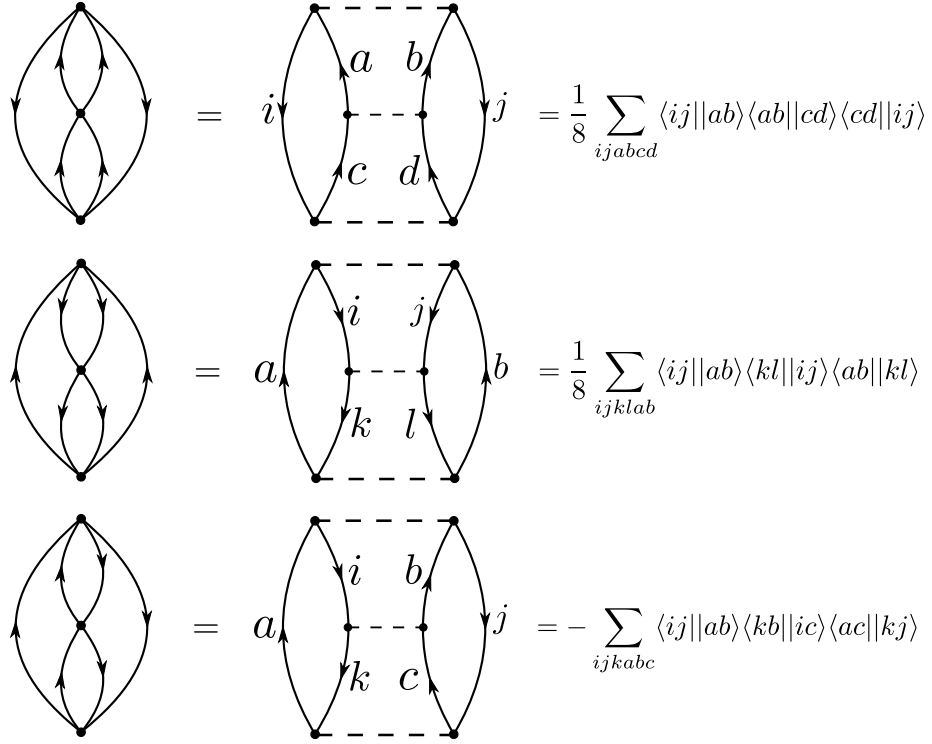
4. Intepret each one-body vertex with the usual

$$\langle\text{line out}|\mathcal{F}|\text{line in}\rangle$$

   arrangement.

5. Assign a phase factor $(-1)^{h-l}$, where h is the number of hole lines and l is the number of loops.

6. Assign a weight factor $(1/2)^n$, where n is the number of equivalent line pairs; two lines are equivalent if they connect the same two verices in the same direction.

We end this section by calculating the matrix element $\langle\Psi_0|W^3|\Psi_0\rangle$ since this will give us the third order term of perturbation theory, which we discuss in chapter 6. The three contributing diagrams are shown in figure 2.8. The first and second diagrams have

$$= i \qquad = \frac{1}{8} \sum_{ijabcd} \langle ij||ab\rangle\langle ab||cd\rangle\langle cd||ij\rangle$$

$$= a \qquad = \frac{1}{8} \sum_{ijklab} \langle ij||ab\rangle\langle kl||ij\rangle\langle ab||kl\rangle$$

$$= a \qquad = - \sum_{ijkabc} \langle ij||ab\rangle\langle kb||ic\rangle\langle ac||kj\rangle$$

Figure 2.8: Hugenholtz and corresponding antisymmetrised Goldstone diagrams for the matrix element $\langle\Psi_0|W^3|\Psi_0\rangle$.

three equivalent line pairs and thus a weight factor of $1/8$, whereas the last diagram has no such pairs and therefore a weight factor of 1. The first diagram has $h = 2$ and $l = 2$, the second diagram has $h = 4$ and $l = 2$, and the third diagram has $h = 3$ and $l = 2$. Hence, the last diagram is accompanied with a minus sign.

2.8   A basis for the fermionic wave function

We end this chapter by stating an important theorem:

If the basis $\{\psi_i\}_{i=1}^{\infty}$ is complete in the Hilbert space of single-particle wave functions, then the set of all Slater determinants constructed from this basis is also complete in the Hilbert space of antisymmetric many-particle functions.

In particular, this means that with the particle-hole formulation introduced above, any state $|\Phi\rangle$ can be written as

$$|\Phi\rangle = C_0|\Psi_0\rangle + \sum_{ia} C_i^a|\Psi_i^a\rangle + \sum_{i<j,a<b} C_{ij}^{ab}|\Psi_{ij}^{ab}\rangle + \dots \qquad (2.91)$$

Note the restriction $i < j$ and $a < b$ on the sum over the two-particle two-hole states. This is necessary because $|\Psi_{ij}^{ab}\rangle = -|\Psi_{ji}^{ab}\rangle = -|\Psi_{ij}^{ba}\rangle = |\Psi_{ji}^{ba}\rangle$.

Chapter 3

Hartree-Fock

The Hartree-Fock method, initially developed by Hartree [9] and improved by Fock [10], is probably the most popular *ab initio* method of quantum chemistry. There are mainly two reasons for this. Firstly, it provides an excellent first approximation to the wave function and energy of the system, often accounting for about 90%-99% of the total energy. Secondly, in cases where an even higher degree of precision is needed, the result from a Hartree-Fock calculation is a very good starting point for other so-called *post-Hartree-Fock methods*. We will look into one such method, namely perturbation theory, in chapter 6.

The general form of the equations is

$$\mathcal{F}\psi_k = \varepsilon_k \psi_k, \tag{3.1}$$

where $\mathcal{F}$ is the Fock operator, defined as

$$
\begin{aligned}
\mathcal{F}(\mathbf{x})\psi_k(\mathbf{x}) =& \Big[-\frac{1}{2}\nabla^2 - \sum_{n=1}^{K} \frac{Z_n}{|\mathbf{R}_n - \mathbf{r}|} \Big]\psi_k(\mathbf{x}) \\
&+ \sum_{l=1}^{N} \int d\mathbf{x}' |\psi_l(\mathbf{x}')|^2 \frac{1}{|\mathbf{r} - \mathbf{r}'|}\psi_k(\mathbf{x}) \\
&- \sum_{l=1}^{N} \int d\mathbf{x}' \psi_l^*(\mathbf{x}') \frac{1}{|\mathbf{r} - \mathbf{r}'|}\psi_k(\mathbf{x}')\psi_l(\mathbf{x}).
\end{aligned}
\tag{3.2}
$$

These are a set of coupled one-electron eigenvalue equations for the spin orbitals ψ_k. The equations are non-linear because the orbitals we are seeking are actually needed in order to obtain the operator $\mathcal{F}$ which determine them. They are therefore often referred to as self consistent field (SCF) equations, and they must be solved iteratively.

The term in the square brackets is the one-body operator which we have called $h(\mathbf{r})$ in equation (2.5). The two extra sums are due to the interactions between the electrons. The first of these represent the Coulomb potential from the mean field set up by the electrons of the system. The last is similar to the first except that the indices of two orbitals have been switched. This is a direct consequence of the fact that in the derivation of the equations, the state is assumed to be a Slater determinant. Note

that due to the last sum, the Fock operator is non-local, that is to say, the value of $\mathcal{F}(\mathbf{x})\psi_k(\mathbf{x})$ depends on the value of $\psi_k(\mathbf{x}')$ at all coordinates $\mathbf{x}' \in \mathbb{R}^3 \oplus \{\uparrow, \downarrow\}$.

In the following section the general Hartree-Fock equations presented above are derived. Thereafter, we will see how to reformulate the equations to a more implementation friendly form. We do this by removing the spin part so that the resulting equations are in terms of spatial orbitals only. However, before doing this, it is necessary to decide how to relate the spin orbitals to the spatial orbitals. We discuss the two most common ways to do this. These result in the so-called restricted and unrestricted Slater determinants, which are discussed in section 3.2. In section 3.4 we show how the restricted determinant leads to the restricted Hartree-Fock (RHF) equations, which is a set of integro-differential equations for the spatial orbitals. In order to solve the equations, the spatial orbitals are expanded in a known basis, which leads to a set of self consistent algebraic equations called the *Roothaan equations*. Thereafter, in section 3.5, we derive the unrestricted Hartree-Fock (UHF) equations from the unrestricted determinant. These are also solved by introducing a set of known basis functions, leading to the so-called *Pople-Nesbet* equations, which is the unrestricted analogue of the Roothaan equations.

The theory of this chapter is covered by Szabo and Ostlund [3] and Thijssen [11].

3.1   Derivation of the Hartree-Fock equations

As discussed in section 2.8, the exact ground state can be written as a linear combination of Slater determinants

$$|\Phi_0\rangle = C_0|\Psi_0\rangle + \sum_{ia} C_i^a|\Psi_i^a\rangle + \sum_{i<j,a<b} C_{ij}^{ab}|\Psi_{ij}^{ab}\rangle + \dots \qquad (3.3)$$

where $|\Psi_0\rangle$ is some chosen reference determinant. In the Hartree-Fock method all determinants except $|\Psi_0\rangle$ are neglected, and the spin orbitals from which $|\Psi_0\rangle$ is constructed are chosen in such a way that the expectation value $E_0 = \langle\Psi_0|H|\Psi_0\rangle$ comes as close to the excact energy $\mathscr{E}_0$ as possible. According to the variational principle, the expectation value E_0 is an upper bound to the exact energy $\mathscr{E}_0$, which means that the optimal choice of spin orbitals are those which minimise E_0. When E_0 is at its minimum, any infinitesimal variation of the spin orbitals will leave E_0 unchanged, which in mathematical terms means that

$$\delta E_0 = \sum_{k=1}^{N}[\langle\delta\psi_k|\mathcal{F}|\psi_k\rangle + \langle\psi_k|\mathcal{F}|\delta\psi_k\rangle] = 0. \qquad (3.4)$$

If each variation could be chosen independently, this would immediately give us N equations to be solved for the N spin orbitals. Unfortunately, the spin orbitals cannot be varied independently, but must remain orthonormal throughout the variation. The orthonormality condition reads

$$\langle\psi_k|\psi_l\rangle - \delta_{kl} = 0. \qquad (3.5)$$

This type of *constrained* optimisation problem can be solved elegantly by the method of Lagrangian multipliers. A good review of the method is given in Boas [12]. The method simply says that if we construct the new functional

$$\mathscr{L} = E_0 - \sum_{k,l=1}^{N} \Lambda_{lk}[\langle \psi_k | \psi_l \rangle - \delta_{kl}], \tag{3.6}$$

we can find the stationary value of E_0 by solving the *unconstrained* variational problem for $\mathscr{L}$. By unconstrained we mean that the variation of each spin orbital can be chosen freely. The multipliers Λ_{lk} are called Lagrange multipliers and will also be determined as part of the solution.

Recall from equation (2.48) that the reference energy is given by

$$E_0 = \langle \Psi_0 | H | \Psi_0 \rangle = \sum_{k=1}^{N} \langle \psi_k | h | \psi_k \rangle + \frac{1}{2} \sum_{k,l=1}^{N} [\langle \psi_k \psi_l | g | \psi_k \psi_l \rangle - \langle \psi_k \psi_l | g | \psi_l \psi_k \rangle]. \tag{3.7}$$

Taking the variation of this yields

$$
\begin{aligned}
\delta E_0 =& \sum_{k=1}^{N} \langle \delta \psi_k | h | \psi_k \rangle \\
&+ \frac{1}{2} \sum_{k,l=1}^{N} [\langle \delta \psi_k \psi_l | g | \psi_k \psi_l \rangle + \langle \psi_k \delta \psi_l | g | \psi_k \psi_l \rangle \\
&\qquad - \langle \delta \psi_k \psi_l | g | \psi_l \psi_k \rangle - \langle \psi_k \delta \psi_l | g | \psi_l \psi_k \rangle] + \text{c.c.} \\
=& \sum_{k=1}^{N} \langle \delta \psi_k | h | \psi_k \rangle \\
&+ \frac{1}{2} \sum_{k,l=1}^{N} [\langle \delta \psi_k \psi_l | g | \psi_k \psi_l \rangle + \langle \delta \psi_l \psi_k | g | \psi_l \psi_k \rangle \\
&\qquad - \langle \delta \psi_k \psi_l | g | \psi_l \psi_k \rangle - \langle \delta \psi_l \psi_k | g | \psi_k \psi_l \rangle] + \text{c.c.} \\
=& \sum_{k=1}^{N} \langle \delta \psi_k | h | \psi_k \rangle + \sum_{k,l=1}^{N} [\langle \delta \psi_k \psi_l | g | \psi_k \psi_l \rangle - \langle \delta \psi_k \psi_l | g | \psi_l \psi_k \rangle] + \text{c.c.}
\end{aligned}
\tag{3.8}
$$

where c.c. represents complex conjugate terms. In the expression after the second equality sign, we have used that $\langle \psi_k \delta \psi_l | g | \psi_k \psi_l \rangle = \langle \delta \psi_l \psi_k | g | \psi_l \psi_k \rangle$, and the last line follows from the fact that the indices k and l can be switched since they are dummy indices. We next define the two operators

$$\mathcal{J}(\mathbf{x}) \psi_k(\mathbf{x}) = \sum_{l=1}^{N} \left[\int d\mathbf{x}' \psi_l^*(\mathbf{x}') g(\mathbf{r}, \mathbf{r}') \psi_l(\mathbf{x}') \right] \psi_k(\mathbf{x}), \tag{3.9}$$

$$\mathcal{K}(\mathbf{x}) \psi_k(\mathbf{x}) = \sum_{l=1}^{N} \left[\int d\mathbf{x}' \psi_l^*(\mathbf{x}') g(\mathbf{r}, \mathbf{r}') \psi_k(\mathbf{x}') \right] \psi_l(\mathbf{x}), \tag{3.10}$$

so that the variation of the energy can be written more compactly as

$$\delta E_0 = \sum_{k=1}^{N} \langle \delta\psi_k | h + \mathcal{J} - \mathcal{K} | \psi_k \rangle + \text{c.c.} \tag{3.11}$$

Next we consider the variation of the constraint:

$$\sum_{k,l=1}^{N} [\Lambda_{lk} \langle \delta\psi_k | \psi_l \rangle + \Lambda_{lk} \langle \psi_k | \delta\psi_l \rangle]. \tag{3.12}$$

We will show that the second term of this equation is in fact the complex conjugate of the first. To realise this, consider the functional $\mathcal{L}$ of equation (3.6). First note that it must be real because E_0 is real and the added constraints are equal to zero. Taking the complex conjugate of $\mathcal{L}$ therefore gives

$$\begin{aligned}
\mathcal{L} &= E_0 - \sum_{k,l=1}^{N} \Lambda_{lk}^* [\langle \psi_k | \psi_l \rangle^* - \delta_{kl}] \\
&= E_0 - \sum_{k,l=1}^{N} \Lambda_{lk}^* [\langle \psi_l | \psi_k \rangle - \delta_{lk}] \\
&= E_0 - \sum_{k,l=1}^{N} \Lambda_{kl}^* [\langle \psi_k | \psi_l \rangle - \delta_{kl}].
\end{aligned} \tag{3.13}$$

This form of $\mathcal{L}$ is identical to the original of (3.6) except that Λ_{lk} has been replaced by Λ_{kl}^*. Since both will yield exactly the same Lagrange multipliers (assuming that the solution is unique), this means that

$$\Lambda_{lk} = \Lambda_{kl}^*, \tag{3.14}$$

that is to say, Λ_{lk} are the elements of a Hermitian matrix. Thus we can write the variation of the constraint as

$$\begin{aligned}
\sum_{k,l=1}^{N} [\Lambda_{lk} \langle \delta\psi_k | \psi_l \rangle + \Lambda_{lk} \langle \psi_k | \delta\psi_l \rangle] &= \sum_{k,l=1}^{N} \Lambda_{lk} \langle \delta\psi_k | \psi_l \rangle + \sum_{k,l=1}^{N} \Lambda_{kl}^* \langle \delta\psi_l | \psi_k \rangle^* \\
&= \sum_{k,l=1}^{N} \Lambda_{lk} \langle \delta\psi_k | \psi_l \rangle + \sum_{k,l=1}^{N} \Lambda_{lk}^* \langle \delta\psi_k | \psi_l \rangle^* \\
&= \sum_{k,l=1}^{N} \Lambda_{lk} \langle \delta\psi_k | \psi_l \rangle + \text{c.c.}
\end{aligned} \tag{3.15}$$

Putting it all together, the variation of $\mathcal{L}$ is now

$$\begin{aligned}
\delta\mathcal{L} &= \sum_{k=1}^{N} \langle \delta\psi_k | \Big[(h + \mathcal{J} - \mathcal{K}) | \psi_k \rangle - \sum_{l=1}^{N} \Lambda_{lk} | \psi_l \rangle \Big] + \text{c.c.} \\
&= 0.
\end{aligned} \tag{3.16}$$

By defining the Fock operator

$$\mathcal{F} = h + \mathcal{J} - \mathcal{K} \tag{3.17}$$

the above equation can be written even more compactly as

$$\delta\mathcal{L} = \sum_{k=1}^{N} \langle \delta\psi_k | \left[\mathcal{F} | \psi_k \rangle - \sum_{l=1}^{N} \Lambda_{lk} | \psi_l \rangle \right] + \text{c.c.} \tag{3.18}$$
$$= 0.$$

Since the variations of the spin orbitals can be chosen freely, each term in the square brackets must be equal to zero, which implies that

$$\mathcal{F}\psi_k = \sum_{l=1}^{N} \Lambda_{lk}\psi_l. \tag{3.19}$$

This equation[1] is not on the same form as the one introduced at the beginning of the chapter. This reason is as follows. Given a solution $\{\psi_k\}$ of the equation above, it is possible to obtain a new set of spin orbitals $\{\psi'_k\}$ via a unitary transformation

$$\psi'_k = \sum_{l} \psi_l \, U_{lk} \tag{3.20}$$

which keeps the expectation value $E_0 = \langle \Psi'_0 | H | \Psi'_0 \rangle$ as well as the form of the Fock operator unchanged, see Szabo and Ostlund [3]. Thus there is some flexibility in the choice of spin orbitals. One particular choice of spin orbitals are the eigenfunctions of the Fock operator

$$\mathcal{F}\psi_k = \varepsilon_k \psi_k, \tag{3.21}$$

which are guaranteed to exist since $\mathcal{F}$ is Hermitian. These particular spin orbitals are solutions of equation (3.19) for the specific case where $\Lambda_{lk} = \varepsilon_k \delta_{lk}$. Equation (3.21) is called the canonical Hartree-Fock equation.

If we are studying a molecular system, that is, if the system has more than a single nucleus, the eigenfunctions of the Hartree-Fock equations are called *molecular orbitals* (MOs). The word molecular is used to emphasise that the orbitals are characterisitic of the molecular system. It is important to distinguish between these and the familiar atomic orbitals because they are usually very different. This means that for molecular systems it is no longer helpful to think of the electrons as occupying atomic orbitals; the atomic orbitals are solutions of the Hartree-Fock equations for *isolated atoms*, but the molecule is an entirely different system with often entirely different solutions.

When the Slater determinant $|\Psi_0\rangle$ is composed of the N lowest eigenfunctions of the Hartree-Fock equations we will call it the Hartree-Fock determinant, and we will refer to E_0 as the Hartree-Fock energy. This will be the case for the remainder of the thesis unless stated otherwise.

---

[1] We are actually talking about a set of N equations for all the spin orbitals $\{\psi_k\}_{k=1}^{N}$, but since we observe that they are all equal, we may refer to *the equation*.

The Hartree-Fock energy can be written in terms of the operators $\mathcal{J}$ and $\mathcal{K}$ as

$$E_0 = \sum_{k=1}^{N} \langle \psi_k | h + \frac{1}{2}(\mathcal{J} - \mathcal{K}) | \psi_k \rangle, \tag{3.22}$$

which shows that the eigenvalues of the Hartree-Fock equations (3.21) do not add up to the ground state energy; the term $(\mathcal{J} - \mathcal{K})$ in the Fock operator is a factor of two too large. However, the energy can be calculated via the eigenvalues in the following two equivalent ways:

$$\begin{aligned} E_0 &= \frac{1}{2} \sum_{k=1}^{N} [\varepsilon_k + \langle \psi_k | h | \psi_k \rangle] \\ &= \sum_{k=1}^{N} [\varepsilon_k - \frac{1}{2} \langle \psi_k | \mathcal{J} - \mathcal{K} | \psi_k \rangle]. \end{aligned} \tag{3.23}$$

3.2 Restricted and unrestricted determinants
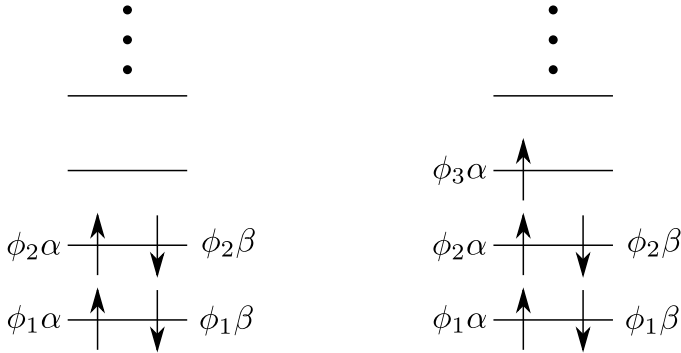
In (3.21) the Hartree-Fock equations are written on their most general form. The unknowns are the eigenvalues ε_k and the spin orbitals ψ_k. However, before solving the equations, it is useful to rewrite them in terms of spatial orbitals ϕ_k instead of spin orbtitals ψ_k. This is done by integrating out the spin part, as will be shown in the next section. But first we must decide how to construct the spin orbitals from the spatial orbitals. There are two ways to do this: One can either form so-called restricted spin orbitals or unrestricted spin orbitals. The two approaches will lead to two different Hartree-Fock methods, namely the restricted Hartree-Fock method (RHF) and the unrestricted Hartree-Fock method (UHF), respectively.

3.2.1 Restricted determinants

Recall from equation (2.8) that a spin orbital ψ_k is a spatial orbital ϕ_k multiplied with a spin function which is either spin up, α, or spin down, β. This means that we can create spin orbitals in the following way

$$\psi_k(\mathbf{x}) = \begin{cases} \phi_l(\mathbf{r})\alpha(s) \\ \quad \text{or} \\ \phi_l(\mathbf{r})\beta(s). \end{cases} \tag{3.24}$$

Spin orbitals on this form are called restricted spin orbitals, and the Slater determinants they form are called restricted determinants. In such determinants, a spatial orbital is either occupied by a single electron or two electrons, see figure 3.1. A determinant which has every spatial orbital doubly occupied, is called a closed shell determinant (left figure), whereas a determinant that has one or more partially filled spatial orbitals, is called an open shell determinant (right figure). If the system has an odd number of electrons, the determinant will always be open shell. However, an even number of electrons does not imply that the determinant is closed shell; if degeneracies apart from that due to spin are present, it can still be open shell.

Figure 3.1: Illustration of the restricted determinant comprised of spin orbitals on the form (3.24). The left and right figures illustrate closed and open shell determinants, respectively.

Throughout this thesis we will limit the use of restricted determinants (and restricted Hartree-Fock) to closed shell systems. This means that the spin orbitals are given by

$$\{\psi_{2k-1}(\mathbf{x}),\, \psi_{2k}(\mathbf{x})\} = \{\phi_k(\mathbf{r})\alpha(s),\, \phi_k(\mathbf{r})\beta(s)\}, \qquad k = 1, \ldots, N/2, \tag{3.25}$$

where N is the number of electrons.
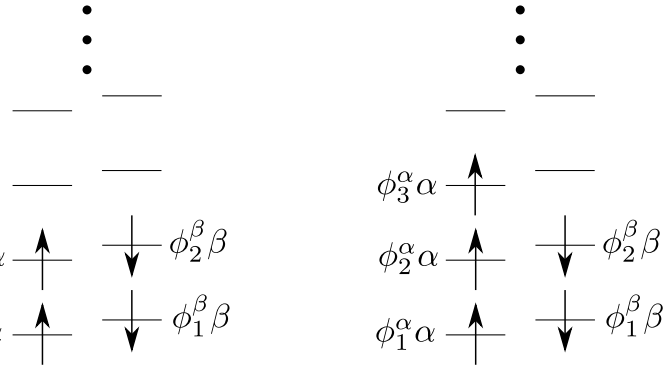
3.2.2   Unrestricted determinants

In equation (3.24) the spin-up electrons are described by the same set of spatial orbitals as the spin-down electrons. For closed shell systems this is often a good assumption. However, consider the open shell determinant illustrated to the right of figure 3.1. The electron occupying the spin orbital $\phi_3\alpha$ will have an exchange interaction with the other spin-up electrons, but not with the spin-down electrons. Hence, it could be energetically favourable to let the spin-up levels shift with respect to the spin-down levels, as shown in figure 3.2. This can be accomplished by letting the spin-up and spin-down electrons be described by different sets of spatial orbitals. Spin orbitals formed in this way, are called unrestricted spin orbitals, and the Slater determinants they form are called unrestricted determinants.

$$\psi_k(\mathbf{x}) = \begin{cases} \phi_l^\alpha(\mathbf{r})\alpha(s) \\ \quad \text{or} \\ \phi_l^\beta(\mathbf{r})\beta(s). \end{cases} \tag{3.26}$$

3.3   Slater determinants and the spin operators

In this section we define the total spin operator for a system of N particles and discuss how it acts on the restricted and unrestricted determinants. The reader is referred to the texts by Griffiths [13] and Shankar [14] for introductory treatments of spin.

Figure 3.2: Illustration of the unrestricted determinant comprised of spin orbitals on the form (3.26). The left and right figures illustrate closed and open shell determinants, respectively.

3.3.1   Single-particle spin operators

The spin operator for a single particle is given by

$$\mathbf{s} = s_x \mathbf{i} + s_y \mathbf{j} + s_z \mathbf{k}, \tag{3.27}$$

where s_x, s_y and s_z are the operators for the spin components along the coordinate axes. The latter satisfy the commutation relations

$$[s_x,\, s_y] = i s_z, \qquad [s_y,\, s_z] = i s_x, \qquad [s_z,\, s_x] = i s_y. \tag{3.28}$$

The squared magnitude of the spin operator is a scalar operator

$$\mathbf{s}^2 = s_x^2 + s_y^2 + s_z^2. \tag{3.29}$$

It commutes with all of the component operators, and it is therefore possible to find a common set of eigenstates for $\mathbf{s}^2$ and *one* of the operators s_x, s_y or s_z. The standard choice in the literature is s_z. A particle with spin s has eigenvalues $s(s+1)$ and m_s

$$\begin{aligned} s^2|s, m_s\rangle &= s(s+1)|s, m_s\rangle, \\ s_z|s, m_s\rangle &= m_s|s, m_s\rangle, \end{aligned} \tag{3.30}$$

where m_s can take the values $\{-s,\, -s + 1, \ldots, s - 1,\, s\}$. Electrons have spin $1/2$, and the Hilbert space describing the spin of electrons is therefore spanned by the two states $|1/2, 1/2\rangle$ and $|1/2, -1/2\rangle$, which we until now have simply called $|\alpha\rangle$ and $|\beta\rangle$ for convenience.

3.3.2   Many-particle spin operators

Analogously, the total spin operator for a system of N particles is given by

$$\mathbf{S} = \sum_{i=1}^{N} \mathbf{s}(i), \tag{3.31}$$

where $\mathbf{s}(i)$ is the spin operator of particle i. Also, the squared magnitude of the total spin operator is given by

$$\mathbf{S}^2 = S_x^2 + S_y^2 + S_z^2, \tag{3.32}$$

where

$$S_I = \sum_{i=1}^{N} s_I(i), \qquad I \in \{x,\, y,\, z\}. \tag{3.33}$$

Since the Hamiltonian does not depend on any of the spin coordinates, it commutes with $\mathbf{S}^2$ as well as S_z

$$[H, \mathbf{S}^2] = [H, S_z] = 0. \tag{3.34}$$

This means that the exact eigenstates of the Hamiltonian $|\Phi_i\rangle$ are also eigenstates of $\mathbf{S}^2$ and S_z [3]

$$\mathbf{S}^2 |\Phi_i\rangle = S(S+1)|\Phi_i\rangle, \tag{3.35}$$

$$S_z |\Phi_i\rangle = M_S |\Phi_i\rangle, \tag{3.36}$$

where S and M_S are the quantum numbers for the total spin and its projection along the z-axis, respectively. A natural question to ask at this point is whether or not the restricted and unrestricted determinants are eigenstates of $\mathbf{S}^2$ and S_z. The answer to this question is as follows:

1. Both restricted and unrestricted determinants are eigenstates of S_z.

2. The restricted closed shell determinant is an eigenstate of $\mathbf{S}^2$ with eigenvalue 0, making it a pure singlet state.

3. The unrestricted determinant is generally not an eigenstate of $\mathbf{S}^2$.

A consequence of point three is that unrestricted determinants can often have a total spin which is larger than the exact value. This is often referred to as spin contamination of the unrestricted determinant. The reader is referred to appendix A for a further discussion of this topic.

3.4   Restricted Hartree-Fock (RHF)

The most general form of the Hartree-Fock equations is given in (3.21), where the Fock operator $\mathcal{F}$ is given by (3.17) and (3.9) - (3.10). We will now derive the equations which result from the restricted assumption in (3.24). Without loss of generality, we may assume that the spin orbital on which the Fock operator acts is spin up:

$$\mathcal{F}(\mathbf{x})\phi_k(\mathbf{r})\alpha(s) = \varepsilon_k \phi_k(\mathbf{r})\alpha(s). \tag{3.37}$$

Writing out the Fock operator explicitly:

$$
\begin{aligned}
\mathcal{F}(\mathbf{x})\phi_k(\mathbf{r})\alpha(s) = {} & h(\mathbf{r})\,\phi_k(\mathbf{r})\alpha(s) \\
& + \Big[\sum_{l=1}^{N} \int d\mathbf{x}'\psi_l^*(\mathbf{x}')g(\mathbf{r},\mathbf{r}')\psi_l(\mathbf{x}')\Big]\phi_k(\mathbf{r})\alpha(s) \\
& - \Big[\sum_{l=1}^{N} \int d\mathbf{x}'\psi_l^*(\mathbf{x}')g(\mathbf{r},\mathbf{r}')\phi_k(\mathbf{r}')\alpha(s)\Big]\psi_l(\mathbf{x}) \\
= {} & \varepsilon_k\phi_k(\mathbf{r})\alpha(s).
\end{aligned}
\tag{3.38}
$$

Our goal is to integrate out the spin of this equation. To do this, we must also express the spin orbitals in the sums in terms of spatial orbitals. We will assume that N is an even number of electrons and that we are dealing with a closed shell determinant. This means that both sums, which run from 0 to N, can be split into two sums which run from 0 to $N/2$:

$$
\begin{aligned}
\mathcal{F}(\mathbf{x})\phi_k(\mathbf{r})\alpha(s) = {} & h(\mathbf{r})\,\phi_k(\mathbf{r})\alpha(s) \\
& + \Big[\sum_{l=1}^{N/2} \int d\mathbf{x}'\phi_l^*(\mathbf{r}')\alpha^*(s')g(\mathbf{r},\mathbf{r}')\phi_l(\mathbf{r}')\alpha(s')\Big]\phi_k(\mathbf{r})\alpha(s) \\
& + \Big[\sum_{l=1}^{N/2} \int d\mathbf{x}'\phi_l^*(\mathbf{r}')\beta^*(s')g(\mathbf{r},\mathbf{r}')\phi_l(\mathbf{r}')\beta(s')\Big]\phi_k(\mathbf{r})\alpha(s) \\
& - \Big[\sum_{l=1}^{N/2} \int d\mathbf{x}'\phi_l^*(\mathbf{r}')\alpha^*(s')g(\mathbf{r},\mathbf{r}')\phi_k(\mathbf{r}')\alpha(s')\Big]\phi_l(\mathbf{r})\alpha(s) \\
& - \Big[\sum_{l=1}^{N/2} \int d\mathbf{x}'\phi_l^*(\mathbf{r}')\beta^*(s')g(\mathbf{r},\mathbf{r}')\phi_k(\mathbf{r}')\alpha(s')\Big]\phi_l(\mathbf{r})\beta(s) \\
= {} & \varepsilon_k\phi_k(\mathbf{r})\alpha(s).
\end{aligned}
\tag{3.39}
$$

We note that the first two sums are in fact equal when the spin coordinate s' is integrated out. Furthermore, the last sum is equal to zero because the integration is over unequal spins. Thus we are left with

$$
\begin{aligned}
\mathcal{F}(\mathbf{x})\phi_k(\mathbf{r})\alpha(s) = {} & h(\mathbf{r})\,\phi_k(\mathbf{r})\alpha(s) \\
& + 2\Big[\sum_{l=1}^{N/2} \int d\mathbf{r}'\phi_l^*(\mathbf{r}')g(\mathbf{r},\mathbf{r}')\phi_l(\mathbf{r}')\Big]\phi_k(\mathbf{r})\alpha(s) \\
& - \Big[\sum_{l=1}^{N/2} \int d\mathbf{r}'\phi_l^*(\mathbf{r}')g(\mathbf{r},\mathbf{r}')\phi_k(\mathbf{r}')\Big]\phi_l(\mathbf{r})\alpha(s) \\
= {} & \varepsilon_k\phi_k(\mathbf{r})\alpha(s).
\end{aligned}
\tag{3.40}
$$

If we now multiply both sides of the equation by $\alpha^*(s)$ and integrate over the spin coordinate s we finally arrive at

$$
\begin{aligned}
\Big[\sum_{s=\uparrow\downarrow} \alpha^*(s)\mathcal{F}(\mathbf{x})\alpha(s)\Big]\phi_k(\mathbf{r}) &= h(\mathbf{r})\,\phi_k(\mathbf{r}) \\
&+ 2\Big[\sum_{l=1}^{N/2}\int d\mathbf{r}'\phi_l^*(\mathbf{r}')g(\mathbf{r},\mathbf{r}')\phi_l(\mathbf{r}')\Big]\phi_k(\mathbf{r}) \\
&- \Big[\sum_{l=1}^{N/2}\int d\mathbf{r}'\phi_l^*(\mathbf{r}')g(\mathbf{r},\mathbf{r}')\phi_k(\mathbf{r}')\Big]\phi_l(\mathbf{r}) \\
&= \varepsilon_k\phi_k(\mathbf{r}).
\end{aligned}
\tag{3.41}
$$

Defining the restricted spatial Fock operator as

$$
F(\mathbf{r}) = \sum_{s=\uparrow\downarrow}\alpha^*(s)\mathcal{F}(\mathbf{x})\alpha(s),
\tag{3.42}
$$

the equation can be written as

$$
F(\mathbf{r})\phi_k(\mathbf{r}) = \varepsilon_k\phi_k(\mathbf{r}),
\tag{3.43}
$$

where

$$
\begin{aligned}
F(\mathbf{r})\phi_k(\mathbf{r}) =&\, h(\mathbf{r})\,\phi_k(\mathbf{r}) + 2\Big[\sum_{l=1}^{N/2}\int d\mathbf{r}'\phi_l^*(\mathbf{r}')g(\mathbf{r},\mathbf{r}')\phi_l(\mathbf{r}')\Big]\phi_k(\mathbf{r}) \\
&- \Big[\sum_{l=1}^{N/2}\int d\mathbf{r}'\phi_l^*(\mathbf{r}')g(\mathbf{r},\mathbf{r}')\phi_k(\mathbf{r}')\Big]\phi_l(\mathbf{r}).
\end{aligned}
\tag{3.44}
$$

The spatial Fock operator can be written more compactly as

$$
F(\mathbf{r}) = h(\mathbf{r}) + 2J(\mathbf{r}) - K(\mathbf{r}),
\tag{3.45}
$$

where

$$
J(\mathbf{r})\phi_k(\mathbf{r}) = \sum_{l=1}^{N/2}\int d\mathbf{r}'\phi_l^*(\mathbf{r}')g(\mathbf{r},\mathbf{r}')\phi_l(\mathbf{r}')\Big]\phi_k(\mathbf{r}),
\tag{3.46}
$$

$$
K(\mathbf{r})\phi_k(\mathbf{r}) = \sum_{l=1}^{N/2}\int d\mathbf{r}'\phi_l^*(\mathbf{r}')g(\mathbf{r},\mathbf{r}')\phi_k(\mathbf{r}')\Big]\phi_l(\mathbf{r}).
\tag{3.47}
$$

Note the factor 2 in front of the direct term, or more to the point, the absence of the factor 2 in front of the exchange term. This is due to the fact that the exchange interaction is only present between electrons of equal spins.

To find the energy, consider the first line of equation (3.23):

$$\begin{aligned}
E_0 &= \frac{1}{2}\sum_{k=1}^{N}[\varepsilon_k + \langle\psi_k|h|\psi_k\rangle] \\
&= \frac{1}{2}\sum_{k=1}^{N}\langle\psi_k|(\mathcal{F}+h)|\psi_k\rangle.
\end{aligned} \tag{3.48}$$

If, as we did above, insert the assumption (3.24) and split the sum in two sums, one with spin up and one with spin down, we get

$$E_0 = \sum_{k=1}^{N/2}\langle\phi_k|(F+h)|\phi_k\rangle. \tag{3.49}$$

3.4.1   Introducing a basis

We have now eliminated the spin from the general Hartree-Fock equations (3.21) and arrived at equation (3.43), which represents a set of integro-differential equations for the spatial orbitals. There is presently no feasible way to solve these as they stand. However, by expressing the orbitals in terms of some known basis

$$\phi_k(\mathbf{r}) = \sum_{\mu=1}^{M}C_{\mu k}\chi_\mu(\mathbf{r}), \tag{3.50}$$

where M is the number of basis functions, the equations can be converted to a set of algebraic equations. Inserting this expansion into equation (3.43) gives

$$\sum_{\nu=1}^{M}F(\mathbf{r})\chi_\nu(\mathbf{r})C_{\nu k} = \varepsilon_k\sum_{\nu=1}^{M}C_{\nu k}\chi_\nu(\mathbf{r}). \tag{3.51}$$

If we now multiply by $\chi_\mu^*(\mathbf{r})$ and integrate with respect to $\mathbf{r}$, we get the so-called *Roothaan equations* [15]

$$\sum_{\nu=1}^{M}F_{\mu\nu}C_{\nu k} = \varepsilon_k\sum_{\nu=1}^{M}S_{\mu\nu}C_{\nu k}, \tag{3.52}$$

or in matrix notation

$$\mathbf{F}\mathbf{C}_k = \varepsilon_k\mathbf{S}\mathbf{C}_k, \tag{3.53}$$

where

$$F_{\mu\nu} = \int d\mathbf{r}\chi_\mu^*(\mathbf{r})F(\mathbf{r})\chi_\nu(\mathbf{r}) \tag{3.54}$$

is the Fock matrix and

$$S_{\mu\nu} = \int d\mathbf{r}\chi_\mu^*(\mathbf{r})\chi_\nu(\mathbf{r}) \tag{3.55}$$

is the overlap matrix. If the basis is orthonormal, the overlap matrix is the identity matrix. However, in molecular calculations Gaussian functions are most often used,

and these are not orthogonal. In section 3.6 we show how equation (3.53) can be transformed to a regular eigenvalue problem

$$\mathbf{F}'\mathbf{C}'_{\mathbf{k}} = \varepsilon_k \mathbf{C}'_k. \tag{3.56}$$

Let us take a closer look at the Fock matrix:

$$
\begin{aligned}
F_{\mu\nu} &= \int d\mathbf{r}\chi_\mu^*(\mathbf{r})F(\mathbf{r})\chi_\nu(\mathbf{r})\\
&= \int d\mathbf{r}\chi_\mu^*(\mathbf{r})[h(\mathbf{r}) + 2J(\mathbf{r}) - K(\mathbf{r})]\chi_\nu(\mathbf{r})\\
&= \langle\mu|h|\nu\rangle + 2\langle\mu|J|\nu\rangle - \langle\mu|K|\nu\rangle.
\end{aligned}
\tag{3.57}
$$

To get the final expression for the matrix, we insert the expansion (3.50) into the operators $J(\mathbf{r})$ and $K(\mathbf{r})$. For $J(\mathbf{r})$ this gives

$$
\begin{aligned}
J(\mathbf{r})\chi_\nu(\mathbf{r}) &= \Big[\sum_{k=1}^{N/2}\int d\mathbf{r}'\phi_k^*(\mathbf{r}')g(\mathbf{r},\mathbf{r}')\phi_k(\mathbf{r}')\Big]\chi_\nu(\mathbf{r})\\
&= \Big[\sum_{k=1}^{N/2}\sum_{\sigma,\lambda=1}^{M}\int d\mathbf{r}'\chi_\sigma^*(\mathbf{r}')g(\mathbf{r},\mathbf{r}')\chi_\lambda(\mathbf{r}')\Big]C_{\sigma k}^*C_{\lambda k}\chi_\nu(\mathbf{r}),
\end{aligned}
\tag{3.58}
$$

so that

$$\langle\mu|J|\nu\rangle = \sum_{k=1}^{N/2}\sum_{\sigma,\lambda=1}^{M}\langle\mu\sigma|g|\nu\lambda\rangle C_{\sigma k}^*C_{\lambda k}, \tag{3.59}$$

where the matrix element $\langle\mu\sigma|g|\nu\lambda\rangle$ is defined in equation (2.47). The expression for $\langle\mu|K|\nu\rangle$ is similar, except that the indices ν and λ switch places in the integral:

$$\langle\mu|K|\nu\rangle = \sum_{k=1}^{N/2}\sum_{\sigma,\lambda=1}^{M}\langle\mu\sigma|g|\lambda\nu\rangle C_{\sigma k}^*C_{\lambda k}. \tag{3.60}$$

Hence, the Fock matrix is given explicitly in terms of the basis functions by

$$F_{\mu\nu} = \langle\mu|h|\nu\rangle + \sum_{k=1}^{N/2}\sum_{\sigma,\lambda=1}^{M}[2\langle\mu\sigma|g|\nu\lambda\rangle - \langle\mu\sigma|g|\lambda\nu\rangle]C_{\sigma k}^*C_{\lambda k}. \tag{3.61}$$

It is useful to define the so-called density matrix

$$P_{\lambda\sigma} = 2\sum_{k=1}^{N/2}C_{\lambda k}C_{\sigma k}^*, \tag{3.62}$$

which allows us to write the Fock matrix more compactly as

$$F_{\mu\nu} = \langle\mu|h|\nu\rangle + \frac{1}{2}\sum_{\sigma,\lambda=1}^{M}P_{\lambda\sigma}[2\langle\mu\sigma|g|\nu\lambda\rangle - \langle\mu\sigma|g|\lambda\nu\rangle]. \tag{3.63}$$

The energy is found by expanding equation (3.49) in the known basis:

$$E_0 = \frac{1}{2}\sum_{\mu,\nu=1}^{M}P_{\nu\mu}[\langle\mu|h|\nu\rangle + F_{\mu\nu}]. \tag{3.64}$$

3.5   Unrestricted Hartree-Fock (UHF)

We now derive the unrestricted Hartree-Fock equations which result from the assumption (3.26). The Hartree-Fock equations (3.21) are now split into two sets of equations

$$\mathcal{F}^\alpha(\mathbf{x})\phi_k^\alpha(\mathbf{r})\alpha(s) = \varepsilon_k^\alpha\phi_k^\alpha(\mathbf{r})\alpha(s), \qquad k = 1, 2, \ldots, N_\alpha, \tag{3.65}$$

$$\mathcal{F}^\beta(\mathbf{x})\phi_k^\beta(\mathbf{r})\beta(s) = \varepsilon_k^\beta\phi_k^\beta(\mathbf{r})\beta(s), \qquad k = 1, 2, \ldots, N_\beta, \tag{3.66}$$

where N^α and N^β are the number of electrons with spin up and spin down, respectively. Again, we want to take out the spin part of the equations. We can insert the unrestricted spin orbitals (3.26) and do the calculations explicitly in the same way as we did for the restricted case. However, using the insight gained during our previous calculation, we can come up with the answer directly. Consider for example the operator $\mathcal{F}^\alpha(\mathbf{x})$. It contains a kinetic term and the potential due to the atomic nuclei. Furthermore, it contains a direct interaction term due to the mean field set up by all electrons, both spin up and spin down. Finally it contains an exchange term due to the mean field set up by the electrons *with spin up only*. Thus we can conclude that the equations for the spatial orbitals ϕ_k^α are given by

$$F^\alpha(\mathbf{r})\phi_k^\alpha(\mathbf{r}) = \varepsilon_k^\alpha\phi_k^\alpha(\mathbf{r}), \tag{3.67}$$

where the unrestricted spin up Fock operator is defined as

$$F^\alpha(\mathbf{r}) = h(\mathbf{r}) + [J^\alpha(\mathbf{r}) - K^\alpha(\mathbf{r})] + J^\beta(\mathbf{r}), \tag{3.68}$$

with

$$J^\alpha(\mathbf{r})\phi_k^\alpha(\mathbf{r}) = \sum_{l=1}^{N^\alpha}\left[\int d\mathbf{r}'\phi_l^\alpha(\mathbf{r}')g(\mathbf{r},\mathbf{r}')\phi_l^\alpha(\mathbf{r}')\right]\phi_k^\alpha(\mathbf{r}), \tag{3.69}$$

$$J^\beta(\mathbf{r})\phi_k^\alpha(\mathbf{r}) = \sum_{l=1}^{N^\beta}\left[\int d\mathbf{r}'\phi_l^\beta(\mathbf{r}')g(\mathbf{r},\mathbf{r}')\phi_l^\beta(\mathbf{r}')\right]\phi_k^\alpha(\mathbf{r}), \tag{3.70}$$

$$K^\alpha(\mathbf{r})\phi_k^\alpha(\mathbf{r}) = \sum_{l=1}^{N^\alpha}\left[\int d\mathbf{r}'\phi_l^\alpha(\mathbf{r}')g(\mathbf{r},\mathbf{r}')\phi_k^\alpha(\mathbf{r}')\right]\phi_l^\alpha(\mathbf{r}). \tag{3.71}$$

The equations for the spatial orbitals ϕ_k^β are the same, except that the indices α and β switch places.

3.5.1   Introducing a basis

To solve the unrestricted Hartree-Fock equations we expand the spatial orbitals in terms of a known basis

$$\phi_k^\alpha(\mathbf{r}) = \sum_{\mu=1}^{M} C_{\mu k}^\alpha \chi_\mu(\mathbf{r}), \tag{3.72}$$

$$\phi_k^\beta(\mathbf{r}) = \sum_{\mu=1}^{M} C_{\mu k}^\beta \chi_\mu(\mathbf{r}), \tag{3.73}$$

just as we did in the restricted case. Inserting the expansion (3.72) into equation (3.67) gives

$$\sum_{\nu=1}^{M} F^{\alpha}(\mathbf{r})\chi_{\nu}(\mathbf{r})C_{\nu k}^{\alpha} = \varepsilon_{k}^{\alpha} \sum_{\nu=1}^{M} C_{\nu k}^{\alpha}\chi_{\nu}(\mathbf{r}). \tag{3.74}$$

If we multiply this equation by $\chi_{\mu}^{*}(\mathbf{r})$ and integrate over $\mathbf{r}$, we get

$$\sum_{\nu=1}^{M} F_{\mu\nu}^{\alpha}C_{\nu k}^{\alpha} = \varepsilon_{k}^{\alpha} \sum_{\nu=1}^{M} S_{\mu\nu}C_{\nu k}^{\alpha}, \tag{3.75}$$

where $S_{\mu\nu}$ is the overlap matrix and $F_{\mu\nu}^{\alpha}$ is the matrix representation of the unrestricted spatial Fock operator

$$F_{\mu\nu}^{\alpha} = \int d\mathbf{r}\chi_{\mu}^{*}(\mathbf{r})F^{\alpha}(\mathbf{r})\chi_{\nu}(\mathbf{r}). \tag{3.76}$$

The corresponding equations for the spin down particles are derived in exactly the same way, of course. In total we have the two sets of equations

$$\mathbf{F}^{\alpha}\mathbf{C}_{k}^{\alpha} = \varepsilon_{k}^{\alpha}\mathbf{S}\mathbf{C}_{k}^{\alpha}, \tag{3.77}$$

$$\mathbf{F}^{\beta}\mathbf{C}_{k}^{\beta} = \varepsilon_{k}^{\beta}\mathbf{S}\mathbf{C}_{k}^{\beta}, \tag{3.78}$$

called the *Pople-Nesbet equations* [16], which are the unrestricted generalisation of the Roothaan equations derived in the previous section. They are nonlinear and coupled since the matrices $\mathbf{F}^{\alpha}$ and $\mathbf{F}^{\beta}$ are functions of both $\{\mathbf{C}_{k}^{\alpha}\}$ and $\{\mathbf{C}_{k}^{\beta}\}$.

The final expression for the Fock matrix $\mathbf{F}^{\alpha}$ is obtained by inserting the expansion (3.72) into equation (3.76). Recalling that the Fock operator $F^{\alpha}(\mathbf{r})$ is given by (3.68) this leads to

$$F_{\mu\nu}^{\alpha} = \langle\mu|h|\nu\rangle + \sum_{k=1}^{N^{\alpha}}\sum_{\sigma,\lambda=1}^{M}\langle\mu\sigma||\nu\lambda\rangle(C_{\sigma k}^{\alpha})^{*}C_{\lambda k}^{\alpha} + \sum_{k=1}^{N^{\beta}}\sum_{\sigma,\lambda=1}^{M}\langle\mu\sigma|g|\nu\lambda\rangle(C_{\sigma k}^{\beta})^{*}C_{\lambda k}^{\beta}, \tag{3.79}$$

and similarly we find

$$F_{\mu\nu}^{\beta} = \langle\mu|h|\nu\rangle + \sum_{k=1}^{N^{\beta}}\sum_{\sigma,\lambda=1}^{M}\langle\mu\sigma||\nu\lambda\rangle(C_{\sigma k}^{\beta})^{*}C_{\lambda k}^{\beta} + \sum_{k=1}^{N^{\alpha}}\sum_{\sigma,\lambda=1}^{M}\langle\mu\sigma|g|\nu\lambda\rangle(C_{\sigma k}^{\alpha})^{*}C_{\lambda k}^{\alpha}, \tag{3.80}$$

where $\langle\mu\sigma|g|\nu\lambda\rangle$ and $\langle\mu\sigma||\nu\lambda\rangle$ are defined in equations (2.47) and (2.58), respectively. If we introduce the density matrices

$$P_{\lambda\sigma}^{\alpha} = \sum_{k=1}^{N^{\alpha}} C_{\lambda k}^{\alpha}(C_{\sigma k}^{\alpha})^{*}, \tag{3.81}$$

$$P_{\lambda\sigma}^{\beta} = \sum_{k=1}^{N^{\beta}} C_{\lambda k}^{\beta}(C_{\sigma k}^{\beta})^{*}, \tag{3.82}$$

$$P_{\lambda\sigma}^{T} = P_{\lambda\sigma}^{\alpha} + P_{\lambda\sigma}^{\beta}, \tag{3.83}$$

the Fock matrices can be written more compactly as

$$F_{\mu\nu}^{\alpha} = \langle\mu|h|\nu\rangle + \sum_{\sigma,\lambda=1}^{M} \left[\langle\mu\sigma||\nu\lambda\rangle P_{\lambda\sigma}^{\alpha} + \langle\mu\sigma|g|\nu\lambda\rangle P_{\lambda\sigma}^{\beta} \right], \tag{3.84}$$

and

$$F_{\mu\nu}^{\beta} = \langle\mu|h|\nu\rangle + \sum_{\sigma,\lambda=1}^{M} \left[\langle\mu\sigma||\nu\lambda\rangle P_{\lambda\sigma}^{\beta} + \langle\mu\sigma|g|\nu\lambda\rangle P_{\lambda\sigma}^{\alpha} \right]. \tag{3.85}$$

The energy can be found from the expectation value of these matrices, keeping in mind that the double counting of the interaction terms must be taken into account. The expression is

$$E_0 = \frac{1}{2}\sum_{k=1}^{N^{\alpha}}\sum_{\mu,\nu=1}^{M} \left[\langle\mu|h|\nu\rangle + F_{\mu\nu}^{\alpha} \right](C_{\mu k}^{\alpha})^* C_{\nu k}^{\alpha} + \frac{1}{2}\sum_{k=1}^{N^{\beta}}\sum_{\mu,\nu=1}^{M} \left[\langle\mu|h|\nu\rangle + F_{\mu\nu}^{\beta} \right](C_{\mu k}^{\beta})^* C_{\nu k}^{\beta}, \tag{3.86}$$

or in terms of the density matrices

$$E_0 = \frac{1}{2}\sum_{\mu,\nu=1}^{M} \left[P_{\nu\mu}^{T}\langle\mu|h|\nu\rangle + P_{\nu\mu}^{\alpha}F_{\mu\nu}^{\alpha} + P_{\nu\mu}^{\beta}F_{\mu\nu}^{\beta} \right]. \tag{3.87}$$

3.6   Solving the generalised eigenvalue problem

In this section we show how the generalised eigenvalue problem

$$\mathbf{F}\mathbf{C}_k = \varepsilon_k \mathbf{S}\mathbf{C}_k, \tag{3.88}$$

can be transformed to the regular eigenvalue problem

$$\mathbf{F}'\mathbf{C}_k' = \varepsilon_k \mathbf{C}_k'. \tag{3.89}$$

We can achieve this if there exists a matrix $\mathbf{X}$ such that

$$\mathbf{X}^{\dagger}\mathbf{S}\mathbf{X} = \mathbf{I}, \tag{3.90}$$

because, if we then let $\mathbf{C_k} = \mathbf{X}\mathbf{C_k'}$, we get

$$\begin{aligned} \mathbf{F}\mathbf{C}_k &= \varepsilon_k \mathbf{S}\mathbf{C}_k \\ \mathbf{F}\mathbf{X}\mathbf{C}_k' &= \varepsilon_k \mathbf{S}\mathbf{X}\mathbf{C}_k' \\ \mathbf{X}^{\dagger}\mathbf{F}\mathbf{X}\mathbf{C}_k' &= \varepsilon_k \mathbf{X}^{\dagger}\mathbf{S}\mathbf{X}\mathbf{C}_k' \\ \mathbf{F}'\mathbf{C}_k' &= \varepsilon_k \mathbf{C}_k', \end{aligned} \tag{3.91}$$

where

$$\mathbf{F}' = \mathbf{X}^{\dagger}\mathbf{F}\mathbf{X}. \tag{3.92}$$

It only remains to show that the matrix $\mathbf{X}$ does indeed exist and how to construct it. First note that the overlap matrix $\mathbf{S}$ is Hermitian:

$$
\begin{aligned}
S_{\mu\nu} &= \int d\mathbf{r}\,\chi_\mu^*(\mathbf{r})\chi_\nu(\mathbf{r}) \\
&= \int d\mathbf{r}\,\chi_\nu(\mathbf{r})\chi_\mu^*(\mathbf{r}) \\
&= S_{\nu\mu}^*.
\end{aligned}
\tag{3.93}
$$

This means that there exists a unitary matrix $\mathbf{U}$ such that

$$
\mathbf{U}^\dagger \mathbf{S} \mathbf{U} = \mathbf{s},
\tag{3.94}
$$

where $\mathbf{s} = \mathrm{diag}(s_1, s_2, \ldots, s_M)$ is a diagonal matrix containing the eigenvalues of $\mathbf{S}$, which are all real, and the columns of $\mathbf{U}$ are the eigenvectors of $\mathbf{S}$. Furthermore, the eigenvalues $\{s_i\}$ are positive. To see this, consider the expansion of some function $f(\mathbf{r})$, not identically equal to zero, in terms of the basis functions $\chi_\mu(\mathbf{r})$:

$$
f(\mathbf{r}) = \sum_\mu A_\mu \chi_\mu(\mathbf{r}).
\tag{3.95}
$$

No matter how the coefficients are chosen, the norm of $f(\mathbf{r})$ will be positive. In particular, if we choose $\mathbf{A} = [A_\mu]$ to be equal to the i'th eigenvector of $\mathbf{S}$, we get

$$
\begin{aligned}
0 < \langle f | f \rangle &= \sum_{\mu\nu} A_\mu^* S_{\mu\nu} A_\nu = \mathbf{A}^\dagger \mathbf{S} \mathbf{A} \\
&= s_i \mathbf{A}^\dagger \mathbf{A} = s_i \|\mathbf{A}\|^2.
\end{aligned}
\tag{3.96}
$$

Now, since all eigenvalues are positive, one can define the matrix

$$
\mathbf{s}^{-1/2} =
\begin{bmatrix}
s_1^{-1/2} & & & \\
& s_2^{-1/2} & & \\
& & \ddots & \\
& & & s_M^{-1/2}
\end{bmatrix}.
\tag{3.97}
$$

Multiplying equation (3.94) from the left and right by $\mathbf{s}^{-1/2}$ yields

$$
\begin{aligned}
\mathbf{s}^{-1/2}\mathbf{U}^\dagger \mathbf{S} \mathbf{U} \mathbf{s}^{-1/2} &= \mathbf{I} \\
(\mathbf{U}\mathbf{s}^{-1/2})^\dagger \mathbf{S} (\mathbf{U}\mathbf{s}^{-1/2}) &= \mathbf{I},
\end{aligned}
\tag{3.98}
$$

which means that

$$
\mathbf{X} = \mathbf{U}\mathbf{s}^{-1/2}.
\tag{3.99}
$$

Chapter 4

Basis functions and integral evaluation

In the previous chapter the general Hartree-Fock equations, which is a set of integro-differential equations, were converted to a set of algebraic equations (the Roothaan equations in the restricted case and the Pople-Nesbet equations in the unrestricted case) by expanding the unknown orbitals in a known set of basis functions. The Fock operator was then reduced to a matrix, the elements of which are integrals involving the chosen basis functions.

We start this chapter by discussing two popular types of basis functions, namely the Slater-type orbtials (STOs) and the Gaussian-type orbitals (GTOs). The latter is more suited for molecular calculations and is the one we will use in this thesis. Thereafter we derive the integration scheme for the Gaussian type orbitals.

4.1   Basis functions

For a molecular system, the eigenfunctions of the Hartree-Fock equations are called *molecular orbitals* (MOs). As discussed earlier, it is important to distinguish these from the perhaps more familiar *atomic orbitals*, and it is erroneous to think that the electrons of molecular systems are occupying atomic orbitals. Consider for example the H_2-molecule. In the ground state the electrons are not occupying the $1s$-orbitals of atomic hydrogen. The molecular system is entirely different from the atomic one, with an entirely different Hamiltonian, and the eigenstates of the Hartree-Fock equations will therefore also be different.

In order to solve the Hartree-Fock equations, we need to expand the molecular orbitals in a known set of basis functions

$$\phi_k(\mathbf{r}) = \sum_{\mu=1}^{M} \chi_{\mu k}(\mathbf{r}). \tag{4.1}$$

The importance of choosing suitable basis functions can hardly be overemphasised; it completely determines the accuracy of the results as well as the computational cost of the calculations. In choosing basis functions, the following criteria should be met:

1. The functions must be physically reasonable, i.e., they should have large proba-
   bility where the electrons are likely to be and small probability elsewhere.

2. It should be possible to integrate the functions efficiently.

3. The solution of the Hartree-Fock equations must converge towards the Hartree-
   Fock limit (see chapter 5) as the number of basis functions increases.

The first point suggests that we choose atomic orbitals as basis functions, which is often
referred to as "linear combination of atomic orbitals" (LCAO). In this thesis we will
let the atomic orbitals be centered at the nuclei. However, this is not strictly required
since the atomic orbitals are merely being used as basis functions, and they are not to
be thought of as orbitals occupied by electrons. In the following two subsections, we
discuss two common types of atomic orbitals, namely the Slater type orbitals (STOs)
and Gaussian type orbitals (GTOs), respectively. Only the GTOs will be applied to
the calculations in this thesis.

4.1.1   Slater-type orbitals (STOs)

The Slater type orbitals are defined as [17]
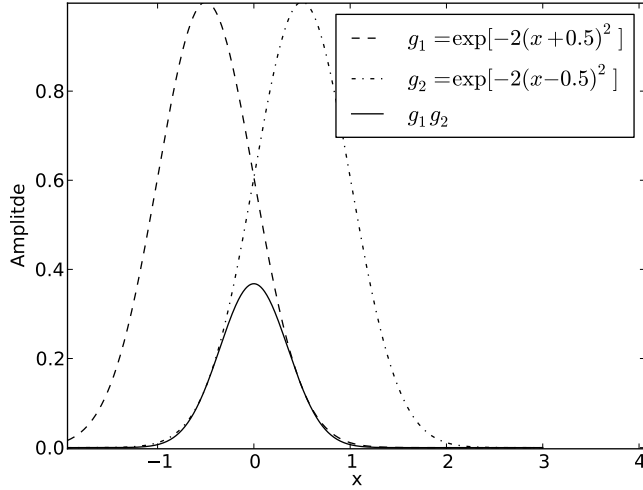
$$\chi^{STO}(r, \theta, \phi, n, l, m) = \frac{(2a)^{n+1/2}}{[(2n)!]^{1/2}} r^{n-1} \exp(-ar) Y_l^m(\theta, \phi), \qquad (4.2)$$

where n is the principal quantum number, l and m are the angular momentum quan-
tum numbers, $Y_l^m(\theta, \phi)$ are the spherical harmonics familiar from the solution of the
Schrödinger equation for the hydrogen atom, and a is an exponent which determines
the radial decay of the function. The main attractive features of the STOs are that they
have the correct exponential decay with increasing r and that the angular components
are hydrogenic. For this reason, they are often used in atomic Hartree-Fock calcula-
tions. When doing molecular calculations, however, they have the disadvantage that
the two-particle integrals $\langle \mu\sigma|g|\nu\lambda \rangle$ occuring in the Fock matrix $F_{\mu\nu}$ have no known
analytical expression. This is because integrals of products of exponentials centered on
different nuclei are difficult to handle. They can of course be calculated numerically,
but for large molecules this is very time consuming.

4.1.2   Gaussian-type orbitals (GTOs)

A clever trick which makes multiple center integrals easier to handle is to replace
the exponential term $\exp(-ar)$ with $\exp(-ar^2)$, i.e., to use Gaussian functions. This
greatly simplifies the integrals because the product of two Gaussians centered on nuclei
with positions $\mathbf{A}$ and $\mathbf{B}$ is equal to *one* Gaussian centered on some point $\mathbf{P}$ on the line
between them:

$$\exp(-a|\mathbf{r} - \mathbf{A}|^2) \cdot \exp(-b|\mathbf{r} - \mathbf{B}|^2) = K_{AB} \exp(-p|\mathbf{r} - \mathbf{P}|^2), \qquad (4.3)$$

Figure 4.1: Illustration of the Gaussian product theorem which says that the product of two Gaussians with centers at points A and B is another Gaussian with center somewhere between A and B.

where

$$K_{AB} \;=\; \exp\Big(-\frac{ab}{a+b}|\mathbf{A}-\mathbf{B}|^2\Big), \tag{4.4}$$

$$\mathbf{P} \;=\; \frac{a\mathbf{A}+b\mathbf{B}}{a+b}, \tag{4.5}$$

$$p \;=\; a+b. \tag{4.6}$$

This is the so-called *Gaussian product theorem*. It is illustrated in the one-dimensional case in figure 4.1.

The general functional form of a normalised Gaussian type orbital centered at $\mathbf{A}$ is given by [17]
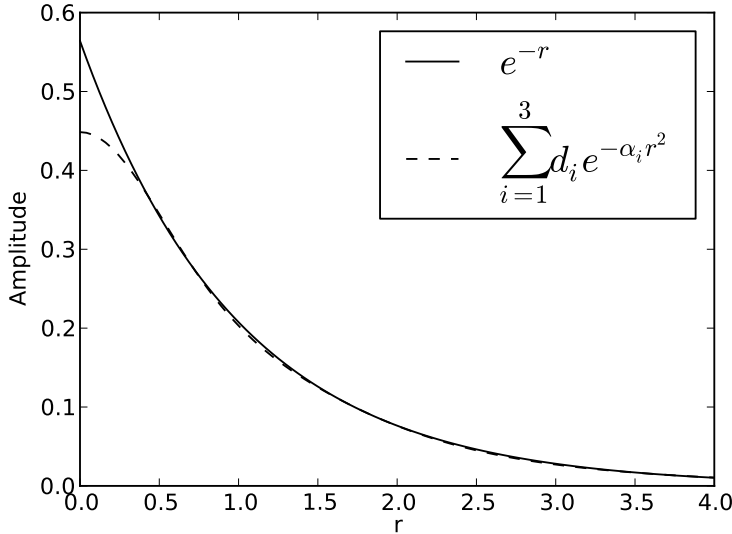
$$G_{ijk}(a,\mathbf{r}_A) = \Big(\frac{2a}{\pi}\Big)^{3/4}\Big[\frac{(8a)^{i+j+k}\,i!\,j!\,k!}{(2i)!\,(2j)!\,(2k)!}\Big]x_A^i\,y_A^j\,z_A^k\,\exp(-ar_A^2), \tag{4.7}$$

where $\mathbf{r}_A = \mathbf{r} - \mathbf{A}$ and the integers i, j, k determine the angular momentum quantum number $l = i + j + k$.

4.1.3   Contracted GTOs

The greatest drawback with Gaussians is that they do not have the proper exponential radial decay. This can be remedied by forming linear combinations of GTOs to resemble the STOs

$$\chi^{CGTO}(\mathbf{r}_A,i,j,k) = \sum_{p=1}^{L} d_p G_{ijk}(a_p,\mathbf{r}_A). \tag{4.8}$$

Figure 4.2: The whole line shows the 1s STO basis function, while the broken line shows a linear combination of three Gaussians.

These are called STO-LG basis functions, where L refers to the number of Gaussians used in the linear combination. Hehre, Stewart and Pople [18] were the first to systematically calculate optimal coefficients d_p and exponentials a_p, and today the STO-LG basis sets are available for most atoms. The individual Gaussians are called *primitive* basis functions and the linear combinations are called *contracted* basis functions, hence the label CGTO (Contracted Gaussian Type Orbital). In this thesis we will only consider CGTOs, and whenever the symbol χ appears without any label, we will always mean CGTO.

A very common choice for the STO-LG basis sets is $L = 3$. Figure 4.2 shows how the $1s$ STO for hydrogen is approximated by 3 GTOs. The exponents a_p and coefficients d_p have been set so that the contracted basis function lies as close to the STO as possible, see table 4.1. It is important to note that the parameters (a_p, d_p) are static and that the linear combination of Gaussians constitute *one single* basis function. Throughout this text the phrase "basis function" will always refer to a contracted basis function.

The STO-LG basis sets belong to the family of *minimal basis sets*. It means that there is one and only one basis function per atomic orbital. The STO-LG basis sets for the hydrogen and helium atoms, for example, contain only one basis function for the $1s$ atomic orbital. This basis function is, as explained above, composed of a linear combination of L primitives. For the atoms lithium through neon the STO-LG basis sets contain 5 basis functions; one for each of the atomic orbitals $1s$, $2s$, $2p_x$, $2p_y$ and $2p_z$.

The reader might be asking herself why the coefficients d_p in the linear combination of the STO-LGs are static. Shouldn't the accuracy of our results actually improve if

Table 4.1: Coefficients and exponents used in the STO-3G basis shown in figure 4.2.

p	1	2	3
d_p	0.1543	0.5353	0.4446
a_p	3.4252	0.6239	0.1688

we let the coefficients vary? The answer to this is yes. However, the linear system to be solved (the Hartree-Fock equations) will then be larger. Thus there is a trade off between accuracy and computational efficiency which must be considered.

However, basis sets where the STO-LG sets have been "decontracted" as described above have actually been used. They belong to the family of ζ-basis sets. The double-ζ and triple-ζ basis sets have two and three basis functions, respectively, for each atomic orbital. As an example, we could create a double-ζ basis set from the STO-3G basis set by contracting the two first primitives and leave the third as a normalised primitive. Similarly, we could counstruct a triple-ζ basis set by treating each primitive as a basis function.

Let us for a moment assume that we use a triple-ζ basis set constructed from the STO-3G to do Hartree-Fock calculations on atomic oxygen. What will the resulting orbitals look like? The lowest orbital will be very close to the definition of the $1s$ orbital of the STO-3G set. This is to be expected since the STO-3G basis functions are constructed to resemble the STO atomic orbitals.

What if we now apply the same triple-ζ basis to calculations on the CO molecule, say? In this case we would probably also find an orbital which resembles the $1s$ orbital of the STO-3G basis for oxygen. This is because it is mostly the valence electrons which contribute in the bonding between atoms, and the core electrons are more or less unaffected. Thus decontracting basis functions corresponding to the core atomic orbitals will generally not pay off, but will merely increase the computational load. Therefore, basis sets have been constructed where only the functions corresponding to the valence atomic orbitals are decontracted. These are the so-called *split-valence* basis sets. An example of a split-valence basis set is the 3-21G. The number before the hyphen (in this case 3) is the number of primitives per core atomic orbital. The fact that there are two numbers after the hyphen signifies that there are two basis functions for each valence atomic orbital. The numbers themselves (in this case 2 and 1) indicate how many primitives the first and second of these are composed of. As an example, the 3-21G basis set for the oxygen atom has one single basis function for the $1s$ orbital (since this is the core orbital), and this basis function consists of three primitives. Furthermore, it has two basis functions for the $2s$, $2p_x$, $2p_y$ and $2p_z$ atomic orbitals (since these are the valence orbitals). The first consists of two primitives, and the second consists of only one primitive. In sum the oxygen atom thus has 9 basis functions which are built up from a total of 15 primitives. Other examples of split-valence basis sets are 4-31G, 6-31G and 6-311G [17].

In many molecular calculations, the split-valence basis sets mentioned thus far do not provide enough flexibility to describe the chemistry appropriately. This is often fixed by adding functions corresponding to atomic orbitals with angular momentum

$l_{max} + 1$, where l_{max} is the highest angular momentum of the atom. Such functions are called *polarisation functions*. For example, the polarisation functions for the Oxygen atom are the *d*-functions. Asterisks (*) are added to the name of the basis set to indicate that polarisation functions are included. One asterisk (as in 6-31G*) indicates that *d*-functions are added to polarise the *p*-functions of first row atoms (Li-Ne). Two asterisks (as in 6-31G**) mean that *p*-functions are added to polarise the *s*-functions of hydrogen and helium as well.

It should be noted that the list of basis sets mentioned here is in no way exhaustive. There is a flora of basis sets out there, see for example Cramer [17] or Helgaker *et al* [19].

4.2   Integral evaluation

As discussed in the previous section, using Gaussian basis functions significantly improves the speed of the integrations which must be done when setting up the Fock matrix. This section discusses the details of how the integration is performed.

We start by summarising the most important properties of the Cartesian Gaussians. Thereafter, we change basis to the so-called Hermite Gaussians, as proposed by Živković and Maksić [20]. Then, following the work of McMurchie and Davidson [21], we show how the one- and two-particle integrals can be expressed compactly in terms of some auxiliary functions. The auxiliary functions are computed via a set of recurrence relations.

A thorough review of the techniques presented can be found in Helgaker *et al* [19].

4.2.1   Cartesian Gaussians

The Cartesian Gaussian functions centered at **A** are given by

$$G_{ijk}(a, \mathbf{r}_A) = x_A^i \, y_A^j \, z_A^k \, \exp(-ar_A^2), \tag{4.9}$$

where $\mathbf{r}_A = \mathbf{r} - \mathbf{A}$. These will be our primitive basis functions. They factorise in the Cartesian components

$$G_{ijk}(a, \mathbf{r}_A) = G_i(a, x_A) \, G_j(a, y_A) \, G_k(a, z_A), \tag{4.10}$$

where

$$G_i(a, x_A) = x_A^i \, \exp(-ax_A^2), \tag{4.11}$$

and the other factors are defined similarly. Each of the components obey the simple recurrence relation

$$x_A \, G_i = G_{i+1}. \tag{4.12}$$

4.2.2   Gaussian overlap distribution

We introduce the following shorthand notation

$$G_a(\mathbf{r}) = G_{ikm}(a, \mathbf{r}_A), \tag{4.13}$$

$$G_b(\mathbf{r}) = G_{jln}(b, \mathbf{r}_B), \tag{4.14}$$

and define the overlap distribution

$$\Omega_{ab}(\mathbf{r}) = G_a(\mathbf{r})\,G_b(\mathbf{r}). \tag{4.15}$$

Using the Gaussian product theorem (4.3) this can be written as

$$\Omega_{ab}(\mathbf{r}) = K_{AB}\,x_A^i\,x_B^j\,y_A^k\,y_B^l\,z_A^m\,z_B^n\,\exp(-p\,r_P^2), \tag{4.16}$$

where

$$
\begin{aligned}
K_{AB} &= \exp\left(-\frac{ab}{a+b}R_{AB}^2\right) \\
\mathbf{R}_{AB} &= \mathbf{A} - \mathbf{B} \\
p &= a + b \\
\mathbf{r}_P &= \mathbf{r} - \mathbf{P} \\
\mathbf{P} &= \frac{a\mathbf{A} + b\mathbf{B}}{a+b}.
\end{aligned}
\tag{4.17}
$$

Because the Gaussians G_a and G_b factorise in their Cartesian components, so does the overlap distribution

$$\Omega_{ab}(\mathbf{r}) = \Omega_{ij}(x)\,\Omega_{kl}(y)\,\Omega_{mn}(z), \tag{4.18}$$

where

$$\Omega_{ij} = K_{AB}^x\,x_A^i\,x_B^j\,\exp(-px_P^2) \tag{4.19}$$

and

$$
\begin{aligned}
K_{AB}^x &= \exp\left(-\frac{ab}{a+b}X_{AB}^2\right) \\
X_{AB} &= A_x - B_x.
\end{aligned}
\tag{4.20}
$$

The distributions $\Omega_{kl}(y)$ and $\Omega_{mn}(z)$ are defined similarly.

4.2.3   Hermite Gaussians

Later we will expand the Cartesian Gaussians in terms of the so-called Hermite Gaussians. This will simplify the integrations significantly. The Hermite Gaussians centered at $\mathbf{P}$ are defined by

$$\Lambda_{tuv}(p,\mathbf{r}_p) = \left(\frac{\partial}{\partial P_x}\right)^t\left(\frac{\partial}{\partial P_y}\right)^u\left(\frac{\partial}{\partial P_z}\right)^v\exp(-p\,r_P^2), \tag{4.21}$$

where $\mathbf{r}_p = \mathbf{r} - \mathbf{P}$. They factorise in the same way as the Cartesian Gaussians do:

$$\Lambda_{tuv}(p,\mathbf{r}_P) = \Lambda_t(p,x_P)\,\Lambda_u(p,y_P)\,\Lambda_v(p,z_P), \tag{4.22}$$

where

$$\Lambda_t(p,x_P) = \left(\frac{\partial}{\partial P_x}\right)^t\exp(-p\,x_P^2), \tag{4.23}$$

and the other factors are defined similarly. However, their recurrence relation is quite different from that of the Cartesian Gaussians:

$$
\begin{aligned}
\Lambda_{t+1}(p, x_P) &= \left(\frac{\partial}{\partial P_x}\right)^t \frac{\partial}{\partial P_x} \exp(-px_P^2) \\
&= \left(\frac{\partial}{\partial P_x}\right)^t 2px_P \exp(-px_P^2) \\
&= 2p\left[-t\left(\frac{\partial}{\partial P_x}\right)^{t-1} + x_P\left(\frac{\partial}{\partial P_x}\right)^t\right]\exp(-px_P^2) \\
&= 2p[-t\Lambda_{t-1} + x_P\Lambda_t],
\end{aligned}
\tag{4.24}
$$

where we have used that

$$
\left(\frac{\partial}{\partial x}\right)^t x f(x) = t\left(\frac{\partial}{\partial x}\right)^{t-1} f(x) + x\left(\frac{\partial}{\partial x}\right)^t f(x).
\tag{4.25}
$$

Thus the recurrence relation reads

$$
x_P\Lambda_t = \frac{1}{2p}\Lambda_{t+1} + t\Lambda_{t-1}.
\tag{4.26}
$$

4.2.4 Overlap integral S_{ab}

Our goal is to compute the overlap integral

$$
S_{ab} = \langle G_a|G_b\rangle = \int d\mathbf{r}\,\Omega_{ab}(\mathbf{r})
\tag{4.27}
$$

between two Gaussians centered at the points $\mathbf{A}$ and $\mathbf{B}$. Note that since the overlap distribution Ω_{ab} factorise in the Cartesian components, the integrals over x, y and z can be calculated independently of each other:

$$
\begin{aligned}
S_{ab} &= \langle G_i|G_j\rangle\langle G_k|G_l\rangle\langle G_m|G_n\rangle \\
&= S_{ij}\,S_{kl}\,S_{mn}.
\end{aligned}
\tag{4.28}
$$

The x component of the overlap integral, for example, is given by

$$
\begin{aligned}
S_{ij} &= \int dx\,\Omega_{ij}(x) \\
&= K_{AB}^x \int dx\,x_A^i x_B^j \exp(-px_P^2).
\end{aligned}
\tag{4.29}
$$

In equation (4.29) the two-center Gaussians have been reduced to a one-center Gaussian. However, the integral is still not straightforward to calculate because of the powers x_A^i and x_B^j. A smart way to deal with this is to express the Cartesian Gaussian in terms of the Hermite Gaussians. Note that (4.23) is a polynomial of order t in x multiplied by the exponential function. In equation (4.29) the polynomial is of order $i+j$. This means that we can express the overlap distribution $\Omega_{ij}(x)$ in equation (4.29) in terms of the Hermite Gaussians in (4.23) in the following way:

$$
\Omega_{ij}(x) = \sum_{t=0}^{i+j} E_t^{ij}\Lambda_t(p, x_P),
\tag{4.30}
$$

where E_t^{ij} are constants. Note that the sum is over t only. The indices i and j are static and are determined from the powers of x in G_i and G_j. We use them as labels on the coefficients E_t^{ij} because different sets of indices will lead to different sets of coefficients.

To get the overlap integral in the x-direction we integrate (4.30) over $\mathbb{R}$, which now turns out to be extremely easy; the only term that survives the integration is the term for $t = 0$:

$$\int dx\, \Lambda_t(p, x_P) \;=\; \int dx\, \left(\frac{\partial}{\partial P_x}\right)^t \exp(-p\, x_P^2), \tag{4.31}$$

$$=\; \left(\frac{\partial}{\partial P_x}\right)^t \int dx\, \exp(-p\, x_P^2), \tag{4.32}$$

$$=\; \sqrt{\frac{\pi}{p}}\, \delta_{t0}. \tag{4.33}$$

We have used Leibniz' rule, which says that the differentiation of an integrand with respect to a variable which is not an integration variable can be moved outside the integral. Thus the integral in (4.29) is simply

$$S_{ij} = E_0^{ij}\, \sqrt{\frac{\pi}{p}}. \tag{4.34}$$

The exact same procedure can be used for the integrals with respect to y and z, which means that the total overlap integral is

$$S_{ab} = E_0^{ij}\, E_0^{kl}\, E_0^{mn}\, \left(\frac{\pi}{p}\right)^{3/2}. \tag{4.35}$$

So far nothing has been said about how we actually determine the coefficients E_t^{ij}. First observe that when $i = j = 0$ in equation (4.30) we obtain

$$E_0^{0,0} = K_{AB}^x. \tag{4.36}$$

The other coefficients are found via the following recurrence relations

$$\begin{aligned}
E_t^{i+1,j} &= \frac{1}{2p} E_{t-1}^{ij} + X_{PA} E_t^{ij} + (t+1) E_{t+1}^{ij} \\
E_t^{i,j+1} &= \frac{1}{2p} E_{t-1}^{ij} + X_{PB} E_t^{ij} + (t+1) E_{t+1}^{ij}.
\end{aligned} \tag{4.37}$$

Analogous expressions hold for the coefficients E_u^{kl} and E_v^{mn}. The first equation in (4.37) can be derived by comparing two equivalent ways of expanding the product $G_{i+1}G_j$ in Hermite Gaussians. The first way is

$$G_{i+1}\, G_j = \sum_{t=0}^{i+j+1} E_t^{i+1,j} \Lambda_t, \tag{4.38}$$

and the second way is

$$G_{i+1}\,G_j = x_A G_i\,G_j$$

$$= [(x - P_x) + (P_x - A_x)] \sum_{t=0}^{i+j} E_t^{ij}\Lambda_t$$

$$= \sum_{t=0}^{i+j} [x_P + X_{PA}]E_t^{ij}\Lambda_t$$

$$= \sum_{t=0}^{i+j} [\frac{1}{2p}\Lambda_{t+1} + t\Lambda_{t-1} + X_{PA}\Lambda_t]E_t^{ij}$$

$$= \sum_{t=0}^{i+j+1} [\frac{1}{2p}E_{t-1}^{ij} + X_{PA}E_t^{ij} + (t+1)E_{t+1}^{ij}]\Lambda_t,$$

(4.39)

where we have used the recurrence relation (4.26) on the fourth line and changed the summation indices on the fifth line. Comparing the two expressions gives the desired result.

Note that the change in summation indices in equation (4.39) implies that we must define

$$E_t^{ij} = 0, \qquad \text{if } t < 0 \text{ or } t > i + j. \tag{4.40}$$

4.2.5   Kinetic integral T_{ij}

Next we turn to the evaluation of the kinetic integral:

$$T_{ab} = -\frac{1}{2}\langle G_a|\nabla^2|G_b\rangle$$

$$= -\frac{1}{2}\langle G_{ikm}(a, \mathbf{r}_A)|\nabla^2|G_{jln}(b, \mathbf{r}_B)\rangle$$

(4.41)

$$= -\frac{1}{2}(T_{ij}\,S_{kl}\,S_{mn} + S_{ij}\,T_{kl}\,S_{mn} + S_{ij}\,S_{kl}\,T_{mn}),$$

where

$$T_{ij} = \int dx\, G_i(a, x_A)\frac{\partial^2}{\partial x^2}G_j(b, x_B), \tag{4.42}$$

and the other factors are defined in the same way. Performing the differentiation yields

$$T_{ij} = 4b^2\,S_{i,j+2} - 2b(2j+1)S_{i,j} + j(j-1)S_{i,j-2}. \tag{4.43}$$

Thus we see that the kinetic integrals are calculated easily as products of the overlap integrals.

4.2.6   Coulomb integral V_{ab}

We now turn to the Coulomb integral due to the interaction between the electrons and the nuclei

$$V_{ab} = \langle G_a|\frac{1}{r_C}|G_b\rangle, \tag{4.44}$$

where $r_C = |\mathbf{r} - \mathbf{C}|$. As before, the overlap distribution is expanded in the Hermite Gaussians:

$$
\begin{aligned}
V_{ab} &= \int d\mathbf{r}\, \frac{\Omega_{ab}(\mathbf{r})}{r_C} \\
&= \sum_{tuv} E_t^{ij} E_u^{kl} E_v^{mn} \int d\mathbf{r}\, \frac{\Lambda_{tuv}(p, \mathbf{r}_P)}{r_C} \\
&= \sum_{tuv} E_{tuv}^{ab} \int d\mathbf{r}\, \frac{\Lambda_{tuv}(p, \mathbf{r}_P)}{r_C}.
\end{aligned}
\tag{4.45}
$$

Here we have used the shorthand notation

$$
E_{tuv}^{ab} = E_t^{ij} E_u^{kl} E_v^{mn}.
\tag{4.46}
$$

In this integral other terms besides Λ_{000} will survive due to the factor $1/r_C$. Let us nonetheless start by evaluating this term

$$
V_p = \int d\mathbf{r}\, \frac{\Lambda_{000}(p, \mathbf{r}_P)}{r_C} = \int d\mathbf{r}\, \frac{\exp(-p\, r_P^2)}{r_C}.
\tag{4.47}
$$

We will show that this three-dimensional integral can actually be converted to a one-dimensional one. The trick is to observe that the factor $1/r_C$ can be replaced by the integral

$$
\frac{1}{r_C} = \frac{1}{\sqrt{\pi}} \int_{-\infty}^{\infty} dt\, \exp(-r_C^2\, t^2).
\tag{4.48}
$$

Inserting this into V_p and using the Gaussian product theorem gives

$$
\begin{aligned}
V_p &= \int \exp(-p\, r_P^2)\left(\frac{1}{\sqrt{\pi}} \int_{-\infty}^{\infty} \exp(-r_C^2\, t^2)\, dt\right) d\mathbf{r} \\
&= \frac{1}{\sqrt{\pi}} \int_{-\infty}^{\infty} \int \exp\left(-\frac{pt^2}{p+t^2} R_{PC}^2\right) \exp[-(p+t^2) r_S^2] d\mathbf{r}\, dt,
\end{aligned}
\tag{4.49, 4.50}
$$

where $\mathbf{R}_{PC} = \mathbf{P} - \mathbf{C}$ and $\mathbf{r}_S = \mathbf{r} - \mathbf{S}$ for some point $\mathbf{S}$. Doing the integral over the spatial coordinates reveals that the specific value of $\mathbf{S}$ is immaterial:

$$
\begin{aligned}
V_p &= \frac{1}{\sqrt{\pi}} \int_{-\infty}^{\infty} \exp\left(-\frac{pt^2}{p+t^2} R_{PC}^2\right)\left(\frac{\pi}{p+t^2}\right)^{3/2} dt \\
&= 2\pi \int_0^{\infty} \exp\left(-\frac{pt^2}{p+t^2} R_{PC}^2\right) \frac{dt}{(p+t^2)^{3/2}}.
\end{aligned}
\tag{4.51, 4.52}
$$

Next we change integration variable from t to u by defining

$$
u^2 = \frac{t^2}{p+t^2}.
\tag{4.53}
$$

This will change the range of integration from $[0, \infty\rangle$ to $[0, 1]$. This is beneficial because the final integral at which we arrive will be calculated numerically. The change of

variables leads to

$$V_p = \frac{2\pi}{p} \int_0^1 \exp(-p\,R_{PC}^2\,u^2)\,du \tag{4.54}$$

$$= \frac{2\pi}{p} F_0(p\,R_{PC}^2), \tag{4.55}$$

where $F_0(x)$ is a special instance of the Boys function $F_n(x)$ which is defined as

$$F_n(x) = \int_0^1 \exp(-xt^2)\,t^{2n}\,dt. \tag{4.56}$$

How to actually evaluate the Boys function will be discussed in section 4.3.

We have now a tremendously simplified way of calculating the integral of Λ_{000}/r_C. However, we need to integrate Λ_{tuv}/r_C for general values of t, u and v. These integrals are actually not that hard to do once the Boys function is calculated:

$$V_{ab} = \sum_{tuv} E_{tuv}^{ab} \int d\mathbf{r}\, \frac{\Lambda_{tuv}(p, \mathbf{r}_p)}{r_C} \tag{4.57}$$

$$= \frac{2\pi}{p} \sum_{tuv} E_{tuv}^{ab} \frac{\partial^{t+u+v} F_0(pR_{PC}^2)}{\partial P_x^t \partial P_y^u \partial P_z^v} \tag{4.58}$$

$$= \frac{2\pi}{p} \sum_{tuv} E_{tuv}^{ab} R_{tuv}(p, \mathbf{R}_{PC}), \tag{4.59}$$

where we have defined

$$R_{tuv}(a, \mathbf{A}) = \frac{\partial^{t+u+v} F_0(aA^2)}{\partial A_x^t \partial A_y^u \partial A_z^v}. \tag{4.60}$$

So we need to know how to calculate derivatives of the function F_0. Note first that

$$\frac{d}{dx} F_n(x) = -F_{n+1}(x). \tag{4.61}$$

This means that it is possible to derive analytical expressions for the Coulomb term V_{ab}. However, in practice they are calculated recursively in a manner similar to the way we calculate the coefficients E_t^{ij}. Before presenting the recursion relations, we introduce the so-called auxiliary Hermite integrals

$$R_{tuv}^n(a, \mathbf{A}) = (-2a)^n \frac{\partial^{t+u+v} F_n(aA^2)}{\partial A_x^t \partial A_y^u \partial A_z^v}. \tag{4.62}$$

By starting with the source terms $R_{000}^n(a, \mathbf{A}) = (-2a)^n F_n(aA^2)$ we can reach the targets $R_{tuv}^0(a, \mathbf{A}) = R_{tuv}(a, \mathbf{A})$ through the following recurrence relations

$$\begin{aligned}
R_{t+1,u,v}^n &= tR_{t-1,u,v}^{n+1} + A_x R_{tuv}^{n+1} \\
R_{t,u+1,v}^n &= uR_{t,u-1,v}^{n+1} + A_y R_{tuv}^{n+1} \\
R_{t,u,v+1}^n &= vR_{t,u,v-1}^{n+1} + A_z R_{tuv}^{n+1}.
\end{aligned} \tag{4.63}$$

The first of these are derived as follows

$$R_{t+1,u,v}^n = (-2a)^n \frac{\partial^{t+u+v}}{\partial A_x^t \partial A_y^u \partial A_z^v} [2aA_x F_n'(aA^2)] \tag{4.64}$$

$$= (-2a)^{n+1} \frac{\partial^{t+u+v}}{\partial A_x^t \partial A_y^u \partial A_z^v} \left[A_x F_{n+1}(aA^2) \right] \tag{4.65}$$

$$= (-2a)^{n+1} \frac{\partial^{u+v}}{\partial A_y^u \partial A_z^v} \left[t \frac{\partial^{t-1}}{\partial A_x^{t-1}} + A_x \frac{\partial^t}{\partial A_x^t} \right] F_{n+1}(aA^2) \tag{4.66}$$

$$= t R_{t-1,u,v}^{n+1} + A_x R_{tuv}^{n+1}, \tag{4.67}$$

where we have used equation (4.25) and the fact that $F_n'(x) = -F_{n+1}(x)$.

4.2.7 Coulomb integral g_{acbd}

Finally we show how to calculate the Coulomb integral due to the interaction between the electrons. It is given by[1]

$$\begin{aligned}
g_{acbd} &= \langle G_a G_c | \frac{1}{r_{12}} | G_b G_d \rangle \\
&= \int \int \frac{\Omega_{ab}(\mathbf{r}_1)\Omega_{cd}(\mathbf{r}_2)}{r_{12}} d\mathbf{r}_1 d\mathbf{r}_2 \\
&= \sum_{tuv} \sum_{\tau\nu\phi} E_{tuv}^{ab} E_{\tau\nu\phi}^{cd} \int \int \frac{\Lambda_{tuv}(p,\mathbf{r}_{1P})\Lambda_{\tau\nu\phi}(q,\mathbf{r}_{2Q})}{r_{12}} d\mathbf{r}_1 d\mathbf{r}_2 \\
&= \sum_{tuv} \sum_{\tau\nu\phi} E_{tuv}^{ab} E_{\tau\nu\phi}^{cd} \frac{\partial^{t+u+v}}{\partial P_x^t \partial P_y^u \partial P_z^v} \frac{\partial^{\tau+\nu+\phi}}{\partial Q_x^\tau \partial Q_y^\nu \partial Q_z^\phi} \\
&\qquad\qquad \int \int \frac{\exp(-pr_{1P}^2)\exp(-qr_{2Q}^2)}{r_{12}} d\mathbf{r}_1 d\mathbf{r}_2,
\end{aligned} \tag{4.68}$$

where, analogous to p and $\mathbf{r}_{1P}$, we have defined

$$\begin{aligned}
q &= c + d \\
\mathbf{r}_{2Q} &= \mathbf{r}_2 - \mathbf{Q} \\
\mathbf{Q} &= \frac{c\,\mathbf{C} + d\,\mathbf{D}}{c+d}.
\end{aligned} \tag{4.69}$$

Thus we need to evaluate the integral

$$V_{pq} = \int \int \frac{\exp(-pr_{1P}^2)\exp(-qr_{2Q}^2)}{r_{12}} d\mathbf{r}_1 d\mathbf{r}_2. \tag{4.70}$$

By first integrating over $\mathbf{r}_1$ and using equation (4.54) this can be written as

$$V_{pq} = \int \left(\frac{2\pi}{p} \int_0^1 \exp(-p\,r_{2P}^2\,u^2)\,du \right) \exp(-qr_{2Q}^2) d\mathbf{r}_2. \tag{4.71}$$

---

[1]Here G_a is combined with G_b and G_c combined with G_d using the Gaussian product rule. In many books on quantum chemistry this is written as
$(G_a(1)G_b(1)|r_{12}^{-1}|G_c(2)G_d(2)) = \int \int d\mathbf{r}_1 d\mathbf{r}_2 G_a(\mathbf{r}_1)G_b(\mathbf{r}_1)r_{12}^{-1}G_c(\mathbf{r}_2)G_d(\mathbf{r}_2)$. However, since this departs from the usual notation of quantum physics, it will not be used in this thesis.

Next we change the order of integration and use the Gaussian product theorem to get

$$
\begin{aligned}
V_{pq} &= \frac{2\pi}{p} \int_0^1 \int \exp(-\frac{pqu^2}{pu^2+q}R_{PQ}^2)\exp[-(pu^2+q)r_{2S}^2]d\mathbf{r}_2 du \\
&= \frac{2\pi}{p}\int_0^1 \exp(-\frac{pqu^2}{pu^2+q}R_{PQ}^2)\Big(\frac{\pi}{pu^2+q}\Big)^{3/2}du,
\end{aligned}
\tag{4.72}
$$

where $\mathbf{R}_{PQ} = \mathbf{P} - \mathbf{Q}$ and $\mathbf{r}_{2S} = \mathbf{r}_2 - \mathbf{S}$ for some point $\mathbf{S}$. Again, the actual coordinates of $\mathbf{S}$ are immaterial. If we now make the change of variable

$$
\frac{v^2}{p+q} = \frac{u^2}{pu^2+q},
\tag{4.73}
$$

we get the result

$$
V_{pq} = \frac{2\pi^{5/2}}{pq\sqrt{p+q}}F_0\Big(\frac{pq}{p+q}R_{PQ}^2\Big).
\tag{4.74}
$$

From this we get the final answer

$$
\begin{aligned}
g_{acbd} &= \frac{2\pi^{5/2}}{pq\sqrt{p+q}}\sum_{tuv}\sum_{\tau\nu\phi}(-1)^{\tau+\nu+\phi}E_{tuv}^{ab}E_{\tau\nu\phi}^{cd} \\
&\qquad\qquad \frac{\partial^{t+u+v+\tau+\nu+\phi}}{\partial P_x^{t+\tau}\partial P_y^{u+\nu}\partial P_z^{v+\phi}}F_0\Big(\frac{pq}{p+q}R_{PQ}^2\Big) \\
&= \frac{2\pi^{5/2}}{pq\sqrt{p+q}}\sum_{tuv}\sum_{\tau\nu\phi}(-1)^{\tau+\nu+\phi}E_{tuv}^{ab}E_{\tau\nu\phi}^{cd}R_{t+\tau,u+\nu,v+\phi}(\alpha,\mathbf{R}_{PQ}),
\end{aligned}
\tag{4.75}
$$

where $\alpha = pq/(p+q)$. The term $(-)^{\tau+\nu+\phi}$ arises due to the fact that

$$
\frac{\partial}{\partial Q_x}F_0\Big(\frac{pq}{p+q}R_{PQ}^2\Big) = -\frac{\partial}{\partial P_x}F_0\Big(\frac{pq}{p+q}R_{PQ}^2\Big).
\tag{4.76}
$$

4.3   The Boys function

As shown in the previous section, calculating the Coulomb integrals boils down to evaluating the Boys function

$$
F_n(x) = \int_0^1 \exp(-xt^2)\,t^{2n}\,dt.
\tag{4.77}
$$

Doing this by standard numerical procedures is compuationally expensive and should therefore be avoided. This section describes one possible way to calculate the Boys function efficiently.

First note that if x is very large, the function value will hardly be affected by changing the upper limit of the integral from 1 to ∞. Doing this is beneficial because then the integral can be calculated exactly. Thus, we have the following approximation for the Boys function for large x:

$$
F_n(x) \approx \frac{(2n-1)!!}{2^{n+1}}\sqrt{\frac{\pi}{x^{2n+1}}}. \qquad\qquad (x \text{ large})
\tag{4.78}
$$

For small values of x there seems to be no escape from numerical calculation. However, instead of doing the integral at the time of computation, it can be tabulated once and for all at regular values of x. For values between the tabulated ones, the function can be calculated by a Taylor expansion centered at the nearest tabulated point x_t:

$$F_n(x_t + \Delta x) = \sum_{k=0}^{\infty} \frac{F_{n+k}(x_t)(-\Delta x)^k}{k!}. \qquad (x \text{ small}) \qquad (4.79)$$

Computational cost can be reduced even further by calculating the Boys function according to the description above only for the highest values of n needed; for lower values of n the function can be found via the recursion relation

$$F_n(x) = \frac{2x F_{n+1}(x) + e^{-x}}{2n + 1}, \qquad (4.80)$$

which can be shown by integrating the function by parts.

4.4   Summary of the integration scheme

In the previous sections the integration scheme for GTOs has been derived. We summarise the results in this section. Some of the results are only elaborated fully for the x-component as the others components are defined similarly.

Gaussian functions

The Gaussian functions are given by

$$\begin{aligned}
G_a(\mathbf{r}) &= G_{ikm}(a, \mathbf{r}_A) = x_A^i\, y_A^k\, z_A^m \exp(-a r_A^2), \\
G_b(\mathbf{r}) &= G_{jln}(b, \mathbf{r}_B) = x_B^j\, y_B^l\, z_B^n \exp(-b r_B^2),
\end{aligned} \qquad (4.81)$$

where $\mathbf{r}_A = \mathbf{r} - \mathbf{A}$ and $\mathbf{r}_B = \mathbf{r} - \mathbf{B}$. We further define

$$\begin{aligned}
p &= a + b, \\
\mathbf{P} &= \frac{a\mathbf{A} + b\mathbf{B}}{a + b}.
\end{aligned} \qquad (4.82)$$

Overlap integral S_{ab}

The overlap integral

$$S_{ab} = \langle G_a | G_b \rangle \qquad (4.83)$$

is calculated as

$$S_{ab} = E_0^{ij}\, E_0^{kl}\, E_0^{mn} \left(\frac{\pi}{p}\right)^{3/2}, \qquad (4.84)$$

where

$$E_0^{i=0,j=0} = \exp\left(-\frac{ab}{a+b} X_{AB}^2\right), \qquad (4.85)$$

and the desired coefficients are found via

$$
\begin{aligned}
E_t^{i+1,j} &= \frac{1}{2p} E_{t-1}^{ij} + X_{PA} E_t^{ij} + (t+1) E_{t+1}^{ij}, \\
E_t^{i,j+1} &= \frac{1}{2p} E_{t-1}^{ij} + X_{PB} E_t^{ij} + (t+1) E_{t+1}^{ij}.
\end{aligned}
\tag{4.86}
$$

Kinetic integral T_{ab}

The kinetic integral is calculated as

$$
T_{ab} = -\frac{1}{2}(T_{ij}\, S_{kl}\, S_{mn} + S_{ij}\, T_{kl}\, S_{mn} + S_{ij}\, S_{kl}\, T_{mn}),
\tag{4.87}
$$

where

$$
T_{ij} = 4b^2\, S_{i,j+2} - 2b(2j+1)S_{i,j} + j(j-1)S_{i,j-2}.
\tag{4.88}
$$

Coulomb integral V_{ab}

The Coulomb integral

$$
V_{ab} = \langle G_a | \frac{1}{r_C} | G_b \rangle
\tag{4.89}
$$

is calculated as

$$
V_{ab} = \frac{2\pi}{p} \sum_{tuv} E_{tuv}^{ab} R_{tuv}(p, \mathbf{R}_{PC}),
\tag{4.90}
$$

where

$$
E_{tuv}^{ab} = E_t^{ij}\, E_u^{kl}\, E_v^{mn},
\tag{4.91}
$$

and $R_{tuv}(a, \mathbf{A})$ is found by first calculating the source term

$$
R_{000}^n(a, \mathbf{A}) = (-2a)^n\, F_n(aA^2)
\tag{4.92}
$$

and then iterating towards the target $R_{tuv}^0(a, \mathbf{A}) = R_{tuv}(a, \mathbf{A})$ via the recurrence relations

$$
\begin{aligned}
R_{t+1,u,v}^n &= t R_{t-1,u,v}^{n+1} + A_x R_{tuv}^{n+1}, \\
R_{t,u+1,v}^n &= u R_{t,u-1,v}^{n+1} + A_y R_{tuv}^{n+1}, \\
R_{t,u,v+1}^n &= v R_{t,u,v-1}^{n+1} + A_z R_{tuv}^{n+1}.
\end{aligned}
\tag{4.93}
$$

Coulomb integral g_{acbd}

The Coulomb integral

$$
g_{acbd} = \langle G_a G_c | \frac{1}{r_{12}} | G_b G_d \rangle
\tag{4.94}
$$

is calculated as

$$
g_{acbd} = \frac{2\pi^{5/2}}{pq\sqrt{p+q}} \sum_{tuv} \sum_{\tau\nu\phi} (-1)^{\tau+\nu+\phi} E_{tuv}^{ab} E_{\tau\nu\phi}^{cd} R_{t+\tau,u+\nu,v+\phi}(\alpha, \mathbf{R}_{PQ}),
\tag{4.95}
$$

where

$$
\alpha = \frac{pq}{p+q}.
\tag{4.96}
$$

Chapter 5

Electron correlations

Even though the Hartree-Fock method often yields quite good results, it has its limitations. This because it is based on the assumption that the electronic state can be written as a single Slater determinant. However, as discussed in section 2.8, an infinite sum of Slater determinants is generally needed. Consequently, no matter how large a basis set we have at our disposal, the Hartree-Fock energy is bound to overestimate the exact energy.[1] The exact solution of the Hartree-Fock equations, obtained in the limit where the basis set approaches completeness, is called the Hartree-Fock limit. The difference between the exact energy, $\mathscr{E}_0$, and the Hartree-Fock limit energy, E_0, is referred to as the correlation energy

$$E_{\text{corr}} = \mathscr{E}_0 - E_0. \tag{5.1}$$

In the author's opinion, this name is somewhat unfortunate since it seems to suggest that the electronic probability distribution obtained from a Hartree-Fock calculation is uncorrelated. However, as we have seen in section 2.4, the Slater determinant, which is the basic starting point of the Hartree-Fock method, does indeed imply a correlated probability distribution. Hence, it is perhaps more appropriate to think of equation (5.1) simply as the systematic error introduced by the Hartree-Fock method and not equate "correlation" in "correlation energy" to the statistical meaning of the word.

Concerning the statistical correlations inherent in the electronic probability distribution, quantum chemists often distinguish between *Fermi* correlations (or *exchange* correlations) and *Coulomb* correlations [22]. The Fermi correlations are defined as those arising purely from the fact that the wave function is antisymmetric, whereas the Coulomb correlations are due to the Coulomb repulsion acting between the electrons. The Coulomb repulsion is included in the Hartree-Fock equations only in an averaged, mean-field sense.

The are a number of so-called *post-Hartree-Fock* methods designed to improve the solution obtained from a Hartree-Fock calculation. The perhaps conceptually simplest is the *configuration interaction* (CI) method. It goes as follows. Assume that we have solved the Hartree-Fock equations for an N-electron system and obtained a set of

---

[1]In this context, exact energy means the exact solution of the Schrödinger equation defined by the Hamiltonian in equation (2.3).

spin orbitals $\{\psi_k\}$, ordered by increasing energy. The Slater determinant constructed from the N lowest spin orbitals, is the familiar reference state $|\Psi_0\rangle$. However, we can construct other Slater determinants by replacing one or more of the occupied spin orbitals with any of the virtual spin orbitals. The exact ground state $|\Phi_0\rangle$ can then be approximated by a linear combination of these Slater determinants:

$$|\Phi_0\rangle \approx C_0|\Psi_0\rangle + \sum_{ia} C_i^a|\Psi_i^a\rangle + \sum_{i<j,a<b} C_{ij}^{ab}|\Psi_{ij}^{ab}\rangle + \ldots \tag{5.2}$$

In fact, if the spin orbitals $\{\psi_k\}$ constitute a complete set of functions, the linear combination above is exact. Diagonalising the matrix representation of the Hamiltonian in the basis of the determinants above is referred to as *full CI*. The lowest eigenvalue is an upper bound for the exact energy (because the basis set must be truncated). However, it is the best one can possibly do within the limit of the single particle basis $\{\psi_k\}$. Hence, full CI is the proper benchmark against which the performance of other post-Hartree-Fock methods should be compared.

The number of Slater determinants grows rapidly with the size of the single particle basis set. Hence, the full CI method becomes intractable for large systems, and we must resort to other methods. Popular candidates are coupled cluster (CC) [5, 23] and many-body perturbation theory (MBPT), which is the method of choice in this thesis, see the next chapter. Many-body methods like density functional theory (DFT) [11], variational Monte Carlo (VMC) [11] and diffusion Monte Carlo (DMC) [11, 24] are other popular methods which go beyond Hartree-Fock, although they are most often not considered as post-Hartree-Fock methods.

For a further discussion on electron correlations, the reader is referred to the clear and readable article by Tew *et al* [22].

Chapter 6

Perturbation theory

6.1 Formal perturbation theory

The basic starting point of perturbation theory is to divide the total Hamiltonian H into two parts: One part, H_0, of which we are able to find the eigenstates and eigenvalues and the remaining part, V, which is called the perturbation:

$$H = H_0 + V. \tag{6.1}$$

When $V = 0$, the known solutions to the Schrödinger equation are given by

$$H_0|\Psi_i^{(0)}\rangle = E_i^{(0)}|\Psi_i^{(0)}\rangle, \tag{6.2}$$

where the superindices indicate that the solutions are of zeroth order, that is, with complete disregard of V. Most often we will be interested in the ground state. Of course, $|\Psi_0^{(0)}\rangle$ is not the actual ground state, but merely an approximation. To obtain the exact ground state $|\Phi_0\rangle$, an (unknown) correction term $|\gamma\rangle$ must be added:

$$|\Phi_0\rangle = |\Psi_0^{(0)}\rangle + |\gamma\rangle. \tag{6.3}$$

The same is true for the energy:

$$\mathscr{E}_0 = E_0^{(0)} + \Delta E. \tag{6.4}$$

In perturbation theory, the goal is to estimate the corrections $|\gamma\rangle$ and ΔE order by order in terms of the perturbation V:

$$|\gamma\rangle = |\Psi_0^{(1)}\rangle + |\Psi_0^{(2)}\rangle + \dots \tag{6.5}$$

$$\Delta E = E_0^{(1)} + E_0^{(2)} + \dots \tag{6.6}$$

where, as before, the superindices indicate the order of the perturbation V. The hope is that most of the physics is captured by the zeroth order Hamiltonian H_0 so that the two series above converge as fast as possible.

It will be assumed that $\langle\Psi_0^{(0)}|\gamma\rangle = 0$, i.e., that there is no overlap between the unperturbed solution and the correction. Furthermore, we will let the unperturbed

solution be normalised, which means that the overlap between the unperturbed and exact solution is equal to unity:

$$\langle \Psi_0^{(0)} | \Phi_0 \rangle = \langle \Psi_0^{(0)} | \left(| \Psi_0^{(0)} \rangle + | \gamma \rangle \right) = 1 + 0 = 1. \tag{6.7}$$

This is often referred to as intermediate normalisation.

The general expression for the energy correction ΔE can be derived from the Schrödinger equation as follows:

$$
\begin{aligned}
(H_0 + V)|\Phi_0\rangle &= \mathscr{E}_0|\Phi_0\rangle, \\
\langle \Psi_0^{(0)}|(H_0 + V)|\Phi_0\rangle &= \mathscr{E}_0 \langle \Psi_0^{(0)}|\Phi_0\rangle, \\
\langle \Psi_0^{(0)}|H_0|\Phi_0\rangle + \langle \Psi_0^{(0)}|V|\Phi_0\rangle &= \mathscr{E}_0, \\
\langle H_0\Psi_0^{(0)}|\Phi_0\rangle + \langle \Psi_0^{(0)}|V|\Phi_0\rangle &= \mathscr{E}_0, \\
E_0^{(0)} + \langle \Psi_0^{(0)}|V|\Phi_0\rangle &= \mathscr{E}_0,
\end{aligned}
\tag{6.8}
$$

so that

$$\Delta E = \langle \Psi_0^{(0)} | V | \Phi_0 \rangle. \tag{6.9}$$

Here we have used equations (6.4) and (6.7) and the fact that H_0 is Hermitian. Once we have an order by order expansion of $|\Phi_0\rangle$, this will give us an order by order expansion also of ΔE.

To make further progress, we define the projection operators P and Q:

$$P = |\Psi_0^{(0)}\rangle\langle\Psi_0^{(0)}|, \tag{6.10}$$

$$Q = \sum_{i=1}^{\infty} |\Psi_i^{(0)}\rangle\langle\Psi_i^{(0)}|. \tag{6.11}$$

When acting on the state $|\Phi_0\rangle$, P picks out the part which is parallel with $|\Psi_0^{(0)}\rangle$. This is easily shown by expressing $|\Phi_0\rangle$ in the basis $\left\{ |\Psi_i^{(0)}\rangle \right\}_{i=0}^{\infty}$:

$$P|\Phi_0\rangle = |\Psi_0^{(0)}\rangle\langle\Psi_0^{(0)}| \sum_{j=0}^{\infty} C_j |\Psi_j^{(0)}\rangle = C_0 |\Psi_0^{(0)}\rangle. \tag{6.12}$$

Similarly, Q picks out the part which is orthogonal to $|\Psi_0^{(0)}\rangle$ since $PQ = QP = 0$. Note also that $P^2 = P$, $Q^2 = Q$ and $P + Q = I$. Furthermore, P commutes with H_0:

$$
\begin{aligned}
H_0 P|\Phi_0\rangle &= H_0 P \sum_{i=0}^{\infty} C_i |\Psi_i^{(0)}\rangle = H_0 C_0 |\Psi_0^{(0)}\rangle = C_0 E_0^{(0)} |\Psi_0^{(0)}\rangle, \\
P H_0 |\Phi_0\rangle &= P H_0 \sum_{i=0}^{\infty} C_i |\Psi_i^{(0)}\rangle = P \sum_{i=0}^{\infty} C_i E_i^{(0)} |\Psi_i^{(0)}\rangle = C_0 E_0^{(0)} |\Psi_0^{(0)}\rangle.
\end{aligned}
\tag{6.13}
$$

Also, since $Q = I - P$, Q commutes with H_0 as well.

We now have the ingredients necessary to find a perturbative expansion of $|\Phi_0\rangle$. The starting point is a slight rewrite of the Schrödinger equation:

$$(\zeta - H_0)|\Phi_0\rangle = (V - \mathscr{E}_0 + \zeta)|\Phi_0\rangle, \tag{6.14}$$

where ζ is a hitherto unspecified parameter. Different choices of ζ will lead to different perturbation schemes. Two very common choices are $\zeta = \mathscr{E}_0$ and $\zeta = E_0^{(0)}$ which lead to Brillouin-Wigner and Rayleigh-Schrödinger perturbation theory, respectively [5]. Acting from the left with the operator Q on both sides, and using the fact that $Q^2 = Q$ and $[Q, H_0] = 0$ leads to

$$Q(\zeta - H_0)Q|\Phi_0\rangle = Q(V - \mathscr{E}_0 + \zeta)|\Phi_0\rangle. \tag{6.15}$$

We now need an expression for the inverse of $Q(\zeta - H_0)Q$. As long as ζ is not equal to any of the eigenvalues $\{E_i^{(0)}\}_{i=1}^\infty$, this exists and is equal to

$$R_0(\zeta) = \frac{Q}{\zeta - H_0} = \sum_{i=1}^\infty \sum_{j=1}^\infty |\Psi_i^{(0)}\rangle\langle\Psi_i^{(0)}|(\zeta - H_0)^{-1}|\Psi_j^{(0)}\rangle\langle\Psi_j^{(0)}|, \tag{6.16}$$

which is called the resolvent of H_0. Writing $R_0(\zeta)$ as the fraction above is justified by the fact that Q commutes with H_0.

Acting with $R_0(\zeta)$ from the left on both sides of equation (6.15) gives

$$Q|\Psi_0\rangle = R_0(\zeta)(V - \mathscr{E}_0 + \zeta)|\Phi_0\rangle, \tag{6.17}$$

and using the fact that $(P + Q)|\Phi_0\rangle = |\Phi_0\rangle$ leads to

$$|\Phi_0\rangle = |\Psi_0^{(0)}\rangle + R_0(\zeta)(V - \mathscr{E}_0 + \zeta)|\Phi_0\rangle. \tag{6.18}$$

Substituting the expression into itself gives

$$\begin{aligned}|\Phi_0\rangle =& |\Psi_0^{(0)}\rangle + R_0(\zeta)(V - \mathscr{E}_0 + \zeta)|\Psi_0^{(0)}\rangle \\ &+ [R_0(\zeta)(V - \mathscr{E}_0 + \zeta)]^2|\Phi_0\rangle,\end{aligned} \tag{6.19}$$

and repeating this process yields the expression we are seeking:

$$|\Phi_0\rangle = \sum_{n=0}^\infty [R_0(\zeta)(V - \mathscr{E}_0 + \zeta)]^n|\Psi_0^{(0)}\rangle. \tag{6.20}$$

The corresponding expansion for the energy is found by inserting this into equation (6.9):

$$\Delta E = \sum_{n=0}^\infty \langle\Psi_0^{(0)}|V[R_0(\zeta)(V - \mathscr{E}_0 + \zeta)]^n|\Psi_0^{(0)}\rangle. \tag{6.21}$$

6.2   Rayleigh-Schrödinger perturbation theory

Rayleigh-Schrödinger perturbation theory, named after Lord Rayleigh [25] and Erwin Scrhrödinger [26], is obtained by setting $\zeta = E_0^{(0)}$, which gives

$$\Delta E = \sum_{n=0}^{\infty} \langle \Psi_0^{(0)} | V [R_0(E_0^{(0)})(V - \Delta E)]^n | \Psi_0^{(0)} \rangle. \tag{6.22}$$

Writing out the first three terms explicitly:

$$\begin{aligned} \Delta E =& \langle \Psi_0^{(0)} | V | \Psi_0^{(0)} \rangle \\ &+ \langle \Psi_0^{(0)} | V R_0 (V - \Delta E) | \Psi_0^{(0)} \rangle \\ &+ \langle \Psi_0^{(0)} | V R_0 (V - \Delta E) R_0 (V - \Delta E) | \Psi_0^{(0)} \rangle + \dots \end{aligned} \tag{6.23}$$

where the dependence of R_0 on $E_0^{(0)}$ has been supressed. This is still not a proper perturbative expansion since ΔE is present also on the right hand side of the equation. We get the correct expansion by inserting the expression itself into every occurence of ΔE on the right hand side. Doing this, and noting that $R_0 | \Psi_0^{(0)} \rangle = 0$, gives

$$\begin{aligned} \Delta E =& \langle \Psi_0^{(0)} | V | \Psi_0^{(0)} \rangle \\ &+ \langle \Psi_0^{(0)} | V R_0 V | \Psi_0^{(0)} \rangle \\ &+ \langle \Psi_0^{(0)} | V R_0 (V - \langle \Psi_0^{(0)} | V | \Psi_0^{(0)} \rangle) R_0 V | \Psi_0^{(0)} \rangle + \cdots \end{aligned} \tag{6.24}$$

The three lines are the first, second and third order corrections, respectively, to the zero order energy.

6.3   Møller-Plesset perturbation theory

To make further progress, it is necessary to specify the zero order Hamiltonian H_0. Setting it equal to the Hartree-Fock Hamiltonian

$$H_0 = \sum_{pq} \langle p | \mathcal{F} | q \rangle a_p^\dagger a_q, \tag{6.25}$$

yields the so-called Møller-Plesset perturbation theory, after Møller and Plesset [27]. If we choose the eigenfunctions of the Fock operator as our single-particle basis, then H_0 simplifies to

$$H_0 = \sum_{pq} \langle p | \varepsilon_q | q \rangle a_p^\dagger a_q = \sum_{pq} \varepsilon_q \delta_{pq} a_p^\dagger a_q = \sum_p \varepsilon_p a_p^\dagger a_p. \tag{6.26}$$

Furthermore, the unperturbed state $| \Psi_0^{(0)} \rangle$ is then equal to the Hartree-Fock determinant $| \Psi_0 \rangle$. It is per definition an eigenstate of the unperturbed Hamiltonian

$$H_0 | \Psi_0 \rangle = \sum_p \varepsilon_p a_p^\dagger a_p | 123 \dots N \rangle = \sum_{i=1}^N \varepsilon_i | \Psi_0 \rangle, \tag{6.27}$$

Thus the zero order energy is the sum of the Hartree-Fock orbital energies

$$E_0^{(0)} = \sum_{i=1}^{N} \varepsilon_i. \tag{6.28}$$

Next we show how this choice of H_0 determines the perturbation V. The Hamiltonian can be written as

$$H = H_0 + (H_1 - H_0 + H_2), \tag{6.29}$$

where H_1 and H_2 are the one- and two-body terms defined in equations (2.55) and (2.57), respectively. This means that

$$
\begin{aligned}
V &= H_1 - H_0 + H_2 \\
&= \sum_{pq}[\langle p|h|q\rangle - \langle p|\mathcal{F}|q\rangle]a_p^\dagger a_q + \frac{1}{4}\sum_{pqrs}\langle pq||rs\rangle a_p^\dagger a_q^\dagger a_s a_r \\
&= -\sum_{pq}\langle p|(\mathcal{J}-\mathcal{K})|q\rangle a_p^\dagger a_q + \frac{1}{4}\sum_{pqrs}\langle pq||rs\rangle a_p^\dagger a_q^\dagger a_s a_r,
\end{aligned}
\tag{6.30}
$$

where $\mathcal{J}$ and $\mathcal{K}$ are defined in equations (3.9) and (3.10), respectively. This form of V seems to suggest that it has a one-body as well as a two-body part. However, normal ordering the operator with respect to $|\Psi_0^{(0)}\rangle$ as the Fermi vacuum reveals that the one-body part of V cancels out. Doing exactly the same calculations as in section 2.6.4 leads to

$$
\begin{aligned}
V = &-\sum_{pq}\langle p|(\mathcal{J}-\mathcal{K})|q\rangle\{a_p^\dagger a_q\} - \sum_{i}\langle i|(\mathcal{J}-\mathcal{K})|i\rangle \\
&+ \frac{1}{4}\sum_{pqrs}\langle pq||rs\rangle\{a_p^\dagger a_q^\dagger a_s a_r\} + \sum_{pq}\sum_{i}\langle pi||qi\rangle\{a_p^\dagger a_q\} \\
&+ \frac{1}{2}\sum_{ij}\langle ij||ij\rangle
\end{aligned}
\tag{6.31}
$$

Noting that $\langle p|(J-K)|q\rangle = \langle pi||qi\rangle$, the one-body parts now cancel, and we arrive at

$$V = \frac{1}{4}\sum_{pqrs}\langle pq||rs\rangle\{a_p^\dagger a_q^\dagger a_s a_r\} - \frac{1}{2}\sum_{ij}\langle ij||ij\rangle. \tag{6.32}$$

This form of the perturbation makes it easier to evaluate the energy corrections.

The first order correction is:

$$E_0^{(1)} = \langle\Psi_0|V|\Psi_0\rangle = -\frac{1}{2}\sum_{ij}\langle ij||ij\rangle, \tag{6.33}$$

since the expectation of the normal product is equal to zero. Comparing equations (6.28) and (6.33) with equation (3.23) shows that the first order correction is included in the Hartree-Fock energy

$$E_0 = E_0^{(0)} + E_0^{(1)}. \tag{6.34}$$

To clearify, E_0 is the Hartree-Fock energy (reference energy), and $E_0^{(i)}$ is the i'th order correction to the exact energy $\mathscr{E}_0$.

$$\text{(diagram)} = a\!\!\!\bigcirc\!\!\!i \quad j\!\!\!\bigcirc\!\!\!b = \sum_{ijab} \frac{\langle ij||ab\rangle\langle ab||ij\rangle}{\varepsilon_i+\varepsilon_j-\varepsilon_a-\varepsilon_b}$$

Figure 6.1: Diagrammatic representation of the second order correction to the energy of Møller-Plesset perturbation theory.

6.4   Second order perturbation theory (MP2)

The expression for the second order correction is somewhat more complicated. It is given by

$$E_0^{(2)} = \langle \Psi_0^{(0)} | V R_0 V | \Psi_0^{(0)} \rangle. \tag{6.35}$$

Because of the resolvent R_0, only the normal product, W, of equation (6.32) survives, so that we get

$$E_0^{(2)} = \langle \Psi_0^{(0)} | W R_0 W | \Psi_0^{(0)} \rangle. \tag{6.36}$$

We have already calculated an almost identical expression in section 2.7. The only difference is that the resolvent

$$R_0 = \frac{Q}{E_0 - H_0} = \sum_{ia}^{\infty} \frac{|\Psi_i^a\rangle\langle\Psi_i^a|}{\varepsilon_i - \varepsilon_a} + \sum_{i<j,a<b} \frac{|\Psi_{ij}^{ab}\rangle\langle\Psi_{ij}^{ab}|}{\varepsilon_i + \varepsilon_j - \varepsilon_a - \varepsilon_b} + \dots \tag{6.37}$$

is squeezed between the two W operators. This simply has the effect that each term in equation (2.90) is divided by an energy denominator

$$\frac{1}{\varepsilon_i + \varepsilon_j - \varepsilon_a - \varepsilon_b} \tag{6.38}$$

which yields the result

$$E_0^{(2)} = \frac{1}{4} \sum_{ijab} \frac{|\langle ij||ab\rangle|^2}{\varepsilon_i + \varepsilon_j - \varepsilon_a - \varepsilon_b}. \tag{6.39}$$

This can be read off directly from the diagram of figure 6.1 according to the rules of section 2.7 and the following additional rule. Draw a horizontal line between each operator in the diagram. Each such line, called resolvent line, will contribute with a factor in the energy denominator. The factor is equal to the sum of all hole lines passing through minus the sum of all particle lines passing through.

6.4.1   MP2 in the RHF-case

In the case of RHF, the spin orbitals are assumed to be on the from

$$\{\psi_{2k}(\mathbf{x}),\, \psi_{2k+1}(\mathbf{x})\} = \{\phi_k(\mathbf{r})\alpha(s),\, \phi_k(\mathbf{r})\beta(s)\}. \tag{6.40}$$

This means that the sum over each spin orbital in equation (6.39) can be replaced by two sums. The sum over i, for example, is

$$\sum_{i=1}^{N} \psi_i = \sum_{i=1}^{N/2} \phi_i\alpha + \sum_{i=1}^{N/2} \phi_i\beta, \tag{6.41}$$

and we get similar sums for the other indices. Inserting this yields

$$
\begin{aligned}
E_0^{(2)} =& \frac{1}{4}\sum_{i,j=1}^{N/2}\sum_{a,b=N/2+1}^{M}\frac{1}{\varepsilon_{ij}^{ab}}\Big[|\langle(\phi_i\alpha)(\phi_j\alpha)||(\phi_a\alpha)(\phi_b\alpha)\rangle|^2 \\
&+ |\langle(\phi_i\beta)(\phi_j\beta)||(\phi_a\beta)(\phi_b\beta)\rangle|^2 + |\langle(\phi_i\alpha)(\phi_j\beta)||(\phi_a\alpha)(\phi_b\beta)\rangle|^2 \\
&+ |\langle(\phi_i\beta)(\phi_j\alpha)||(\phi_a\beta)(\phi_b\alpha)\rangle|^2 + |\langle(\phi_i\alpha)(\phi_j\beta)||(\phi_a\beta)(\phi_b\alpha)\rangle|^2 \\
&+ |\langle(\phi_i\beta)(\phi_j\alpha)||(\phi_a\alpha)(\phi_b\beta)\rangle|^2\Big],
\end{aligned}
\tag{6.42}
$$

where M is the number of spatial orbitals (equal to the number of spatial basis functions) and

$$
\varepsilon_{ij}^{ab} = \varepsilon_i + \varepsilon_j - \varepsilon_a - \varepsilon_b.
\tag{6.43}
$$

Terms which are automatically zero due to spin have not been included. Integrating out spin now yields

$$
\begin{aligned}
E_0^{(2)} =& \frac{1}{4}\sum_{i,j=1}^{N/2}\sum_{a,b=N/2+1}^{M}\frac{1}{\varepsilon_{ij}^{ab}}\Big[|\langle\phi_i\phi_j||\phi_a\phi_b\rangle|^2 \\
&+ |\langle\phi_i\phi_j||\phi_a\phi_b\rangle|^2 + |\langle\phi_i\phi_j|g|\phi_a\phi_b\rangle|^2 \\
&+ |\langle\phi_i\phi_j|g|\phi_a\phi_b\rangle|^2 + |\langle\phi_i\phi_j|g|\phi_b\phi_a\rangle|^2 \\
&+ |\langle\phi_i\phi_j|g|\phi_b\phi_a\rangle|^2\Big].
\end{aligned}
\tag{6.44}
$$

Note that the first two terms in the sum have both the direct term and the exchange term, whereas in the rest of the terms only one of these (direct or exchange) survives. Collecting equal terms finally gives

$$
E_0^{(2)} = \sum_{i,j=1}^{N/2}\sum_{a,b=N/2+1}^{M}\frac{\langle ij|g|ab\rangle\big(2\langle ab|g|ij\rangle - \langle ab|g|ji\rangle\big)}{\varepsilon_{ij}^{ab}}.
\tag{6.45}
$$

Note that in this expression the explicit appearance of ϕ has been supressed. To avoid confusion as to whether the sum is over spin orbitals or spatial orbitals (in this case it is the latter), we shall use the following convention. If the summation ranges are given explicitly, the sum is over spatial orbitals. Otherwise, the sum is over spin orbitals.

6.4.2 MP2 in the UHF-case

In the case of UHF, the spinorbitals are assumed to be on the form

$$
\{\psi_{2k}(\mathbf{x}),\,\psi_{2k+1}(\mathbf{x})\} = \{\phi_k^\alpha(\mathbf{r})\alpha(s),\,\phi_k^\beta(\mathbf{r})\beta(s)\}.
\tag{6.46}
$$

Inserting this in equation (6.39) and integrating out spin in the same manner as above yields

$$
\begin{aligned}
E_0^{(2)} =& \frac{1}{4} \sum_{i=1}^{N^\alpha} \sum_{j=1}^{N^\alpha} \sum_{a=N^\alpha+1}^{M} \sum_{b=N^\alpha+1}^{M} \frac{|\langle \phi_i^\alpha \phi_j^\alpha || \phi_a^\alpha \phi_b^\alpha \rangle|^2}{\varepsilon_i^\alpha + \varepsilon_j^\alpha - \varepsilon_a^\alpha - \varepsilon_b^\alpha} \\
&+ \frac{1}{4} \sum_{i=1}^{N^\beta} \sum_{j=1}^{N^\beta} \sum_{a=N^\beta+1}^{M} \sum_{b=N^\beta+1}^{M} \frac{|\langle \phi_i^\beta \phi_j^\beta || \phi_a^\beta \phi_b^\beta \rangle|^2}{\varepsilon_i^\beta + \varepsilon_j^\beta - \varepsilon_a^\beta - \varepsilon_b^\beta} \\
&+ \frac{1}{4} \sum_{i=1}^{N^\alpha} \sum_{j=1}^{N^\beta} \sum_{a=N^\alpha+1}^{M} \sum_{b=N^\beta+1}^{M} \frac{|\langle \phi_i^\alpha \phi_j^\beta | g | \phi_a^\alpha \phi_b^\beta \rangle|^2}{\varepsilon_i^\alpha + \varepsilon_j^\beta - \varepsilon_a^\alpha - \varepsilon_b^\beta} \\
&+ \frac{1}{4} \sum_{i=1}^{N^\beta} \sum_{j=1}^{N^\alpha} \sum_{a=N^\beta+1}^{M} \sum_{b=N^\alpha+1}^{M} \frac{|\langle \phi_i^\beta \phi_j^\alpha | g | \phi_a^\beta \phi_b^\alpha \rangle|^2}{\varepsilon_i^\beta + \varepsilon_j^\alpha - \varepsilon_a^\beta - \varepsilon_b^\alpha} \\
&+ \frac{1}{4} \sum_{i=1}^{N^\alpha} \sum_{j=1}^{N^\beta} \sum_{a=N^\beta+1}^{M} \sum_{b=N^\alpha+1}^{M} \frac{|\langle \phi_i^\alpha \phi_j^\beta | g | \phi_b^\alpha \phi_a^\beta \rangle|^2}{\varepsilon_i^\alpha + \varepsilon_j^\beta - \varepsilon_b^\alpha - \varepsilon_a^\beta} \\
&+ \frac{1}{4} \sum_{i=1}^{N^\beta} \sum_{j=1}^{N^\alpha} \sum_{a=N^\alpha+1}^{M} \sum_{b=N^\beta+1}^{M} \frac{|\langle \phi_i^\beta \phi_j^\alpha | g | \phi_b^\beta \phi_a^\alpha \rangle|^2}{\varepsilon_i^\beta + \varepsilon_j^\alpha - \varepsilon_b^\beta - \varepsilon_a^\alpha}.
\end{aligned}
\tag{6.47}
$$

Since the last four terms are equal, this is reduced to

$$
\begin{aligned}
E_0^{(2)} =& \frac{1}{4} \sum_{i=1}^{N^\alpha} \sum_{j=1}^{N^\alpha} \sum_{a=N^\alpha+1}^{M} \sum_{b=N^\alpha+1}^{M} \frac{|\langle \phi_i^\alpha \phi_j^\alpha || \phi_a^\alpha \phi_b^\alpha \rangle|^2}{\varepsilon_i^\alpha + \varepsilon_j^\alpha - \varepsilon_a^\alpha - \varepsilon_b^\alpha} \\
&+ \frac{1}{4} \sum_{i=1}^{N^\beta} \sum_{j=1}^{N^\beta} \sum_{a=N^\beta+1}^{M} \sum_{b=N^\beta+1}^{M} \frac{|\langle \phi_i^\beta \phi_j^\beta || \phi_a^\beta \phi_b^\beta \rangle|^2}{\varepsilon_i^\beta + \varepsilon_j^\beta - \varepsilon_a^\beta - \varepsilon_b^\beta} \\
&+ \sum_{i=1}^{N^\alpha} \sum_{j=1}^{N^\beta} \sum_{a=N^\alpha+1}^{M} \sum_{b=N^\beta+1}^{M} \frac{|\langle \phi_i^\alpha \phi_j^\beta | g | \phi_a^\alpha \phi_b^\beta \rangle|^2}{\varepsilon_i^\alpha + \varepsilon_j^\beta - \varepsilon_a^\alpha - \varepsilon_b^\beta}
\end{aligned}
\tag{6.48}
$$

6.5   Third order perturbation theory (MP3)

The third order correction is given by

$$
E_0^{(3)} = \langle \Psi_0^{(0)} | V R_0 (V - E_0^{(1)}) R_0 V | \Psi_0^{(0)} \rangle,
\tag{6.49}
$$

which, when using that $V = W + E^{(1)}$ and $R_0 |\Psi_0^{(0)}\rangle = 0$, can be written as

$$
E_0^{(3)} = \langle \Psi_0^{(0)} | W R_0 W R_0 W | \Psi_0^{(0)} \rangle.
\tag{6.50}
$$

We can evaluate this expression in the same manner as the second order correction, the only difference now being that there are two resolvent lines. The diagrams for this term was set up and discussed in section 2.7. The result is shown in figure 6.2.

Figure 6.2: Diagrammatic representation of the third order correction to the energy of Møller-Plesset perturbation theory.

Integrating out the spin part of these equations are a little bit more involved and tedious than for the second order case, and the derivation and results are therefore shown in appendix B.

Chapter 7

Nelder-Mead minimisation method

So far we have discussed how we can calculate the energy of a molecular system for a given configuration. The set of all possible configurations is called the configuration space. If we calculate the energy of the system for the entire configuration space, we get the so-called potential energy surface (often abbreviated PES in the literature). From the potential energy surface, it is possible to classically simulate the trajectories of the atoms as a function of time. This is exactly what is done in molecular dynamics simulations.

When the temperature of a system is very low, the atoms will vibrate in the neighbourhood of their equilibrium positions. The corresponding point in configuration space will then oscillate in the vicinity of some local minimum. Hence, searching for an equilibrium configuration is mathematically equivalent to searching for a minimum of the potential energy surface.

In this chapter we discuss the Nelder-Mead method [28], which is a rather simple method for minimizing functions in many-dimensional space. The method is quite popular in compuational chemistry, largely due to the fact that functional derivatives are not needed, which in many cases can be difficult to calculate.

7.1   The algorithm

Assume that we are given a function $f : \mathbb{R}^n \to \mathbb{R}$ which is to be minimised. Whereas Newton-Raphson type methods use the function value and its derivatives in a *single point* to iterate forward towards a minimum, the Nelder-Mead method uses function values in *several points* in space to decide in which direction to move. The method proceeds as follows.

1. Generate a simplex with vertices $\mathbf{x}_1, \mathbf{x}_2, \ldots, \mathbf{x}_{n+1}$. (The simplex is defined below.)

2. Order the the points so that $f(\mathbf{x}_1) \leq f(\mathbf{x}_2) \leq \cdots \leq f(\mathbf{x}_{n+1})$.

3. Calculate the *center of gravity* $\mathbf{x}_g$ of all the points excluding the worst:

$$\mathbf{x}_g = \frac{1}{n} \sum_{i=1}^{n} \mathbf{x}_i. \tag{7.1}$$

4. Compute the coordinates of the *reflected point*

$$\mathbf{x}_r = \mathbf{x}_g + \alpha(\mathbf{x}_g - \mathbf{x}_{n+1}), \tag{7.2}$$

see figure 7.1a. We then have the following possibilities:

(a) The reflected point is better than the next worst point but not better than the best, that is, $f(\mathbf{x}_1) \leq f(\mathbf{x}_r) < f(\mathbf{x}_n)$. If so, replace $\mathbf{x}_{n+1}$ with $\mathbf{x}_r$ and move to step 2.

(b) The reflected point is the new best point, that is, $f(\mathbf{x}_r) < f(\mathbf{x}_1)$. If so, proceed to step 5.

(c) The reflected point is not better than the next worst point, that is, $f(\mathbf{x}_r) \geq f(\mathbf{x}_n)$. If so, move to step 6.

5. Compute the coordinates of the *expanded point*

$$\mathbf{x}_e = \mathbf{x}_g + \gamma(\mathbf{x}_g - \mathbf{x}_{n+1}), \tag{7.3}$$

see figure 7.1b. We then have the following possibilities:

(a) The expaned point is better than the reflected point, that is, $f(\mathbf{x}_e) < f(\mathbf{x}_r)$. If so, replace $\mathbf{x}_{n+1}$ with $\mathbf{x}_e$ and move to step 2.

(b) The expanded point is not better than the reflected point, that is, $f(\mathbf{x}_e) \geq f(\mathbf{x}_r)$. If so, replace $\mathbf{x}_{n+1}$ with $\mathbf{x}_r$ and move to step 2.

6. Compute the coordinates of the *contracted point*

$$\mathbf{x}_c = \mathbf{x}_g + \rho(\mathbf{x}_g - \mathbf{x}_{n+1}), \tag{7.4}$$

see figure 7.1c. Consider then the following possibilities:

(a) The contracted point is better than the worst point, that is, $f(\mathbf{x}_c) < f(\mathbf{x}_{n+1})$. If so, replace $\mathbf{x}_{n+1}$ with $\mathbf{x}_c$ and move to step 2.

(b) The contracted point is not better than the worst point, that is, $f(\mathbf{x}_c) \geq f(\mathbf{x}_{n+1})$. If so, go to step 7.

7. *Reduction.* For all but the best point $\mathbf{x}_1$ replace the point with

$$\mathbf{x}_i' = \mathbf{x}_1 + \sigma(\mathbf{x}_i - \mathbf{x}_1), \qquad \text{for all } i \in \{2, \ldots, n+1\}, \tag{7.5}$$

see figure 7.1d, and go to step 2.

The search is terminated after some convergence criterium is reached. In this thesis we have chosen to stop the search when

$$f(\mathbf{x}_{n+1}) - f(\mathbf{x}_1) < \varepsilon_{\text{toler}}, \tag{7.6}$$

where $\varepsilon_{\text{toler}}$ is some predefined tolerance.

The coefficients α, γ, ρ and σ are called the reflection, expansion, contraction and shrink coefficients, respectively. Standard values are $\alpha = 1$, $\gamma = 2$, $\rho = -1/2$ and $\sigma = 1/2$.

The search is initiated by defining a simplex. A simplex is the generalisation of a triangle to many dimensions. A triangle is a simplex in two dimensions and a tetrahedron is a simplex in three dimensions. The general definition is as follows. If $\mathbf{x}_1, \ldots, \mathbf{x}_{n+1}$ are points in $\mathbb{R}^n$ such that the vectors $\mathbf{x}_2 - \mathbf{x}_1, \ldots, \mathbf{x}_{n+1} - \mathbf{x}_1$ are linearly independent, the simplex C is the set

$$C = \left\{ \sum_{i=1}^{n+1} \theta_i \mathbf{x}_i \,\middle|\, \theta_i \geq 0 \,\forall\, i, \quad \sum_{i=1}^{n+1} \theta_i = 1 \right\}. \tag{7.7}$$

The various operations of the method can heuristically be explained as follows. Since $\mathbf{x}_{n+1}$ is the point with the largest function value, one can expect the minimum to be located somewhere on the line between $\mathbf{x}_{n+1}$ and the center of gravity of the other points. The default guess is to try the reflected point $\mathbf{x}_r$ (figure 7.1a). If this point is the lowest point so far, the search should be extended further in the same direction (figure 7.1b). On the other hand, if the reflected point is not better than any of the points $\{\mathbf{x}_1, \ldots, \mathbf{x}_n\}$, it seems that we have moved past the minimum. Thus it is reasonable to try the contracted point (figure 7.1c). If this is not better than the worst point $\mathbf{x}_{n+1}$, we are not sufficiently close to a local minimum, and the simplex size is therefore shrinked towards the best point $\mathbf{x}_1$ (figure 7.1d).

7.2   Removing rigid body motions
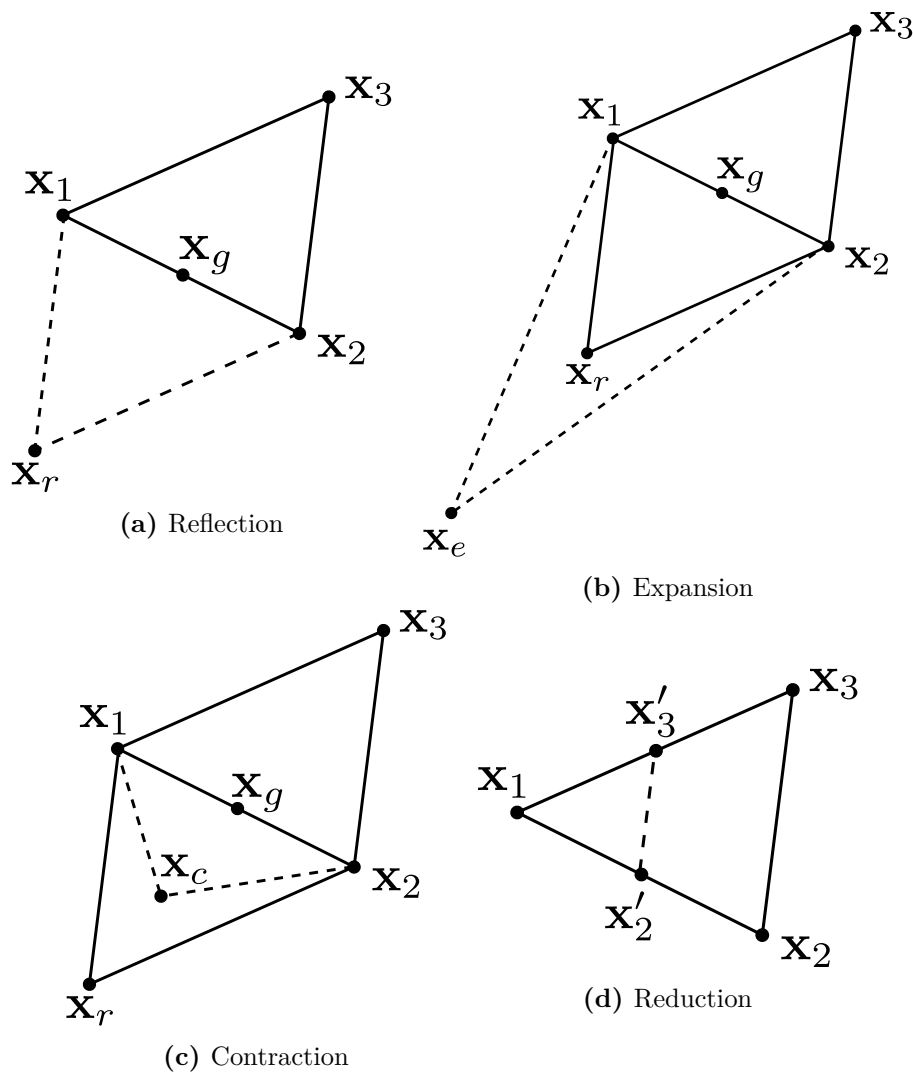
Consider a system of K atoms, where the nucleus of atom number i is centered at

$$\mathbf{R}_i = [R_{ix}, R_{iy}, R_{iz}]. \tag{7.8}$$

The vector $\mathbf{x}$ considered in the previous section will then be the $3K$-dimensional vector

$$\mathbf{x} = [\mathbf{R}_1, \mathbf{R}_2, \ldots, \mathbf{R}_K]. \tag{7.9}$$

However, since rigid body motions do not change the energy of the system, we should remove translational and rotational degrees of freedom associated with rigid body motions before searching for an energy minimum. For a system of two atoms, there is only one degree of freedom to vary during minimisation, namely the distance between them. For systems of $K > 2$ atoms, there are $3K - 6$ degrees of freedom after the removal of three translations and three rotations. In the code, the degrees of freedom associated with rigid body motions are eliminated in the following way.

(a) Reflection

(b) Expansion

(c) Contraction

(d) Reduction

Figure 7.1: Illustration of the various operations in the Nelder-Mead algorithm in the two-dimensional case.

1. The system is translated so that the first atom is located at the origin.

2. The system is rotated so that the second atom is located at the x-axis. (Two rotations: One around the z-axis and one around the y-axis.)

3. If there are more than two atoms, the system is rotated so that the third atom is placed on the xy-plane. (One rotation around the x-axis.)

4. During minimisation, the following coordinates, which are now equal to zero, are removed from the vector $\mathbf{x}$: $R_{1x}, R_{1y}, R_{1z}, R_{2y}, R_{2z}, R_{3z}$. The last coordinate is of course only removed if there are three atoms or more.

Part II

Implementation

Chapter 8

Program structure and classes

8.1 Introduction

The Hartree-Fock method and Møller-Plesset perturbation theory are coded in the C++ programming language. The program is written in an object oriented fashion, making it relatively easy to extend with new features. This chapter describes the structure of the program and how various routines have been implemented in different classes. The entire program is available at https://github.com/henrikei/HartreeFock.
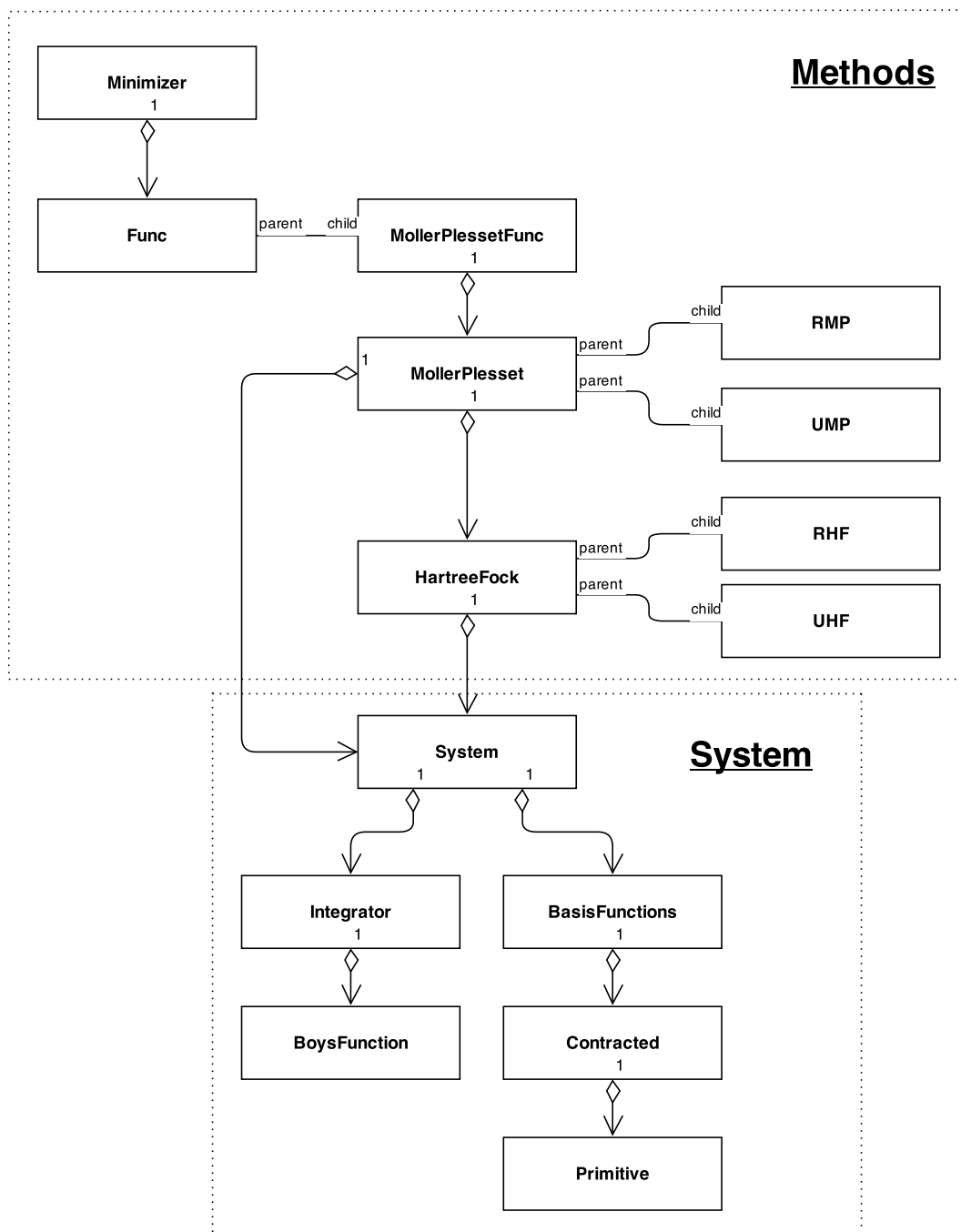
The various classes and their relations are shown in figure 8.1. Vertical arrows indicate a "member of" relation, while horizontal lines indicate a "parent-child" relation. As the dotted lines in the figure indicate, we have tried to distinguish between the system and the methods. However, what do we define as being part of the system and part of the methods? Variables such as the positions and charges of the nuclei and the number of electrons are obviously system variables. But what about the basis functions? One might intuitively define them as part of the methods as they are purely man made objects. However, recall that we are using basis functions which mimic the atomic orbitals. For this reason, we have chosen to let class System hold all information about the basis functions. Furthermore, since we are using only one type of basis functions, namely Gaussians, class System has a method for performing the integration as well.

The code makes extensive use of the linear algebra library Armadillo [29], which greatly simplifies the mathematics. Not only does it have standard objects such as vectors and matrices, but it also offers higher dimensional objects such as cubes and fields. A cube is the same as a matrix except that it has three indices instead of two. A field object is similar to a vector, matrix or cube except that, instead of each element being a scalar, each element can be a vector, matrix or cube.

8.2 Class HartreeFock

The central piece of the program is the rather short and simple virtual class HartreeFock. The main tasks of this class are to:

- Obtain and store the overlap integrals $\langle \mu | \nu \rangle$, one-particle integrals $\langle \mu | h | \mu \rangle$ and

Methods

Minimizer
1

Func

parent   child

MollerPlessetFunc
1

RMP

child

parent

1   MollerPlesset
1

parent

child

UMP

RHF

child

parent

HartreeFock
1

parent

child

UHF

System

System
1   1

Integrator
1

BasisFunctions
1

BoysFunction

Contracted
1

Primitive

Figure 8.1: Diagram of the various classes of the program. Vertical arrows indicate a "member of" relation, while horizontal lines signify a "parent-child" relation.

two-particle integrals $\langle \mu\sigma|g|\nu\lambda \rangle$.

- Solve a single iteration of the self-consistent field equations.

The overlap and one-particle integrals are stored in Armadillo matrices `m_S` and `m_h`, respectively, and the two-particle integrals are stored in a two-dimensional field `m_Q` with each element `m_Q(i,j)` beging a matrix.

The HartreeFock class obtains these integrals by calling the System class, which is responsible for storing and providing all the information about the system. For example, the overlap and one-particle integrals are obtained in the following way:

```
rowvec oneElectronIntegrals;
for (int i = 0; i < m_matDim; i++){
    for (int j = i; j < m_matDim; j++){
        oneElectronIntegrals = m_system->getOneElectronIntegrals(i,j);
        m_S(i,j) = oneElectronIntegrals(0);
        m_S(j,i) = m_S(i,j);
        m_h(i,j) = oneElectronIntegrals(1);
        m_h(j,i) = m_h(i,j);
    }
}
```

Here, `m_system` is an instance of the System class. Note that the HartreeFock class need not know anything about the details of the system under consideration. It simply passes the indices (i, j) to the System class, which processes this and returns the integrals of interest.

The function

```
void solveSingle(const mat &Fock, mat &Coeffs, mat &P, colvec &fockEnergy, int
    nElectrons);
```

of the HartreeFock class solves the set of equations defined by the matrix `Fock` and stores the resulting eigenvalues and eigenvectors in the matrices `fockEnergy` and `Coeffs`, respectively. It also returns the corresponding density matrix `P`. When solving the self-consistent field equations, this function is called iteratively until convergence is obtained.

The HartreeFock class has two subclasses RHF and UHF in which the specifics of the restricted and unrestricted Hartree-Fock methods are implemented, respectively. The difference between these two methods lies mainly in the way the Fock matrices are constructed. In the RHF class, the Fock matrix is constructed according to equation (3.63), whereas in class UHF the spin-up and spin-down Fock matrices are constructed according to equations (3.84) and (3.85). When solving the self-consistent field equations, both subclasses call the function solveSingle of parent class HartreeFock. The only difference lies in the arguments being passed to the function. For example, in the RHF class, the self-consistent field equations are solved as follows:

```
double fockEnergyOld;
double energyDiff = 1.0;
```

```
while (energyDiff > m_toler){
    fockEnergyOld = m_fockEnergy(0);
    buildFockMatrix();
    solveSingle(m_F, m_C, m_P, m_fockEnergy, m_nElectrons);
    energyDiff = fabs(fockEnergyOld − m_fockEnergy(0));
}
```

where `m_toler` is the tolerance, which is set equal to $1.0 \cdot 10^{-12}$.

Before moving on to describe how the System class works, we need to discuss the classes holding information about the basis functions.

8.3   Class Primitive

The Primitive class is a small class which simply stores the exponent, coefficient, powers $(x^i y^j z^k)$ and center of a Gaussian primitive function.

8.4   Class Contracted

The Contracted class, also quite short, holds an std vector of pointers to one or more Primitives:

```
vector<Primitive*> m_primitives;
```

8.5   Class BasisFunctions

The BasisFunctions class holds an std vector of pointers to all the contracted objects of the system under consideration:

```
vector<Contracted*> m_contracteds;
```

The class has a parser which reads input files on the TurboMole format. Contracted basis functions are added by calling the function addContracteds:

```
p_basisFunctions−>addContracteds("../../HartreeFock/
                                 inFiles/basisSets/O_431G.dat", 0);
```

The first argument is the path to the input file, and the second argument is an integer which identifies the nucleus at which the basis set is to be centered.[1] In the above example, the 4-31G basis set for oxygen is specified for the first nucleus (the position itself is specified in the System class, which we describe below). The input file is given by

_____

[1] Each basis function is always centered at one of the nuclei in this thesis.

```
#  4-31G  EMSL  Basis Set Exchange Library  4/16/14 1:15 PM
# Elements                            References
# --------                            ----------
# H, C - F: R. Ditchfield, W.J. Hehre and J.A. Pople, J. Chem. Phys. 54, 724
#           (1971).
# He, Ne:   Gaussian 90
# Li, Be:   These are actually 5-21G basis sets.
# Na - Ar:  M.S. Gordon, J.S. Binkley, J.A. Pople, W.J. Pietro and W.J. Hehre,
#           J. Am. Chem. Soc. 104, 2797 (1983).
#


$basis
*
o   4-31G
*
    4  s
    883.2728600              0.0175506
    133.1292800              0.1228292
     29.9064080              0.4348836
      7.9786772              0.5600108
    3  s
     16.1944470             -0.1134010
      3.7800860             -0.1772865
      1.0709836              1.1504079
    1  s
      0.2838798              1.0000000
    3  p
     16.1944470              0.0685453
      3.7800860              0.3312254
      1.0709836              0.7346079
    1  p
      0.2838798              1.0000000
*
$end
```

The first and second column contain the exponents and coefficients of the primitives, respectively. In this example, a total of 9 contracted objects are specified for the first oxygen atom (with index 0): Three s-, two p_x-, two p_y- and two p_z-functions. The contracted objects are simply appended to the std vector `m_contracteds`. Thus every contracted basis function is automatically assigned a unique number, namely its position in the vector `m_contracteds`. All the input files have been taken from the EMSL Basis Set Library [30].

There are two potential pitfalls regarding these input files which should be noted. First, the coefficients are to be used with *normalised* Gaussian primitives. When discussing the integration scheme in chapter 4, the normalisation coefficient was left out for notational convenience. The normalised Gaussian function is given in equation (4.7).

Second, there is an ambiguity concerning the atomic orbitals with $l > 1$. For example, when $l = 2$, there are a total of six possible combinations of index values (i, j, k) which sum to two. This leads to the possible prefactors x^2, y^2, z^2, xy, yz and xz. These functions are called Cartesian d functions. However, the solution of

the Schrödinger equation for the hydrogen atom has only five d functions. Many program packages therefore also choose to use five d functions, referred to as canonical d functions. These are often taken to be xy, xz, yz, $x^2 - y^2$ and $3z^2 - r^2$ [17]. The same ambiguity presents itself for higher values of l. We will use Cartesian atomic orbitals throughout this thesis.

8.6 Class System

The system to be analysed is defined in an instance of the System class. The most important member variables of this class are:

- `mat m_nucleiPositions` which contains the positions of the nuclei.

- `rowvec m_charges` which contains the nuclei charges.

- `int m_nElectronsUp`, `int m_nElectronsDown` and `int m_nElectrons` storing the number of spin-up and spin-down electrons as well as the total number of electrons.

- `BasisFunctions *m_basisFunctions` holding all information about the basis functions.

- `Integrator *m_integrator` which performs the integrations.

The main task of the class is to pass computed integrals to the HartreeFock class upon request. In the previous section we saw how the HartreeFock class calls the function getOneElectronIntegrals of the System class. This function then returns the integral in question in the following manner:

```
rowvec2 System::getOneElectronIntegrals(int p, int q)
{
Contracted* contractedA = m_basisFunctions->getContracted(p);
Contracted* contractedB = m_basisFunctions->getContracted(q);

int nPrimitivesA = contractedA->getNumOfPrimitives();
int nPrimitivesB = contractedB->getNumOfPrimitives();

double overlap = 0;
double energy = 0;

Primitive* primitiveA;
Primitive* primitiveB;
for (int v = 0; v < nPrimitivesA ; v++){
    primitiveA = contractedA->getPrimitive(v);
    m_integrator->setPrimitiveA(primitiveA);
    for (int w = 0; w < nPrimitivesB; w++){
        primitiveB = contractedB->getPrimitive(w);
        m_integrator->setPrimitiveB(primitiveB);
        m_integrator->setE_AB("oneParticle");

        energy += m_integrator->kinetic()*primitiveA->getCoeff()*primitiveB->
            getCoeff();
```

```
        for (int x = 0; x < m_nNuclei; x++){
            m_integrator->setNucleusPosition(m_nucleiPositions.row(x));
            energy += -m_integrator->coulomb1()*m_charges(x)*primitiveA->getCoeff
                ()*primitiveB->getCoeff();
        }

        overlap += m_integrator->overlap()*primitiveA->getCoeff()*primitiveB->
            getCoeff();
    }
}

rowvec2 oneElectronIntegrals = {overlap, energy};
return oneElectronIntegrals;
}
```

For a given combination of indices (p, q), this functions fetches the overlap and one-particle integrals between contracted basis number p and contracted basis number q. It does this by looping through all combinations of primitives in these contracted objects and passing them to the Integrator class, which performs the integration. The function getTwoParticleIntegrals works similarly.

8.7   Class Integrator

The main task of the Integrator class is to return the overlap and one-particle integrals between two primitives, as well as the two-particle integrals between four primitives. This is were the integration scheme of chapter 4 is implemented. The overlap integral is calculated from equation (4.84). The one-particle integrals are the sum of the kinetic integrals (4.87) and the Coulomb interaction between the electrons and the nuclei (4.90). Finally, the two-particle integrals are computed by equation (4.95). As the expressions show, in order to compute these quantities, the coefficients $E_{tuv}^{ab} = E_t^{ij} E_u^{kl} E_v^{mn}$ and R_{tuv} are needed. We will postpone the description of how to calculate these until the next chapter. For now we will simply assume that they are readily available.

As an example, we illustrate how the Coulomb interaction between the electrons and the nuclei is calculated. Continuing the discussion in the previous section, first the two primitives in question are passed to the integrator object. Thereafter, when the funtion `m_integrator->coulomb1()` is called, the Coulomb integral is calculated according to equation (4.90) as follows:

```
double Integrator::coulomb1()
{
    int i = m_primitiveA->getPow()(0);
    int j = m_primitiveB->getPow()(0);
    int k = m_primitiveA->getPow()(1);
    int l = m_primitiveB->getPow()(1);
    int m = m_primitiveA->getPow()(2);
    int n = m_primitiveB->getPow()(2);

    return coulomb1(i, j, k, l, m, n);
}
```

```cpp
double Integrator::coulomb1(int i, int j, int k, int l, int m, int n)
{
    int tMax = i + j;
    int uMax = k + l;
    int vMax = m + n;

    rowvec3 A = m_primitiveA->getPos();
    rowvec3 B = m_primitiveB->getPos();

    double alpha = m_primitiveA->getExp();
    double beta = m_primitiveB->getExp();
    double p = alpha + beta;
    rowvec3 P = (alpha*A + beta*B)/p;
    rowvec3 PC = P - m_nucleusPosition;

    setR(p, PC, tMax, uMax, vMax);

    double value = 0;
    for (int t = 0; t < tMax + 1; t++){
        for (int u = 0; u < uMax + 1; u++){
            for (int v = 0; v < vMax + 1; v++){
                value += m_E_AB[0](i,j,t)*m_E_AB[1](k,l,u)
                            *m_E_AB[2](m,n,v)*m_R.at(0)(t,u,v);
            }
        }
    }
    value *= 2*M_PI/p;
    return value;
}
```

The integers i, j, k, l, m, n are the powers of the two primitives in question:

$$G_a(\mathbf{r}) = G_{ikm}(a, \mathbf{r}_A) = x_A^i \, y_A^k \, z_A^m \exp(-ar_A^2), \tag{8.1}$$

$$G_b(\mathbf{r}) = G_{jln}(b, \mathbf{r}_B) = x_B^j \, y_B^l \, z_B^n \exp(-br_B^2), \tag{8.2}$$

and $t_{max} = i + j$, $u_{max} = k + l$ and $v_{max} = m + m$ are the upper limits of the loop in equation (4.90). Before entering the loop, the coefficients R_{tuv} are calculated in the function `setR` (the coefficients $E_{tuv}^{ab} = E_t^{ij} E_u^{kl} E_v^{mn}$ are set before the function `m_integrator->coulomb1()` is called, see the code snippet in the previous section).

8.8   Class MollerPlesset

The Møller-Plesset perturbation theory is implemented in the MollerPlesset class. This class uses the eigenvalues and eigenvectors, as well as the integrals $\langle \mu\sigma|g|\nu\lambda \rangle$, obtained from a Hartree-Fock calculation to compute the Møller-Plesset perturbative terms. The integrals $\langle \mu\sigma|g|\nu\lambda \rangle$ are so-called *atomic orbital integrals* (AOIs) since they are calculated with the *atomic orbitals* (basis functions) $\chi_\mu, \chi_\sigma, \chi_\nu$ and χ_λ. However, the integrals needed in the perturbation sums are *molecular orbital integrals* (MOIs). The

molecular orbitals are simply

$$\phi_k(\mathbf{r}) = \sum_{\mu=1}^{M} C_{\mu k} \chi_\mu(\mathbf{r}), \tag{8.3}$$

in the restricted case and

$$\phi_k^\alpha(\mathbf{r}) = \sum_{\mu=1}^{M} C_{\mu k}^\alpha \chi_\mu(\mathbf{r}), \tag{8.4}$$

$$\phi_k^\beta(\mathbf{r}) = \sum_{\mu=1}^{M} C_{\mu k}^\beta \chi_\mu(\mathbf{r}), \tag{8.5}$$

in the unrestricted case, where $\{\mathbf{C}_k\}$, $\{\mathbf{C}_k^\alpha\}$ and $\{\mathbf{C}_k^\beta\}$ are the eigenvectors obtained from the Hartree-Fock calculations. Thus, before calculating the perturbation sums, the following transformation must be performed for every combination of p, q, r, s:

$$\langle pq|g|rs \rangle = \sum_{\mu,\sigma,\nu,\lambda=1}^{M} \langle \mu\sigma|g|\nu\lambda \rangle C_{\mu p} C_{\sigma q} C_{\nu r} C_{\lambda s}. \tag{8.6}$$

The most economical way of doing this is to perform the transformation for each index p, q, r and s one at a time. That is, first do the transformation

$$\langle \mu\sigma|g|\nu\lambda \rangle \rightarrow \langle p\sigma|g|\nu\lambda \rangle = \sum_{\mu=1}^{M} \langle \mu\sigma|g|\nu\lambda \rangle C_{\mu p}, \tag{8.7}$$

for every combination of p, σ, ν and λ. Thereafter, do the same by summing over the index σ:

$$\langle p\sigma|g|\nu\lambda \rangle \rightarrow \langle pq|g|\nu\lambda \rangle = \sum_{\sigma=1}^{M} \langle p\sigma|g|\nu\lambda \rangle C_{\sigma q}, \tag{8.8}$$

for every combination of p, q, λ and ν. Continuing in this manner, we obtain the desired MOIs. This transformation is the most costly part of the Møller-Plesset scheme, scaling as $\mathcal{O}(M^5)$, where M is the number of basis functions.

Since the restricted Hartree-Fock equations are different from the unrestricted ones, the expressions for the Møller-Plesset corrections naturally reflect this. The MollerPlesset class is therefore subclassed into the classes RMP (restricted Møller-Plesset) and UMP (unrestricted Møller-Plesset). Each of these subclasses holds an instance of class RHF and UHF, respectively.

The second order corrections are calculated according to equations (6.45) and (6.48) for the restricted and unrestricted cases, respectively. These terms scale as $\mathcal{O}(O^2 V^2)$, where O and V are the numbers of occupied and virtual spatial orbitals, respectively. The third order corrections are calculated as the sum of equations (B.8), (B.9) and (B.11) in the restricted case and as the sum of equations (B.13), (B.14) and (B.15) in the unrestricted case. The third order terms scale as $\mathcal{O}(O^3 V^3) + \mathcal{O}(O^2 V^4)$.

8.9   Class Minimizer

The Nelder-Mead minimisation method, described in detail in chapter 7, is implemented in the Minimizer class. The method's greatest asset is that it only needs to evaluate the function value at various points in space (no derivatives needed) to perform the minimisation. It is quite general and can minimise any many-dimensional scalar function. In order to achieve this, it holds an object of a purely virtual class named Func. The latter class contains no more than two purely virtual functions:

```cpp
class Func
{
public:
    Func();
    ~Func();
    virtual rowvec getx()=0;
    virtual double getValue(rowvec x)=0;
};
```

As their names suggest, these functions are supposed to return the coordinate and function value, respectively. The specific function which is to be minimised, must be be implemented as a subclass of parent class Func. Of interest in this thesis, of course, is the minimisation of the energy of molecules as calculated at the Hartree-Fock or Møller-Plesset level of theory. To achieve this, we have created the subclass MollerPlessetFunc, which returns the energy of the molecule under consideration at the desired level of theory (first, second or third order Møller-Plesset theory[2]).

---

[2]Recall that the first order Møller-Plesset energy is the same as the Hartree-Fock energy.

Chapter 9

Computational details

The previous chapter described the program structure and the tasks assigned to the various classes. However, many details were left out so not to smokescreen the outline of the program. Nevertheless, many of the left out details deserve further discussion. We address some of these details in this chapter.

9.1 Solving the SFC equations

As described in chapter 3, solving the Hartree-Fock equations boils down to solving the set of algebraic equations (3.53) or (3.77) and (3.78) in the restricted and unrestricted case, respectively. In the following, we focus on the restricted set of equations (the unrestricted equations are solved analogously). The equations are often referred to as self consistent field (SCF) equations because they must be solved in an iterative manner until there is consistency between the solution $\{\mathbf{C}_k\}$ and the Fock matrix $\mathbf{F}$. In the code, this is done as shown schematically in figure 9.1. First the system is defined in the System class as described in the previous chapter. Thereafter, the one-particle integrals $\langle \mu | h | \nu \rangle$, two-particle integrals $\langle \mu\sigma | g | \nu\lambda \rangle$ and overlap integrals $\langle \mu | \nu \rangle$ are computed. Then, the transformation matrix $\mathbf{X}$ is calculated. It is constructed so that

$$\mathbf{X}^\dagger \mathbf{S} \mathbf{X} = \mathbf{I}. \tag{9.1}$$

Recall from section 3.6 that this is needed in order to transform the generalized eigenvalue problem

$$\mathbf{F}\mathbf{C}_k = \varepsilon_k \mathbf{S}\mathbf{C}_k, \tag{9.2}$$

to an ordinary eigenvalue problem

$$\mathbf{F}'\mathbf{C}'_k = \varepsilon_k \mathbf{C}'_k, \tag{9.3}$$

where

$$\mathbf{F}' = \mathbf{X}^\dagger \mathbf{F} \mathbf{X} \tag{9.4}$$

and

$$\mathbf{C}'_k = \mathbf{X}^{-1}\mathbf{C}_k. \tag{9.5}$$

Details concerning how to construct the transformation matrix $\mathbf{X}$ is discussed in section 3.6. Finally, before entering the SCF-loop, an initial guess is made for the density matrix[1]

$$P_{\sigma\lambda} = 2\sum_{k=1}^{N/2} C_{\sigma k}C_{\lambda k}, \tag{9.6}$$

which is neeeded in order to computed the first Fock matrix $\mathbf{F}$. In this code it is simply set equal to the zero matrix, which corresponds to a system of non-interacting electrons.

After entering the SCF-loop, the Fock matrix of the current eigenvalue problem is calculated based on the solution of the previous eigenvalue problem. The loop is continued until

$$|\varepsilon_1^{\mathrm{cur}} - \varepsilon_1^{\mathrm{prev}}| < \epsilon_{\mathrm{toler}}, \tag{9.7}$$

where $\varepsilon_1^{\mathrm{cur}}$ and $\varepsilon_1^{\mathrm{prev}}$ are the lowest eigenvalues of the current and previous iteration, respectively, and $\epsilon_{\mathrm{toler}}$ is the tolerance. In the code the tolerance is set equal to $\epsilon_{\mathrm{toler}} = 1,0\cdot 10^{-8}$ by default.

9.1.1   Symmetries of the two-particle integrals

The two-particle integrals $\langle\mu\sigma|g|\nu\lambda\rangle$ have symmetries which imply that not all elements need to be calculated. Firstly, since we are using real basis functions, the swapping $\mu \leftrightarrow \nu$ and $\sigma \leftrightarrow \lambda$ of indices do not change the value of the integral. And secondly, since the two-particle operator is symmetric with respect to particle one and particle two, the switching $(\mu, \nu) \leftrightarrow (\sigma, \lambda)$ also keeps the integral unchanged. Hence, we can save time by truncating the limits of the looping indices as follows:

```cpp
for (int i = 0; i < m_matDim; i++){
    for (int j = 0; j < i+1; j++){
        for (int k = 0; k < i+1; k++){
            for (int l = 0; l < j+1; l++){
                m_Q(i,j)(k,l) =m_system->getTwoElectronIntegral(i,j,k,l);
                m_Q(k,j)(i,l) = m_Q(i,j)(k,l);
                m_Q(i,l)(k,j) = m_Q(i,j)(k,l);
                m_Q(k,l)(i,j) = m_Q(i,j)(k,l);

                m_Q(j,i)(l,k) = m_Q(i,j)(k,l);
                m_Q(j,k)(l,i) = m_Q(i,j)(k,l);
                m_Q(l,i)(j,k) = m_Q(i,j)(k,l);
                m_Q(l,k)(j,i) = m_Q(i,j)(k,l);
            }
        }
    }
}
```
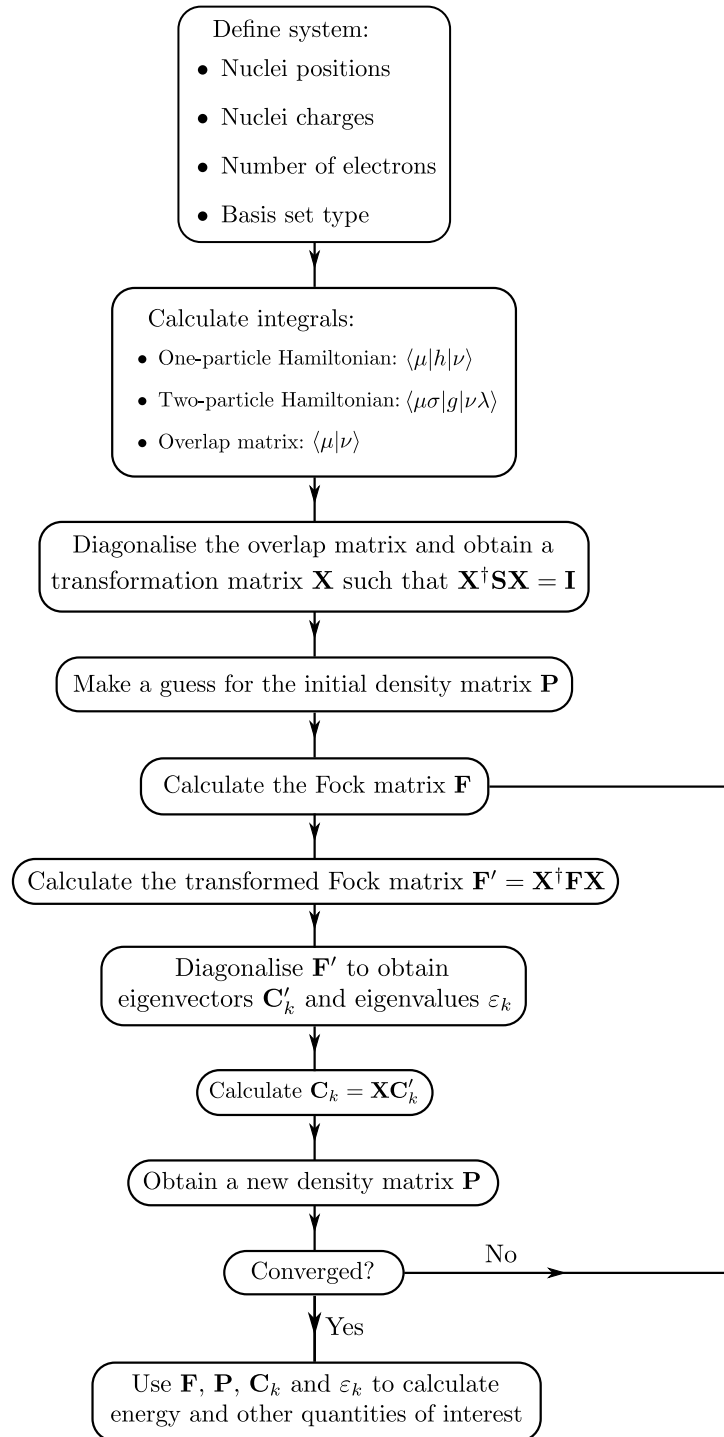
The two-particle integrals $\langle\mu\sigma|g|\nu\lambda\rangle$ are stored in member variable `m_Q`. The variable `m_Q` is an Armadillo object of type field. A field object is similar to a vector, matrix or cube except that, instead of each element being a scalar, each element can be a vector,

---

[1]We have here simply written $C_{\sigma k}$ instead of $C_{\sigma k}^*$ since we are using real basis functions.

Figure 9.1: Diagram of the self consistency solver in the RHF class. The solver in the UHF class is similar except that, instead of a single Fock matrix, there are two matrices $\mathbf{F}^\alpha$ and $\mathbf{F}^\beta$ which are diagonalised simultaneously.

matrix or cube. In the snippet above, `m_Q` is a two-dimensional field with each element `m_Q(i,j)` being a matrix.

9.2   Calculating the Hermite coefficients E_t^{ij}

The Hermite coefficients are computed in the Integrator class. They are necessary for the computation of the overlap integrals (equation (4.84)), single-particle integrals (equations (4.87) and (4.90)) and the two-particle integrals (equation (4.95)). There are three distinct sets of coefficients which need to be computed, namely $\{E_t^{ij}\}$, $\{E_u^{kl}\}$ and $\{E_v^{mn}\}$, which are related to the overlap distributions in the x, y and z directions, respectively. They are all determined exactly the same way, and in the following we will therefore only discuss $\{E_t^{ij}\}$.

Before continuing, recall that i and j are the exponents of the two primitives in question:

$$\begin{aligned} G_i(a, x_A) &= x_A^i \exp(-ax_A^2), \\ G_j(b, x_B) &= x_B^j \exp(-bx_B^2), \end{aligned} \tag{9.8}$$

where $x_A = x - A_x$ and $x_B = x - B_x$, as usual. The starting point is the zeroth element

$$E_0^{0,0} = \exp\left(\frac{ab}{a+b}X_{AB}\right), \tag{9.9}$$

and all other coefficients are found via the recurrence relations
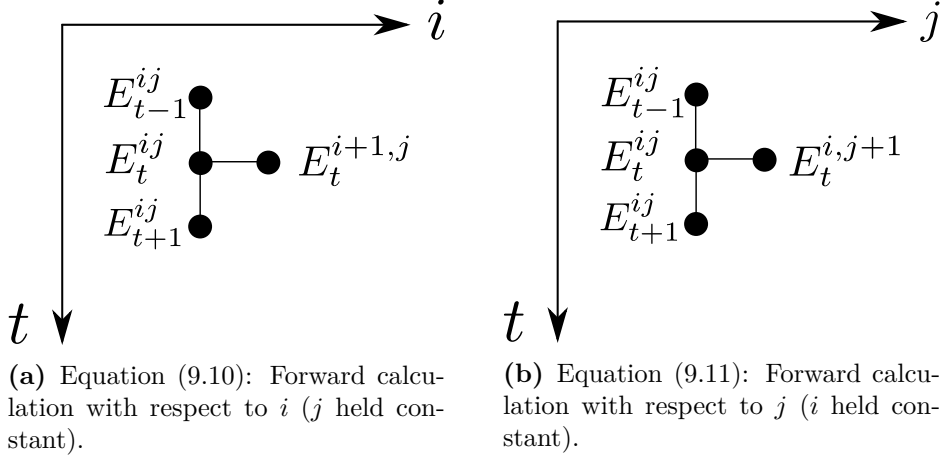
$$E_t^{i+1,j} = \frac{1}{2p}E_{t-1}^{ij} + X_{PA}E_t^{ij} + (t+1)E_{t+1}^{ij}, \tag{9.10}$$

$$E_t^{i,j+1} = \frac{1}{2p}E_{t-1}^{ij} + X_{PB}E_t^{ij} + (t+1)E_{t+1}^{ij}, \tag{9.11}$$

where $X_{PA} = P_x - A_x$, $X_{PB} = P_x - B_x$ and $\mathbf{P}$ is defined in equation (4.17). By definition, $E_t^{ij} = 0$ if $t < 0$ or $t > i + j$. First note that if E_{t-1}^{ij}, E_t^{ij} and E_{t-1}^{ij} are known, the coefficient $E_t^{i+1,j}$ can be calculated from the first of the above relations. If we draw a grid with i as horizontal axis and t as vertical axis, and also assume j to be constant, the calculation of $E_t^{i+1,j}$ can be viewed geometrically as in figure 9.2a. Next, note that $E_t^{0,0}$ is zero for all values of t except $t = 0$. Hence, $E_t^{0,0}$ is known for all values of t, and from figure 9.2a it is then clear that we can calculate $E_t^{1,0}$ for all values of t. Thereafter, once these have been determined, we can calculate $E_t^{2,0}$ for all values of t. In this manner we are able to compute $E_t^{i,0}$ for all values of i and t.

We can of course determine $E_t^{0,j}$ for all values of j and t in exactly the same way using the second of the above recurrence relations, which is shown graphically in figure 9.2b. However, we can now do more than this. Since we know $E_t^{i,0}$ for all i and t, we can use $E_t^{1,0}$ to compute $E_t^{1,j}$ for all j and t, and we can use $E_t^{2,0}$ to compute $E_t^{2,j}$ for all j and t, and so forth. Hence, in this manner we are able to compute E_t^{ij} for all i, j and t. The algorithm is implemented in the code as follows:

```
// First loop over t and i with j = 0
```

(a) Equation (9.10): Forward calculation with respect to i (j held constant).

(b) Equation (9.11): Forward calculation with respect to j (i held constant).

Figure 9.2: Graphical illustration of the recurrence relations in equations (9.10) and (9.11).

```
E[dir](0,0,0) = exp(−alpha*beta*AB(dir)*AB(dir)/p);
for (int i = 0; i < iMax; i++){
    // Treat the case t=0 separately due to (t−1) term
    E[dir](i+1,0,0) = PA(dir)*E[dir](i,0,0) + E[dir](i,0,1);
    for (int t = 1; t <= i + 0 + 1; t++){
        E[dir](i+1,0,t) = E[dir](i,0,t−1)/(2*p) + PA(dir)*E[dir](i,0,t) + (t+1)*E
            [dir](i,0,t+1);
    }
}

// Second loop over t and j and i

// Must here let i <= l because the forward loop is on index j
for (int i = 0; i <= iMax; i++){
    for (int j = 0; j < iMax; j++){
        E[dir](i,j+1,0) = PB(dir)*E[dir](i,j,0) + E[dir](i,j,1);
        for (int t = 1; t <= i + j + 1; t++){
            E[dir](i,j+1,t) = E[dir](i,j,t−1)/(2*p) + PB(dir)*E[dir](i,j,t) + (t
                +1)*E[dir](i,j,t+1);
        }
    }
}
```
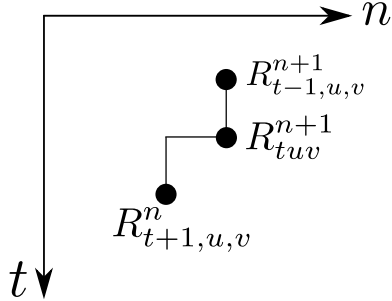
9.3   Calculating the Hermite integrals R_{tuv}

The Hermite integrals R_{tuv} are calculated in class Integrator. They are needed in order to calculate the one-particle Coulomb integrals in equation (4.90) and two-particle Coulomb integrals in equation (4.95). The algorithm for determining them is reminiscent of the one described in the previous section.

The starting point is the auxiliary Hermite integrals

$$R_{000}^n(a, \mathbf{A}) = F_n(aA^2), \tag{9.12}$$

Figure 9.3: Equation (9.13): Forward calculation with respect to t (u and v held constant).

where $a = p$ and $\mathbf{A} = \mathbf{R}_{PC}$ when calculating the one-particle Coulomb integral, $a = \alpha$ and $\mathbf{A} = \mathbf{R}_{PQ}$ when calculating the two-particle Coulomb integral, and F_n is the Boys function defined in equation (4.77). The reader is referred to sections 4.2.6 and 4.2.7 to refresh her memory on these quantities.

In the following discussion we will for simplicity assume that we are seeking the coefficients needed for the one-particle Coulomb interaction between the electrons and a nucleus, so that $a = p$ and $\mathbf{A} = \mathbf{R}_{PC}$. We start by calculating R_{000}^n for all $n \in \{0, 1, \ldots, n_{\max}\}$ where $n_{\max}$ is some maximum value. The value of $n_{\max}$ will become clear at the end of the discussion. Our target values are $R_{tuv}^0 = R_{tuv}$. These coefficients are computed via the recurrence relations
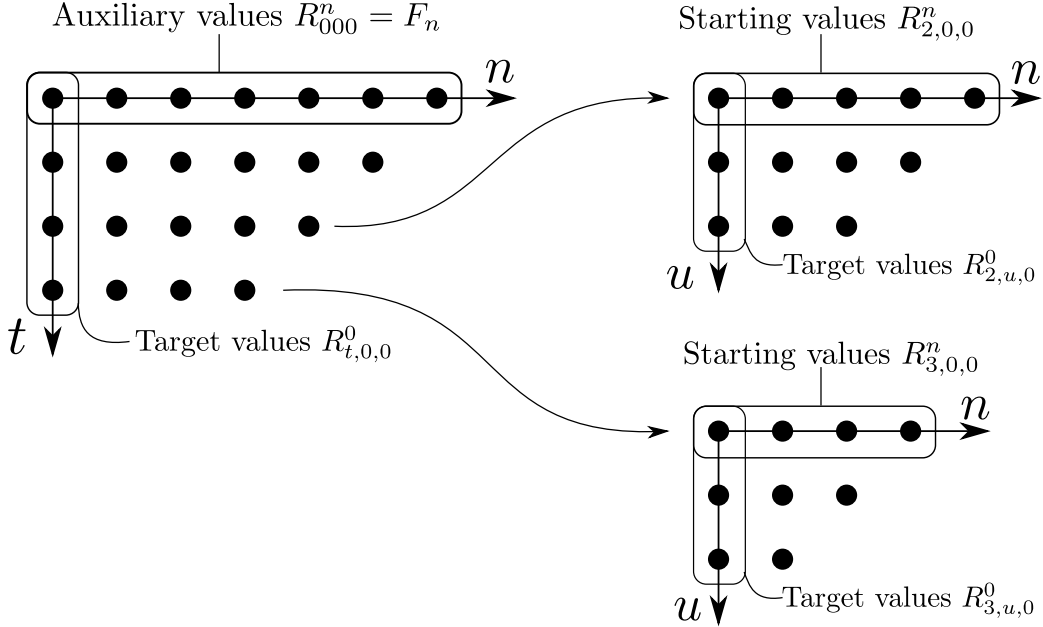
$$R_{t+1,u,v}^n = tR_{t-1,u,v}^{n+1} + A_x R_{tuv}^{n+1}, \tag{9.13}$$

$$R_{t,u+1,v}^n = uR_{t,u-1,v}^{n+1} + A_y R_{tuv}^{n+1}, \tag{9.14}$$

$$R_{t,u,v+1}^n = vR_{t,u,v-1}^{n+1} + A_z R_{tuv}^{n+1}. \tag{9.15}$$

It is useful to visualize the above relations graphically as we did in the previous section. The computational molecule of equation (9.13) is shown in figure 9.3. The other relations have similar molecules. From the figure it is clear that starting with the coefficients R_{000}^n we can calculate $R_{1,0,0}^n$ for all $n \in \{0, 1, \ldots, n_{\max} - 1\}$. [Note that $R_{-1,0,0}^n$ is not needed since it is multiplied by 0.] Thereafter, using the latter coefficients we can calculate $R_{2,0,0}^n$ for all $n \in \{0, 1, \ldots, n_{\max} - 2\}$. We can continue this process as illustrated in the left diagram of figure 9.4. Note that on every row we have the restriction $n + t \leq n_{\max}$. This is due to the structure of the computational molecule of figure 9.3. We can thus compute coefficients for increasing values of t until we reach $t = t_{\max}$. Recall that $t_{\max} = i + j$, where i and j are the powers of the primitive Gaussians $G_i(a, x_A)$ and $G_j(b, x_B)$, respectively. Similarly $u_{\max} = k + l$ and $v_{\max} = m + n$, where k, l and m, n are the powers of the y and z factors of the Gaussians, respectively. We have then obtained the target values $R_{t,0,0}^0$ for $t \in \{0, 1, \ldots, t_{\max}\}$.

Each row in the left diagram of figure 9.4 will serve as a starting row for similar diagrams with axes (u, n) in which equation (9.14) is used for the forward iteration. For example, the third row, i.e. the row with $t = 2$, will provide the initial values from which one can compute $R_{2,u,0}^n$ for all n and u such that $u \leq u_{\max}$ and $n + 2 + u \leq n_{\max}$. Similarly, the fourth row will give $R_{3,u,0}^n$ for all n and u such that $u \leq u_{\max}$ and $n + 3 + u \leq n_{\max}$. This is illustrated in the right diagrams of figure 9.4. In this way one

Figure 9.4: The left diagram illustrates how the target values $R_{t,0,0}^0$ are calculated starting with the auxiliary values R_{000}^n. The right diagrams show how the third and fourth rows of the left diagram are used as initial values of new diagrams from which the target values $R_{2,u,0}^0$ and $R_{3,u,0}^0$ are computed.

can calculate $R_{t,u,0}^n$ for all n, t and u such that $t \leq t_{\max}$, $u \leq u_{\max}$ and $n+t+u \leq n_{\max}$.

Finally, the coefficients $R_{t,u,0}^n$ will serve as initial values for the computation of R_{tuv}^n for all n, t, u and v such that $t \leq t_{\max}$, $u \leq u_{\max}$, $v \leq v_{\max}$ and $n + t + u + v \leq n_{\max}$. We have then found the target values $R_{tuv}^0 = R_{tuv}$ for all $t \leq t_{\max}$, $u \leq u_{\max}$ and $v \leq v_{\max}$.

From the discussion above it is now clear that we must set $n_{\max} = t_{\max}+u_{\max}+v_{\max}$. However, so far we have had the one-particle Coulomb integral of equation (4.90) in mind. When calculating the two-particle Coulomb integral of equation (4.95) we must replace $t_{\max}$ by $t_{\max} + \tau_{\max}$, $u_{\max}$ by $u_{\max} + \nu_{\max}$ and $v_{\max}$ by $v_{\max} + \phi_{\max}$.

9.4   Calculating the Boys function

The Hermite integrals R_{tuv} discussed in the previous section are all obtained from an initial calculation of the Boys function

$$F_n(x) = \int\limits_0^1 \exp(-xt^2)\, t^{2n}\, \mathrm{d}t. \qquad (9.16)$$

Throughout the thesis, the Boys function has been calculated as follows.

First, the largest value of n is determined. When calculating the Coulomb interaction between the electrons and a nucleus, as in equation (4.90), we set

$$n_{\max} = t_{\max} + u_{\max} + v_{\max}, \qquad (9.17)$$

where $t_{\max} = i + j$, $u_{\max} = k + l$ and $v_{\max} = m + n$. The integers i, j, k, l, m, n are the powers of the Gaussian funtions G_a and G_b, see equations (4.13) and (4.14). When calculating the Coulomb interaction between the electrons, as in equation (4.95), we set

$$n_{\max} = t_{\max} + u_{\max} + v_{\max} + \tau_{\max} + \nu_{\max} + \phi_{\max}, \tag{9.18}$$

where $t_{\max}$, $u_{\max}$ and $v_{\max}$ are sums of powers of the Gaussians G_a and G_b, and $\tau_{\max}$, $\nu_{\max}$ and $\phi_{\max}$ are sums of powers of the Gaussians G_c and G_d.

Second, the Boys function is evaluated for $n = n_{\max}$ by

$$F_n(x) = \frac{(2n-1)!!}{2^{n+1}} \sqrt{\frac{\pi}{x^{2n+1}}}, \qquad \text{if } x > 50, \tag{9.19}$$

and by

$$F_n(x) = \sum_{k=0}^{6} \frac{F_{n+k}(x_t)(-\Delta x)^k}{k!}. \qquad \text{if } x \leq 50, \tag{9.20}$$

where the functions $F_{n+k}(x_t)$ are tabulated at x_t and $\Delta x = x - x_t$. The Boys function is tabulated at 1000 equispaced points x_t on the interval $[0, 50]$. The tabulated values have been calculated by the trapeziodal rule with $1.0 \cdot 10^6$ points.

Third, the Boys function for all $n < n_{\max}$ is calculated by the recursion formula

$$F_n(x) = \frac{2x F_{n+1}(x) + e^{-x}}{2n + 1}. \tag{9.21}$$

9.5 Parallelization

In the Hartree-Fock solver, the biggest computational load is by far undertaken by the Integrator class when calulating the two-particle integrals $\langle \mu\sigma|g|\nu\lambda \rangle$ and the Minimizer class when transforming the AOIs to MOIs. These particular parts of the program have therefore been coded to run in parallel using the library Open MPI.

Chapter 10

Code development and validation

10.1 Code development in Qt Creator

The code has been written using the Qt Creator integrated development environment (IDE). The IDE uses the tool qmake which automates the generation of Makefiles and greatly simplifies the build process. The Makefile is generated based on the information in one or more project files. For example, if a project consists of the files

```
/
├──main.cpp
└──myclass/
    ├──myclass.h
    └──myclass.cpp
```

the project file (.pro) should be placed in the same directory as main.cpp and should look something like

```
TEMPLATE = app
TARGET = myapp
CONFIG -= qt
SOURCES += main.cpp \
           myclass/myclass.cpp
HEADERS += myclass/myclass.h
INCLUDEPATH += myclass
```

The `TEMPLATE` variable is set to app, which means that the Makefile builds an application (executable). The `TARGET` variable specifies the name of the executable. Since it is not a Qt application, qt is subtracted from the `CONFIG` variable. The variables `SOURCES` and `HEADERS` specifies the source and header files which are used in the project. Directories in which qmake searches for header files can be added to the `INCLUDEPATH` variable. This is not essential, but has the effect that include directives can be changed from

```
#include "myclass/myclass.h"
```

to

```
#include "myclass.h"
```

With qmake one also has the option to create subprojects. For example, it is possible to have one subproject which creates a library from the source files, and one or more other subprojects which use this library. This is especially useful during code development, since one can then have one subproject which is the main application and another subproject which tests the various classes of the source code. This approach has been used in this thesis. The file structure of the project is as follows

```
/
├── mainproject.pro
├── defaults.pri
├── src/
│   ├── src.pro
│   ├── myclass1/
│   │   ├── myclass1.h
│   │   └── myclass1.cpp
│   ├── myclass2/
│   │   ├── myclass2.h
│   │   └── myclass2.cpp
│   └── ...
├── app/
│   ├── app.pro
│   └── main.cpp
└── tests/
    ├── tests.pro
    └── main.cpp
```

With such a setup, the main project as well as each subproject must have its own project file. The mainproject.pro files should look something like

```
TEMPLATE = subdirs
SUBDIRS = \
src \
app \
tests
CONFIG += ordered
```

where `TEMPLATE` is now set to subdirs, which signifies that each subdirectory, specified in the `SUBDIRS` variable, will be a subproject. The variable `CONFIG` is set equal to ordered so that each subproject is built in the order indicated. This is important, since the file src.pro will have `TEMPLATE` set equal to lib, telling qmake to create a library, and the other subprojects app and tests will use this library. The file src.pro looks something like:

```
include(../defaults.pri)
CONFIG −= qt
TARGET = myapp
TEMPLATE = lib
SOURCES += myclass1/myclass1.cpp \
           myclass2/myclass2.cpp \
           ...
HEADERS += myclass1/myclass1.h \
           myclass2/myclass2.h \
           ...
```

The first line includes the file defaults.pri in which default settings shared by all sub-projects are set. This can for example be the inclusion of libraries such as Armadillo,

Lapack, Blas etc. The project file for the application, which uses the library, should look something like:

```
include(../defaults.pri)
TEMPLATE = app
CONFIG -= qt
SOURCES += main.cpp
LIBS += -L../src -lmyapp
```

Here the library created in subproject src is included in the `LIBS` variable. The project file of the tests project is essentially the same.

10.2   Testing the classes

Throughout the code development, many of the classes and routines of the project have been tested and validated in the tests subproject. The tests have been implemented using the library UnitTest++, which is very easy to use. All the tests are written in the file main.cpp. For example, the Boys function can be tested by defining the test

```
TEST(BoysIntegrals){
    BoysFunction boys(3);
    boys.setx(2.3252);
    CHECK_CLOSE(boys.returnValue(1), 1.0007267355e-01, 1.0E-10);
    CHECK_CLOSE(boys.returnValue(3), 2.5784878802e-02, 1.0E-10);
    CHECK_CLOSE(boys.returnValue(6), 1.0688807154e-02, 1.0E-10);
    CHECK_CLOSE(boys.returnValue(10), 5.8076406817e-03, 1.0E-10);
}
```

before `int main()`. The function `CHECK_CLOSE` checks the value returned by the function `boys.returnValue()` against a precalculated value up to a presicion of $1.0 \cdot 10^{-10}$. Tests for other classes and routines have been defined similarly. The tests are run simply by calling the function `RunAllTests()`:

```
int main()
{
    return UnitTest::RunAllTests();
}
```

10.3   Code validation

It is important to confirm that the code is able to reproduce results published in the literature. Table 10.1 shows calculated energies for the closed shell molecule NH_4^+ and open shell molecule CN together with values given by Gill *et al* [31] and Boldyrev *et al* [32]. The NH_4^+ molecule has been analysed with a restricted determinant and the 6-31++G** basis set (46 basis functions), whereas the CN molecule has been analysed with an unrestricted determinant and the STO-3G basis set (10 basis functions). All

Table 10.1: Total energies for the CN and NH_4^+ molecules validated against Gill *et al* [31] and Boldyrev *et al* [32], respectively. The STO-3G basis set (10 basis functions) and unrestricted determinant was used for the CN molecule, whereas the 6-31++G** basis set (46 basis functions) and restricted determinant was used for the NH_4^+ molecule. The frozen core approximation was used in both cases, freezing the two and one lowest orbitals of the CN and NH_4^+ molecules, respectively.

Mol.	Det.	Bond length (Å)	Work	Energy (a.u.)		
				HF	MP2	MP3
CN	Restr.	1.235	This	-91.02639	-91.10287	-91.11262
			[31]	-91.02639	-91.10287	-91.11262
NH_4^+	Unrestr.	1.022	This	-56.545683	-56.734616	-56.749123
			[32]	N.A.	N.A.	-56.749124

energies have been calculated up to the level of third order Møller-Plesset perturbation theory. The frozen core approximation was used in both cases. This means that the core molecular orbitals have been left out of the perturbation sum. The core molecular orbitals are defined as the *n molecular* orbitals of lowest energy, where n is the number of core *atomic* orbitals of the system. This definition might sound rather unsophisticated. Nonetheless, it is the definition used in most quantum chemistry program packages, see for example the documentation for NWCHem [33]. Note that we are talking about spatial orbitals here; freezing n molecular orbitals corresponds to freezing $2n$ electrons.

The nitrogen atom, being the only atom of NH_4^+ with core atomic orbitals, have one core atomic orbital, namely the $1s$ orbital. This means that the molecular orbital of lowest energy is left out of the perturbation sums of this molecule. On the other hand, both atoms of the CN molecule have core atomic orbitals, namely the $1s$ orbital. Hence, the two molecular orbitals of lowest energy are ignored in the perturbation sums for this molecule.

As the numbers show, the code reproduces the results from the literature. The only discrepancy is at the eighth significant digit of the MP3 energy for the NH_4^+. However, this discrepancy is extremely small, and should cause no worry.

Part III

Results and conclusion

Chapter 11

Results

In this chapter we present results from calculations on various molecular systems. We first discuss the hydrogen molecule which, although a simple system, serves to illustrate some interesting aspects of the various methods. Thereafter, we move on to larger systems, both closed shell and open shell molecules. The chapter ends with an investigation of the C-C dissociation energy of the C_2H_6 molecule (ethane). Throughout the chapter, we try to discuss the computational methods as well as the physics involved.

11.1   The hydrogen molecule
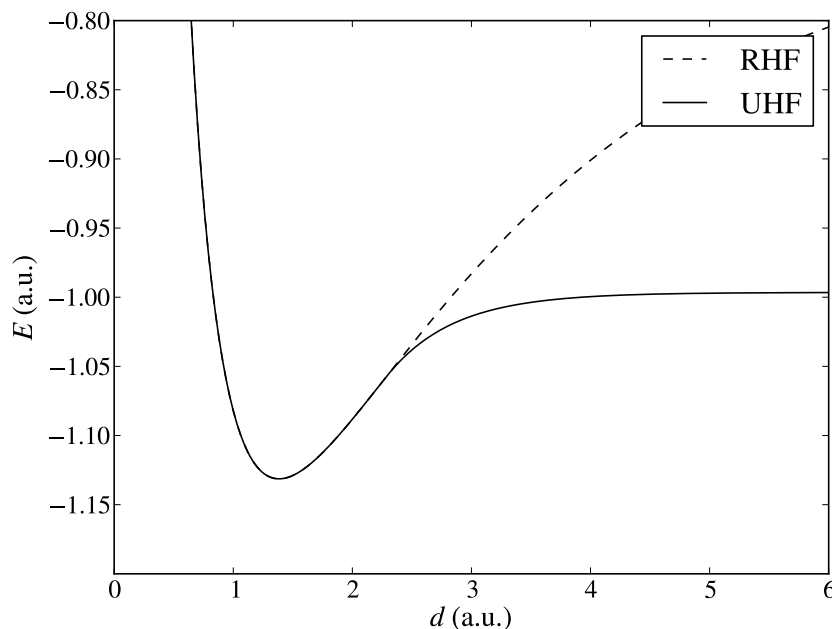
The hydrogen molecule is the simplest molecule one can think of. Nevertheless, it is an interesting case to study using the methods discussed in the previous chapters. There are mainly two reasons for this. First, it has been studied thoroughly by chemists by a vast number of different methods, and it therefore serves as a means to validate the code. Second, although a simple system, it illuminates some interesting aspects of the methods.

Table 11.1: Restricted Hartree-Fock energies in a.u. for H_2 for a selection of basis sets. The internuclear distance has been set to $d = 1.4$ a.u. The results are in perfect agreement with Szabo *et al* [3].
[a] Schulman *et al* [34]
[b] Moskowitz *et al* [35]

Basis set	E_{HF}
STO-3G	-1.116714
4-31G	-1.126743
6-31G**	-1.131284
HF-limit[a]	-1.134

Experimental energy[b]: -1.1746
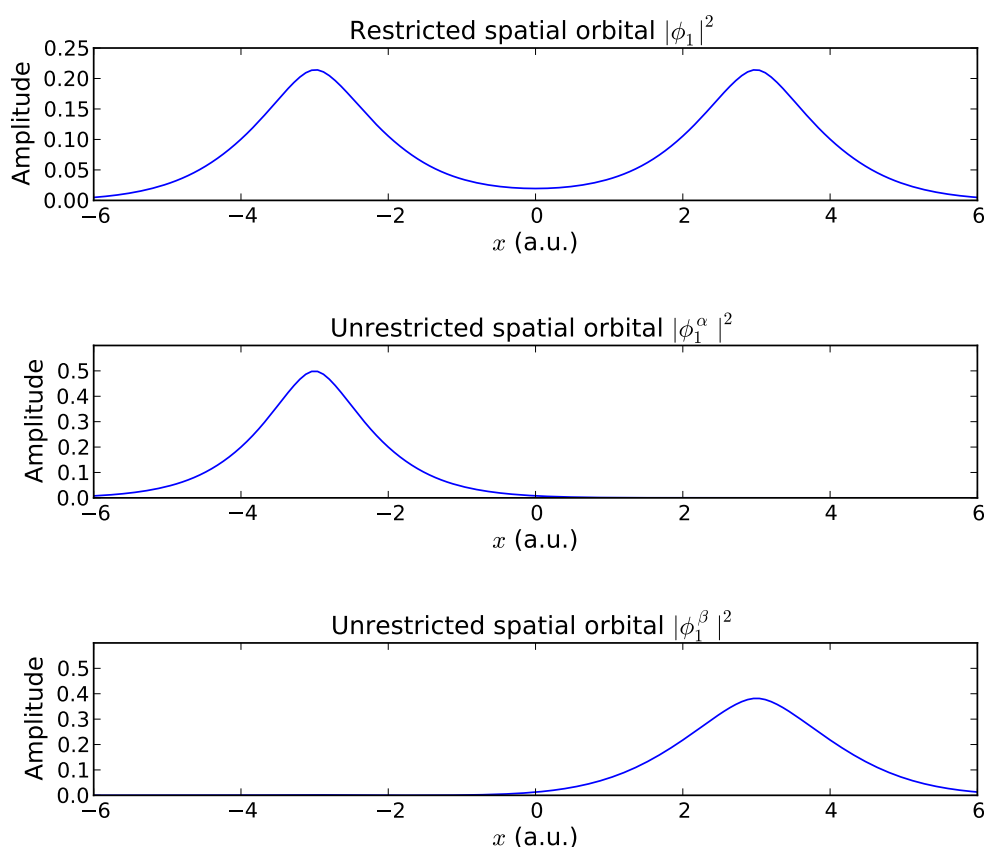
Figure 11.1: The energy of the H_2 molecule as a function of the internuclear distance d. The 6-31G** basis set was used in the calculations.

11.1.1   Hartree-Fock energies

Table 11.1 shows the energies from a restricted Hartree-Fock calculation with the internuclear distance set equal to 1.4 a.u., which is close to the experimental bond length. All results are in perfect agreement with those of Szabo *et al* [3]. The STO-3G, 4-31G and 6-31G** basis sets have a total of 2, 4 and 10 basis functions, respectively. It is clear that the results improve as we increase the size of the basis set. However, there is a threshold, the Hartree-Fock limit, beyond which the Hartree-Fock method cannot take us. With the 6-31G** basis set, the energy nearly reaches this limit and accounts for 96.3% of the total energy.

Figure 11.1 shows the energy as a function of the internuclear distance d obtained from restricted and unrestricted Hartree-Fock calculations with the 6-31G** basis set. For distances not far from the equilibrium bond length, both curves have the shape we expect. However, they exhibit radically different behaviour when the distance is large. Clearly, the restricted calculation gives unsatisfactory results in this case. We know this since the energy of the system should approach that of two single hydrogen atoms, which is -1.0 a.u., as $d \to \infty$. Thus, even though we have a closed shell system near the equilibrium bond length, it is apparently not well described by a closed shell determinant as the molecule dissociates. The reason for this is as follows.

Recall that a restricted determinant is characterised by requiring two and two spin orbitals to have identical spatial parts. When the internuclear distance is close to equilibrium, this is a feasable assumption; the nuclei "share" electrons, and a single

Figure 11.2: Comparison of the spatial orbitals resulting from restricted and unrestricted Hartree-Fock calculations of the hydrogen molecule. The curves represent the squared magnitude of the orbtitals projected onto the x-axis. The nuclei are located at $x = -3$ and $x = 3$. In the RHF calculations, both electrons are confined to occupy the same spatial orbital, as shown in the uppermost plot, whereas in the UHF calculations, the electrons can occupy distinct spatial orbitals, as shown in the two lowermost plots.

electron is equally likely to be located near one as the other. However, as the distance increases, the molecule dissociates into two single hydrogen atoms. Hence, it no longer makes physical sense to force both electrons to occupy the same spatial orbital; the two electrons are now located at different nuclei. This can only be accomplished by the unrestricted determinant. Figure 11.2 illustrates this point. It shows the spatial orbitals obtained from restricted and unrestricted calculations with an internuclear distance of 6.0 a.u. The restricted spin orbitals are given by

$$\begin{aligned} \psi_1(x,s) &= \phi_1(x)\alpha(s) \\ \psi_2(x,s) &= \phi_1(x)\beta(s), \end{aligned} \tag{11.1}$$

where $\phi_1(x)$ is the spatial orbital in the uppermost diagram of figure 11.2, and the unrestricted spin orbitals are given by

$$\begin{aligned} \psi_1(x,s) &= \phi_1^\alpha(x)\alpha(s) \\ \psi_2(x,s) &= \phi_1^\beta(x)\beta(s), \end{aligned} \tag{11.2}$$

where $\phi_1^\alpha(x)$ and $\phi_1^\beta(x)$ are the spatial orbitals of the two lowermost diagrams. Clearly, the restricted spin orbitals are unfeasable for large bond lengths.

11.1.2   Møller-Plesset energies

Table 11.2 shows results obtained from second and third order perturbation theory at an internuclear distance of 1.4 a.u. It is clear that the perturbative contribution increases with the size of the basis set, as expected. With the 6-31G* basis set, the third order perturbation theory accounts for 99.0% of the exact energy. We mention that all the results listed are in perfect agreement with those of Szabo *et al* [3].
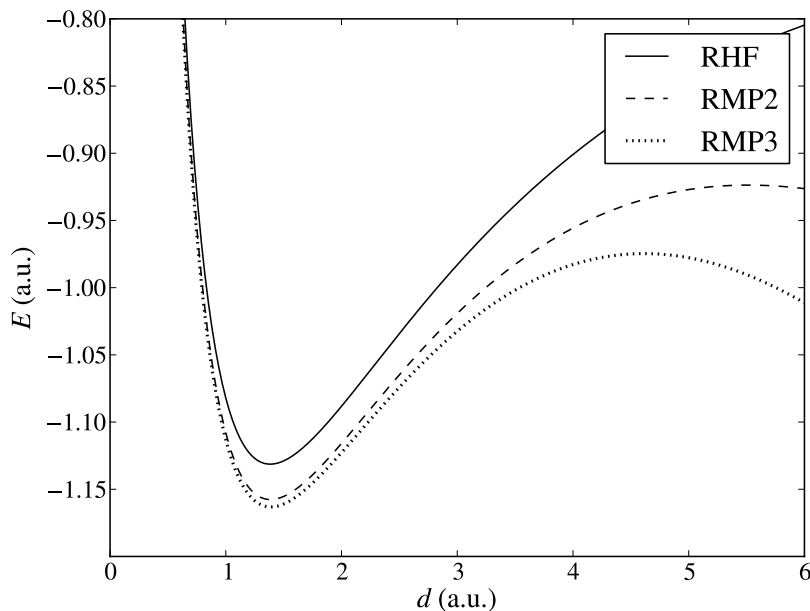
Table 11.2: Restricted Møller-Plesset energies in a.u. for a selection of basis sets. The internuclear distance has been set to $d = 1.4$ a.u. The results are in perfect agreement with Szabo *et al* [3].
[a] Schulman *et al* [34]
[b] Moskowitz *et al* [35]
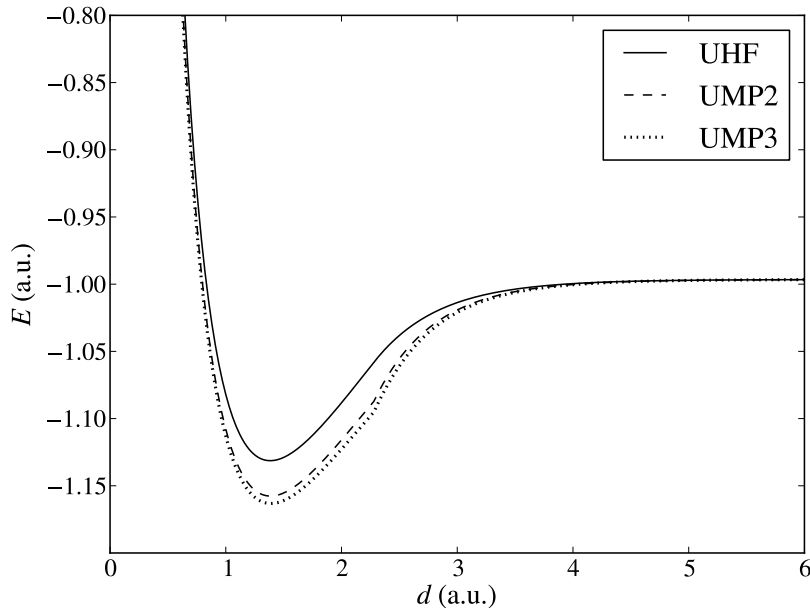
Basis set	E_{RHF}	E_{RMP2}	E_{RMP3}
STO-3G	-1.116714	-1.129872	-1.134718
4-31G	-1.126743	-1.144133	-1.149342
6-31G**	-1.131284	-1.157626	-1.163142
HF-limit[a]	-1.134		

Experiment[b]: -1.1746

Figure 11.3 shows potential energy curves obtained from calculations at different levels of theory. Near the equilibrium bond length, the RMP2 and RMP3 curves have the shape we expect them to have. And for larger bond lengths, they behave somewhat better than the RHF curve. However, the RMP2 and RMP3 energies diverge towards negative infinity as $d \to \infty$.

(a) Restricted calculation.

(b) Unrestricted calculation.

Figure 11.3: The energy of the H_2 molecule as a function of the internuclear distance d obtained from calculations at different levels of theory. The 6-31G** basis set was used in the calculations.

The unrestricted curves behave more realistically, converging towards approximately -1 as $d \to \infty$. It is evident that correlations play an important role for small bond lengths. However, as the bond length increases, the correlation energy gradually decreases towards zero, as it should; two independent hydrogen atoms have no correlations.

11.1.3 Equilibrium bond length

One of the most common uses of Hartree-Fock and Møller-Plesset perturbation theory, is the calculation of equilibrium geometries of molecules. This is a rather easy task for the H_2 molecule since the potential energy surface has only one variable. Nevertheless, it serves as a good first test for the minimiser. The computed bond lengths are shown in table 11.3. All but one value underestimates the bond length. However, larger basis sets and the inclusion perturbative corrections brings us closer to the experimental value.

Table 11.3: Equilibrium bond lengths of the H_2 molecule calculated with different levels of theory.
[a] Szabo *et al* [3]

Basis set	RHF	RMP2	RMP3
STO-3G	1.346	1.368	1.380
4-31G	1.379	1.394	1.402
6-31G**	1.384	1.387	1.390

Experimental bond length [a]: 1.401

11.2 Closed shell molecules: H_2O, CH_4, NH_3 and FH

11.2.1 Energies

The energies for the so-called ten-electron series are listed in table 11.4. Consider first the Hartree-Fock energies. Even for the minimal basis set STO-3G, the calculated energy is not too far from the Hartree-Fock limit, merely 1.4% above in average. The largest basis set 6-31G** reduces the deviation to 0.1% in average. Within the Hartree-Fock approximation, there is little to be gained from increasing the size of the basis set further; the difference between the exact energy and the calculated Hartree-Fock energy is almost entirely due to correlations at this point.

For the specific atoms considered here, the contribution from second order Møller-Plesset perturbation theory typically affects the third significant digit, whereas the third order contrubution affects the fourth digit. This indicates that most of the correlation energy is accounted for by the second order term.
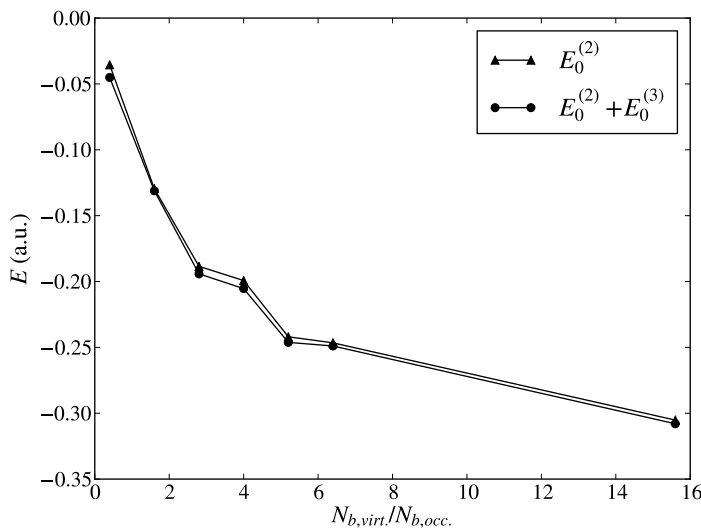
The STO-3G basis set for H_2O has a total of 7 basis functions, and the system itself is composed of 10 electrons. Thus, within this basis set, there are only 2 virtual spatial orbitals to which the 5 occupied orbitals may be excited, and the perturbative terms cannot be expected to improve the energies significantly. On the other hand, the

Table 11.4: Energies in a.u. of the ten electron series.
[a] Hariharan *et al* [36]

Mol.	Basis set	Bond length	Bond angle	RHF	RMP2	RMP3
H_2O	STO-3G	1.809	104.52°	−74.962940	−74.998439	−75.008031
	4-31G			−75.907391	−76.036868	−76.038497
	6-31G*			−76.010527	−76.199006	−76.204711
	6-31G**			−76.023159	−76.222419	−76.228538
	HF-lim[a]:			−76.065		
CH_4	STO-3G	2.050	109.47°	−39.726853	−39.782880	−39.797785
	4-31G			−40.139728	−40.240297	−40.253737
	6-31G*			−40.195168	−40.336980	−40.352991
	6-31G**			−40.201700	−40.369855	−40.388048
	HF-lim[a]:			−40.225		
NH_3	STO-3G	1.913	106.67°	−55.454079	−55.501291	−55.513485
	4-31G			−56.102428	−56.219981	−56.227471
	6-31G*			−56.184112	−56.357331	−56.368890
	6-31G**			−56.195205	−56.386897	−56.399477
	HF-lim[a]:			−56.225		
FH	STO-3G	1.733		−98.570787	−98.588134	−98.593660
	4-31G			−99.887258	−100.016682	−100.015452
	6-31G*			−100.002862	−100.183850	−100.185387
	6-31G**			−100.011348	−100.196683	−100.198231
	HF-lim[a]:			−100.071		

6-31G** basis set contains 25 basis functions, meaning that each occupied orbital may be excited to 20 different virtual orbitals. Clearly, we should expect this basis set to give a more substantial correction to the Hartree-Fock energies. The tabulated results confirm this.

How many basis functions should be included in order to obtain good results from perturbation theory? To answer this, we have investigated how the perturbative corrections from MP2 and MP3 depend on the choice of basis set for the H_2O molecule. Calculations were performed in the configuration given in table 11.4 for the following basis sets: STO-3G, 4-31G, 6-31G*, 6-31G**, 6-311G**, 6-311++G**, 6-311++G(3df,3pd). They have a total of 7, 13, 19, 25, 31, 37 and 83 basis functions, respectively. The corrections are plotted as a function of the ratio $N_{b,virt.}/N_{b,occ.}$ in figure 11.4. Here $N_{b,virt.}$ and $N_{b,occ.}$ are the numbers of virtual and occupied spatial orbitals, respectively. The plot suggests that it is optimal to include approximately 5 times as many virtual states as occupied states or more.
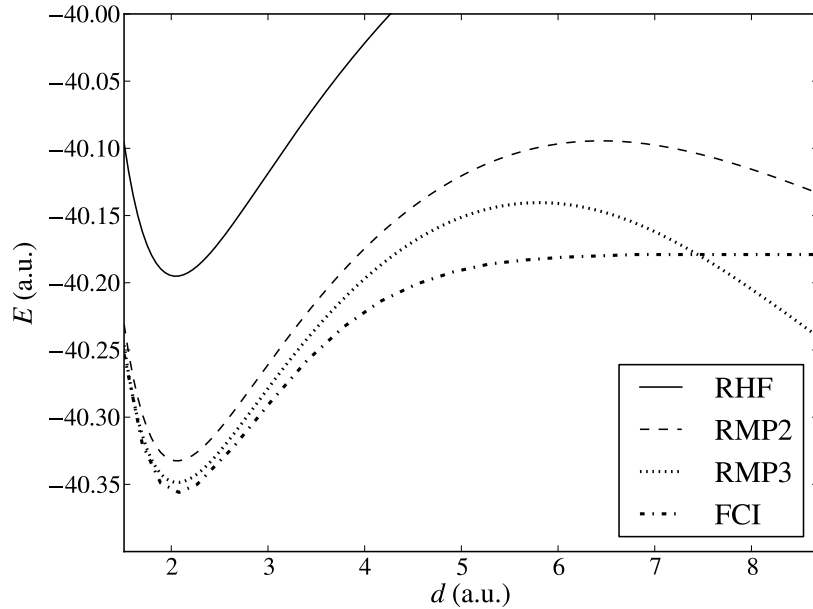
Figure 11.4: Plot of energy corrections for the H_2O molecule obtained from second and third order Møller-Plesset perturbation theory as a function of $N_{\text{b,virt.}}/N_{\text{b,occ.}}$, where $N_{\text{b,virt.}}$ and $N_{\text{b,occ.}}$ are the numbers of virtual and occupied spatial orbitals, respectively.

## 11.2.2   Potential energy curves
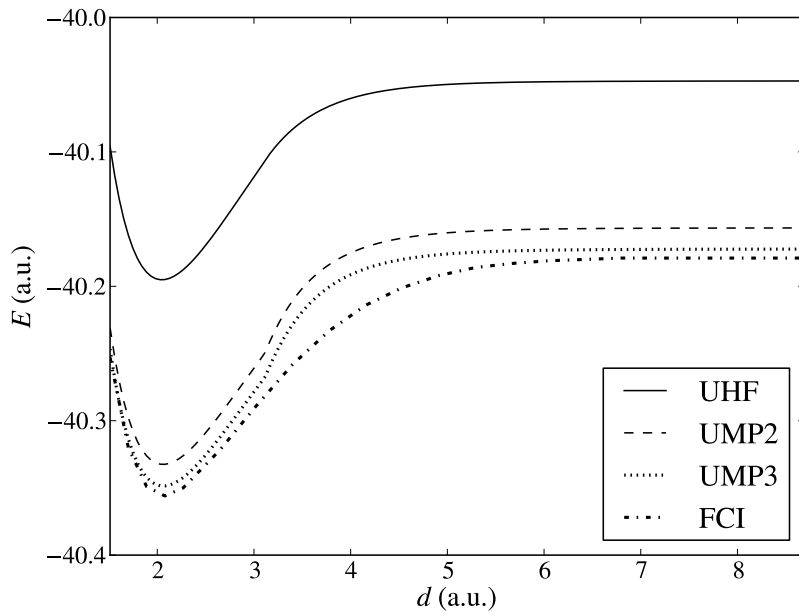
As explained in chapter 5, the proper way to judge the quality of results obtained from perturbation theory, is to compare them to full configuration interaction results. Figures 11.5 and 11.6 do this for the CH_4 and FH molecules. The plots show the energy as a function of bond length. In the calculations for the CH_4 molecule, the length of a single CH bond is varied while all others are kept at a constant length of 1.086 Å. The calculations have been performed with the 6-31G* and 6-31G** basis sets, respectively. The full CI results are taken from Dutta *et al* [37]. The frozen-core approximation has been used throughout (see section 10.3).

From figure 11.5 and 11.6 we see that, for bond lengths near the equilibrium value, most of the correlation energy is indeed taken care of by the second order term. This is particularly the case for the FH molecule. The inclusion of the third order term brings the energy almost all the way down to the full CI energy. This is is the case for the restricted as well as the unrestricted results. For large bond lengths, however, the RHF curve overshoots the energy drastically, just as we saw for the hydrogen molecule. The perturbation theory corrects for some of this error, but the RMP2 and RMP3 curves are still far from the full CI curve. Furthermore, they diverge to negative infinity as the bond length increases. Thus, the restricted calculations are not suitable when studying bond dissociation. On the other hand, the unrestricted results behave

Before discussing the results in detail, it is worth mentioning that Dutta *et al* [37] also performed calculations at the RHF, UHF, RMP2 and UMP2 levels (as well as coupled cluster and DFT, but not RMP3 or UMP3), and that our results match theirs perfectly, thus validating large portions of the code. They tabulated values with a precision of 8-9 significant digits.
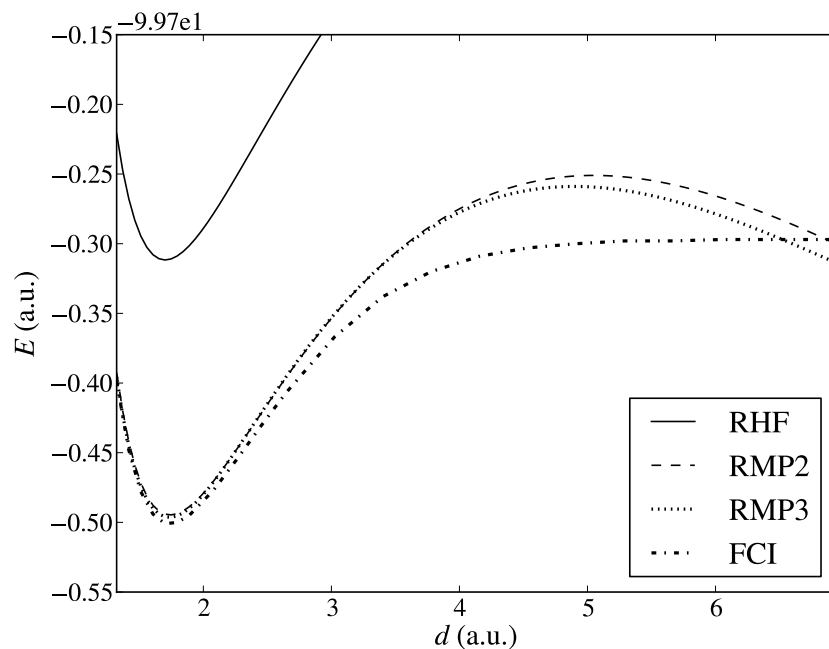
(a) Restricted calculation.
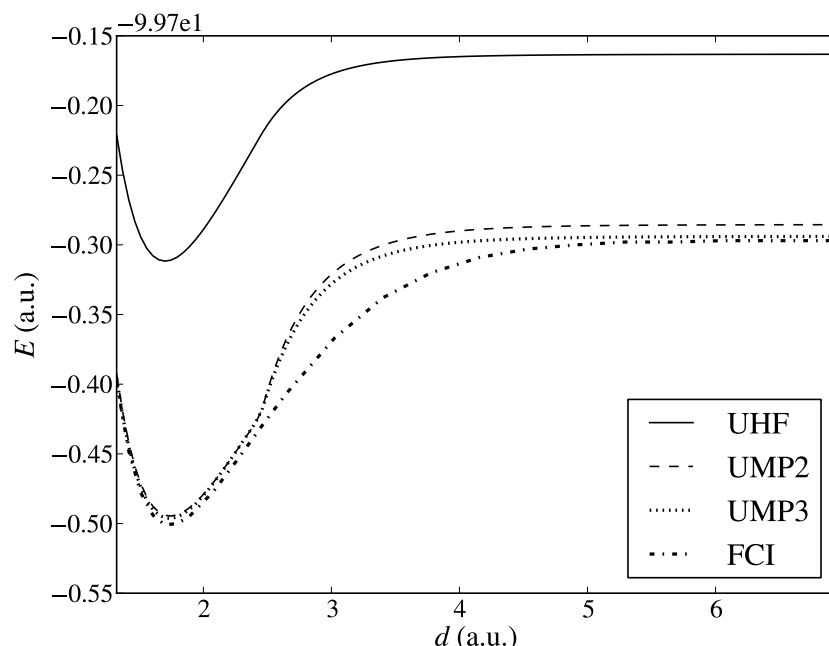
(b) Unrestricted calculation.

Figure 11.5: Potential energy curves of the CH_4 molecule as a function of the distance d between one of the hydrogen atoms and the carbon atom. All other hydrogen atoms are kept at a distance of 1.086 Å. The calculations were performed with the 6-31G* basis set, and the frozen core approximation was used (see main text). The FCI results are taken from Dutta *et al* [37].

(a) Restricted calculation.

**(b)** Unrestricted calculation.

Figure 11.6: Potential energy curve of the FH molecule as a function of the internuclear distance d. The calculations were performed with the 6-31G** basis set, and the frozen core approximation was used (see main text). The FCI results are taken from Dutta *et al* [37].

correctly for large bond lengths.

However, it is clear that also the unrestricted results are flawed: For intermediate bond lengths, approximately $3 - 5$ a.u. for the CH_4 molecule and $2.5 - 4$ a.u. for the FH molecule, the unrestricted energies behave rather strangely. Evidently, the Møller-Plesset perturbation theory converges poorly in this range. This type of behaviour has also been observed and discussed by other authors, and it is hypothesised [31, 38, 39] that it is due to spin contamination of the unrestricted determinant. We will investigate this in the following.

An exact state of a system composed of N^α spin-up electrons and N^β spin-down electrons, is an eigenstate of $\mathbf{S}^2$ and S_z with eigenvalues $S(S + 1)$ and $M_S = (N^\alpha - N^\beta)/2$, respectively, where S can take the values

$$S \in \left\{ \frac{|n^\alpha - n^\beta|}{2}, \frac{|n^\alpha - n^\beta|}{2} + 1, \ldots, \frac{n^\alpha + n^\beta}{2} \right\}, \tag{11.3}$$
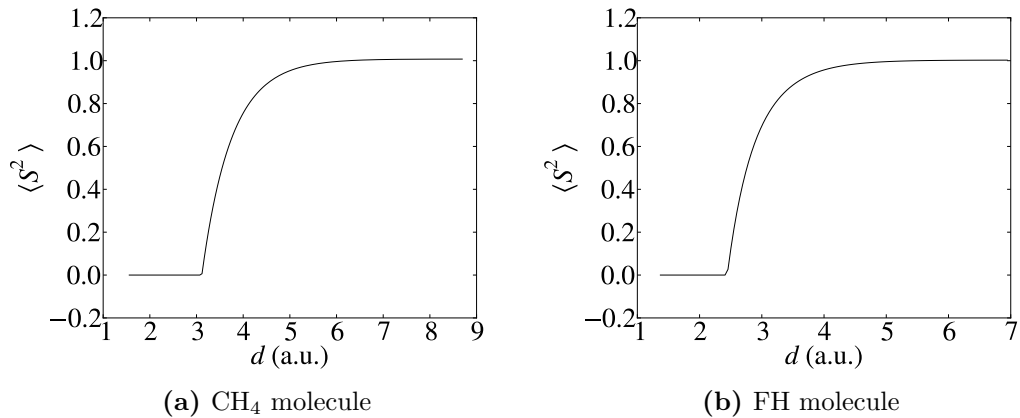
and where n^α and n^β are the numbers of *unpaired* spin-up and spin-down electrons, respectively [17]. In most cases $S = (N^\alpha - N^\beta)/2$. However, the unrestricted determinant is not an eigenstate of $\mathbf{S}^2$. Rather, the expectation value of $\mathbf{S}^2$ calculated with the unrestricted determinant is given by (see appendix A)

$$\langle \mathbf{S}^2 \rangle = \frac{N^\alpha - N^\beta}{2} \left(\frac{N^\alpha - N^\beta}{2} + 1 \right) + N^\beta - \sum_{i=1}^{N^\alpha} \sum_{j=1}^{N^\beta} |\langle \phi_i^\alpha | \phi_j^\beta \rangle|^2. \tag{11.4}$$

Assume for simplicity that $N^\alpha \geq N^\beta$. The equation above then reveals that the expectation value is correct only if the two last terms cancel. This can for example happen if every spin-down orbital is 'paired' with a spin-up orbital, meaning that their spatial parts are identical. If this is the case, then $\phi_i^\alpha = \phi_i^\beta$ for $i \leq N^\beta$. Furthermore, $\langle \phi_i^\alpha | \phi_j^\beta \rangle = 0$ for $i \neq j$ since the set of functions $\{\phi_i^\alpha\}_{i=1}^{N^\alpha}$ is orthonormal. Thus $|\langle \phi_i^\alpha | \phi_j^\beta \rangle|^2 = \delta_{ij}$, the sum reduces to N^β, and the last two terms cancel.

What we have just described is a restricted determinant. However, the whole point of introducing unrestricted determinants is to relax the constraint of pairing every spin-down orbital with a spin-up orbital. A consequence of this relaxation is that the spin-up electrons may occupy regions of space which to a less extent are occupied by the spin-down electrons. If this is the case, the last term of the above equation will not sum up to N^β, and $\langle \mathbf{S}^2 \rangle$ will be too large. We say that the determinant is contaminated with higher multiplets of spin.

The ground states of FH and CH_4 have $N^\alpha = N^\beta$, and the correct value of S is therefore $S = 0$. We can test the degree of spin contamination by calculating the expectation value in equation (11.4) and comparing it with the correct value $\langle \mathbf{S}^2 \rangle = 0$. This has been done in figure 11.7, which shows $\langle \mathbf{S}^2 \rangle$ as a function of bond length for (a) CH_4 and (b) FH. From the figure it is clear that $\langle \mathbf{S}^2 \rangle = 0$ for small values of d. In fact, for these values, the unrestricted Hartree-Fock solution collapses to the restricted solution and is therefore an eigenstate of $\mathbf{S}^2$. However, at $d \approx 3.2$ a.u. for CH_4 and $d \approx 2.5$ a.u. for FH, the value of $\langle \mathbf{S}^2 \rangle$ diverges rather abruptly away from zero. Seen in relation to figure 11.5b and 11.6b, this supports the hypothesis that spin

(a) CH$_4$ molecule   **(b)** FH molecule

Figure 11.7: Plots of $\langle S^2 \rangle$ (equation (11.4)) as a function of bond length.

contamination plays a role in the poor convergence of the Møller-Plesset perturbation theory at intermediate bond lengths.

We end the discussion of spin contamination by mentioning that there exist methods which aim to remedy this issue. One such method is to use so-called projection operators which are designed to annihilate the higher multiplets of spin. This method have been applied by Schlegel [40] and Knowles *et al* [41].

11.2.3   Orbital energies and ionisation potentials
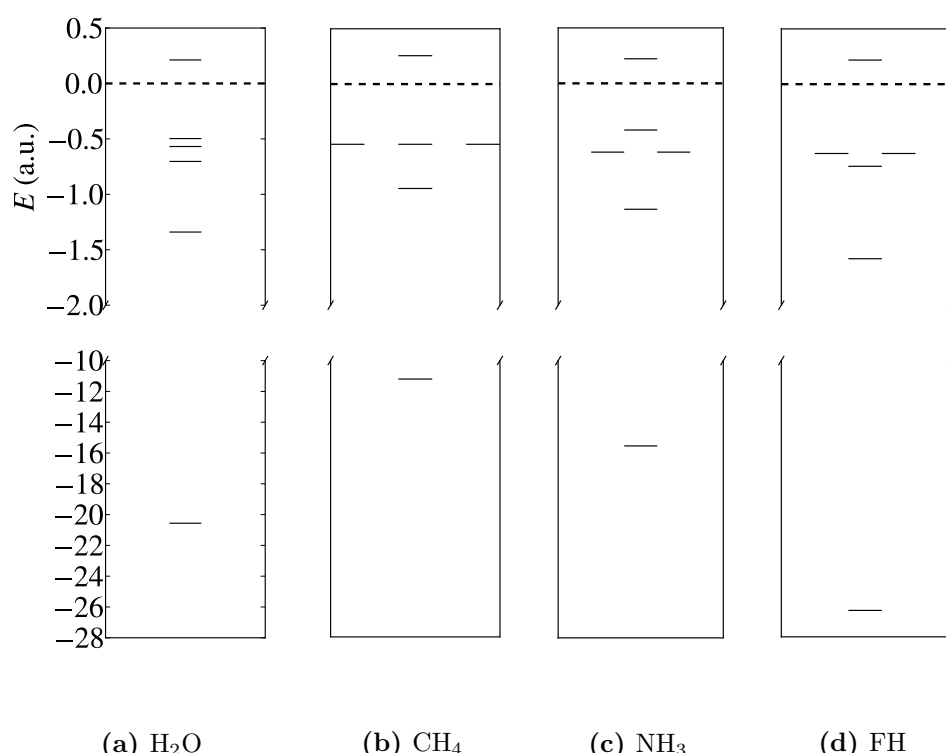
The orbital energies can be written as

$$
\begin{aligned}
\varepsilon_i &= \langle \psi_i | \mathcal{F} | \psi_i \rangle \\
&= \langle \psi_i | h | \psi_i \rangle + \sum_j \langle \psi_i \psi_j || \psi_i \psi_j \rangle.
\end{aligned}
\tag{11.5}
$$

From this we see that ε_i is equal to the energy of the electron in spin orbital ψ_i: It has a kinetic energy term, a Coloumb term due to the interaction with the nuclei, and a Coulomb term due to the interaction with all other electrons of the system. One can therefore think of $-\varepsilon_i$ as the energy needed to remove said electron from the molecule (ionisation potential), where the minus sign is placed in front because the energy must be negative in order to describe a bound state. Although this is not strictly correct, there is a theorem due to Koopmans [42] which says that $-\varepsilon_i$ can nevertheless be a good *approximation* for the ionisation potential.

Koopmans' theorem states: *Given an N-electron Hartree-Fock single determinant $|^N\Psi_0\rangle$ with occupied spin orbital energies ε_i, then the ionisation potential to produce an $(N-1)$-electron single determinant $|^{N-1}\Psi_i\rangle$ with identical spin orbitals, obtained by removing an electron from spin orbital ψ_i, is $-\varepsilon_i$.*

The orbital energies of the H$_2$O, CH$_4$, NH$_3$ and FH molecules are shown in figure 11.8. The dashed line in the diagrams marks the separation between the occupied and virtual states. According to Koopmans' theorem, the highest occupied molecular orbital (often abbreviated HOMO) is approximately equal to the ionisation potential.

(a) H_2O **(b)** CH_4 **(c)** NH_3 **(d)** FH

Figure 11.8: Orbital energies (a.u.) obtained from restricted Hartree-Fock calculations with the 6-31G** basis set.

11.2.4   Equilibrium geometries

One of the most useful applications of Hartree-Fock and Møller-Plesset perturbation theory is the calculation of equilibrium geometries of molecules. Results for the ten electron series are shown in tables 11.5 and 11.6. The initial geometries given to the Nelder-Mead minimiser as well as the resulting geometries are shown in figure 11.9. The inital geometry was set rather unrealistically to test the minimiser. It should be noted, however, that for larger molecules it is important to make an intelligent first guess. Otherwise, convergence can be very slow, or in the worst case, the nuclei can get stuck in the wrong configuration.

From table 11.5, we see that Hartree-Fock theory usually underestimates bond lengths. One might guess that increasing the size of the basis set would increase the bond length towards the correct value. Suprisingly, however, there is no such trend. The MP2 and MP3 results predict longer bond lengths in better agreement with the experimental values. In general, the use of MP3 with the basis set 6-31G** seems to give best results, deviating from the exact bond lengths by no more than 0.02 a.u. in the results presented here.

The calculated bond angles are shown in table 11.6. It is seen that the angles have a greater spread than the bond lengths. Some of the numbers stand out. First of all, we notice the poor performance of the STO-3G basis set. In the RHF calculations, it estimates a bond angle of 100.0° for H_2O, undershooting the exact value by 4.5°. Surprisingly, the RMP2 and RMP3 calculations actually worsen the results. However, as discussed in the previous subsection, it does not make much sense to use perturbation theory with a minimal basis set.

However, perhaps even more suprising is the fact that increasing the basis set to 4-31G worsens the RHF results, although this time in the opposite direction. For example, the RHF method overestimates the bond angle of the NH_3 molecule by as much as 9.1°. However, as soon as we use the 6-31G* basis sets, the angles are in quite good agreement with the experimental values. This could indicate that polarising functions (see subsection 4.1.3) play an important role when estimating bond angles.

The MP3 level of theory combined with the 6-31G* or 6-31G** basis sets gives the best estimates for the bond angles, resulting in a maximum error of 0.6° for the molecules considered.

11.2.5   Electron density

The solution of the Hartree-Fock equations gives direct access to the electron density
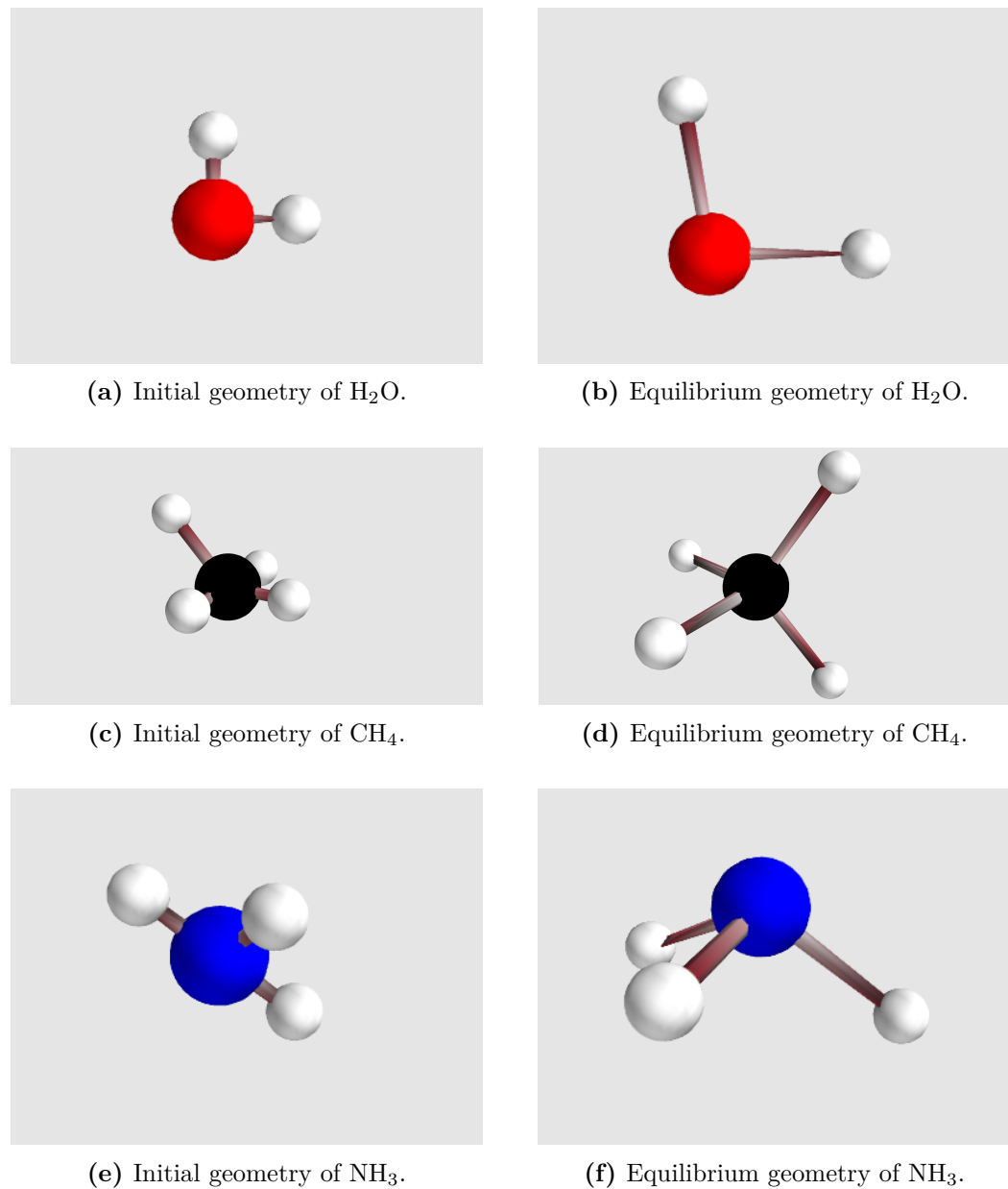
$$\tilde{\rho}(\mathbf{x}) = N \int d\mathbf{x}_2 \, d\mathbf{x}_3 \cdots d\mathbf{x}_N \, |\Psi_0(\mathbf{x}, \mathbf{x}_2, \mathbf{x}_3, \ldots, \mathbf{x}_N)|^2. \tag{11.6}$$

Note that $\tilde{\rho}(\mathbf{x})$ depends upon the spatial coordiantes $\mathbf{r}$ as well as spin s. It is common practice to integrate over the spin coordinate and define the electron density as

$$\rho(\mathbf{r}) = \sum_{s=\uparrow\downarrow} \tilde{\rho}(\mathbf{r}, s), \tag{11.7}$$

Table 11.5: Equilibrium bond lengths in a.u. of the ten electron series.
[a] Rosenberg *et al* [43]
[b] Meyer *et al* [44]
[c] Rauk *et al* [45]
[d] Cade *et al* [46]
[e] Szabo *et al* [3]

Mol.	Basis set	RHF	RMP2	RMP3
H_2O	STO-3G	1.870	1.915	1.932
	4-31G	1.796	1.842	1.838
	6-31G*	1.790	1.830	1.827
	6-31G**	1.782	1.816	1.810
	Near-HF-lim.[a]:	1.776		
	Experiment[e]:	1.809		
CH_4	STO-3G	2.047	2.077	2.086
	4-31G	2.043	2.066	2.069
	6-31G*	2.048	2.059	2.061
	6-31G**	2.048	2.049	2.049
	Near-HF-lim.[b]:	2.048		
	Experiment[e]:	2.050		
NH_3	STO-3G	1.951	1.998	2.012
	4-31G	1.873	1.907	1.908
	6-31G*	1.894	1.921	1.921
	6-31G**	1.891	1.912	1.910
	Near-HF-lim.[c]:	1.890		
	Experiment[e]:	1.912		
FH	STO-3G	1.806	1.843	1.863
	4-31G	1.743	1.791	1.786
	6-31G*	1.721	1.765	1.761
	6-31G**	1.702	1.740	1.735
	Near-HF-lim.[d]:	1.696		
	Experiment[e]:	1.733		

(a) Initial geometry of H_2O.

(b) Equilibrium geometry of H_2O.

(c) Initial geometry of CH_4.

(d) Equilibrium geometry of CH_4.

(e) Initial geometry of NH_3.

(f) Equilibrium geometry of NH_3.

Figure 11.9: Initial and equilibrium geometries obtained from calculations with the STO-3G basis set.

Table 11.6: Equilibrium bond angles in degrees of the ten electron series.
[a] Rosenberg et *et al* [43]
[b] Rauk *et al* [45]
[c] Szabo *et al* [3]

Mol.	Basis set	RHF	RMP2	RMP3
H_2O	STO-3G	100.0	97.3	96.8
	4-31G	111.2	108.9	109.2
	6-31G*	105.5	104.0	104.2
	6-31G**	106.0	103.9	104.3
	Near-HF-limit[a]	106.1		
	Experiment[c]:	104.5		
NH_3	STO-3G	104.2	100.9	100.4
	4-31G	115.8	113.9	113.5
	6-31G*	107.2	106.4	106.3
	6-31G**	107.6	106.1	106.1
	Near-HF-limit[b]	107.2		
	Experiment[c]:	106.7		

which is the definition we will use throughout this thesis. For a restricted determinant, equation (11.7) simplifies to

$$\rho(\mathbf{r}) = 2 \sum_{k=1}^{N/2} |\phi_k(\mathbf{r})|^2, \tag{11.8}$$

which, when inserting the solution obtained from the Hartree-Fock equations

$$\phi_k(\mathbf{r}) = \sum_{\mu=1}^{M} C_{\mu k}\chi_\mu(\mathbf{r}), \tag{11.9}$$

can be written as

$$\rho(\mathbf{r}) = \sum_{\mu,\nu=1}^{M} P_{\mu\nu}\chi_\mu(\mathbf{r})\chi_\nu^*(\mathbf{r}), \tag{11.10}$$
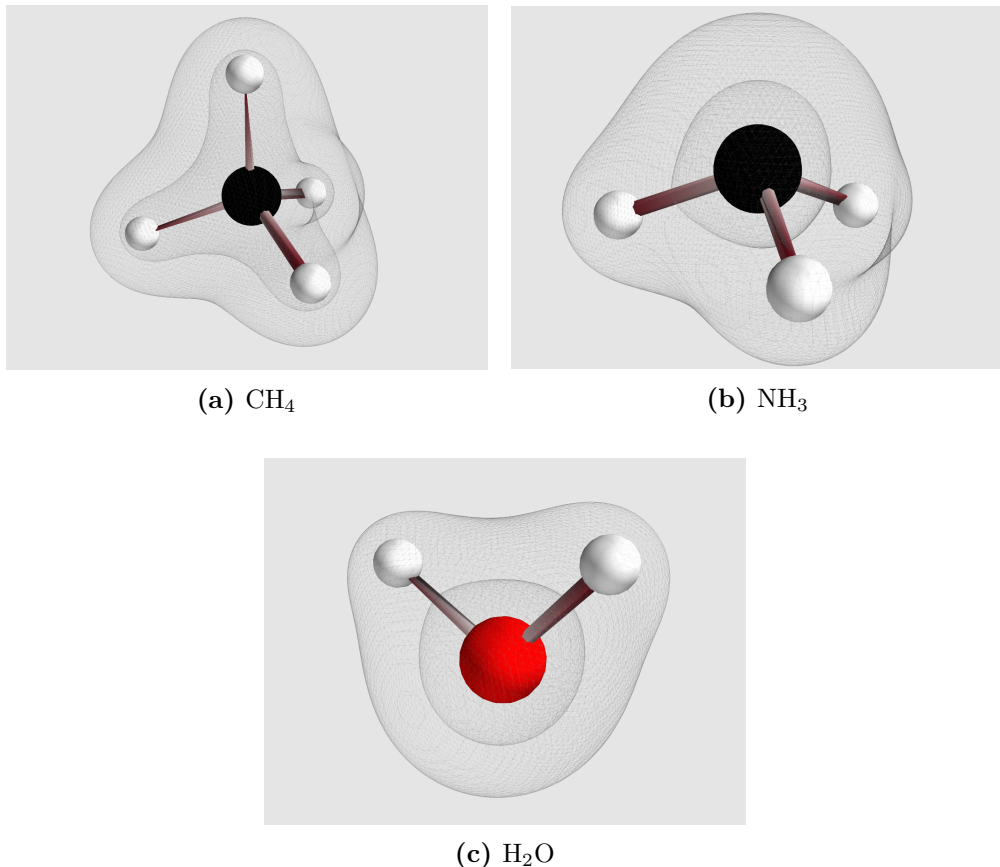
where $P_{\mu\nu}$ is the density matrix defined in equation (3.62). Similarly, the electron density for the unrestricted determinant reads

$$\rho(\mathbf{r}) = \rho^\alpha(\mathbf{r}) + \rho^\beta(\mathbf{r}), \tag{11.11}$$

where

$$\rho^\alpha(\mathbf{r}) = \sum_{\mu,\nu=1}^{M} P_{\mu\nu}^\alpha\chi_\mu(\mathbf{r})\chi_\nu^*(\mathbf{r}), \tag{11.12}$$

$$\rho^\beta(\mathbf{r}) = \sum_{\mu,\nu=1}^{M} P_{\mu\nu}^\beta\chi_\mu(\mathbf{r})\chi_\nu^*(\mathbf{r}), \tag{11.13}$$

(a) CH_4

(b) NH_3

(c) H_2O

Figure 11.10: Charge density calculated on the RHF level of theory using the 6-31G** basis set.

are the spin-up and spin-down densities, respectively, and $P_{\mu\nu}^\alpha$ and $P_{\mu\nu}^\beta$ are defined in equations (3.81) and (3.82). Plots of the electron densities for H_2O, CH_4 and NH_3 are shown in figure 11.10.

The quantity $\rho(\mathbf{r})d\mathbf{r}$ is the probability of finding an electron in the volume $d\mathbf{r}$ at $\mathbf{r}$. Molecules which do not bond will tend to have non-overlapping electron densities (due to the Pauli principle). Hence, the electron density tells us something about the size of a molecule. Furthermore, since covalent bonds between atoms are due to overlapping orbitals, the electron density gives information about how the atoms are bonded within a molecule.

11.3   Open shell molecules: CH_3 and O_2

In the previous section we studied mulecules which were all in a singlet spin state. This means that, when placed in or near their equilibrium configurations, they are well described by restricted closed shell determinants. In fact, we could equally well have analysed the molecules with unrestricted determinants, but these would then

automatically reduce to the corresponding restricted determinants.

However, molecules which are not singlets cannot be analysed by restricted closed shell determinants. We will study two such examples in this section.

11.3.1   The CH$_3$ radical

The CH$_3$ radical has 9 electrons, and the quantum number for the z-component of spin must therefore be nonzero. If we think in terms of molecular orbitals, we can picture placing the first electron in the lowest molecular orbital with spin up, then placing the second electron in the same orbital, but with spin down (due to the Pauli principle). The first orbital is then filled, and the third electron must be placed in the second orbital. Continuing like this, we end up with 5 spin-up electrons and 4 spin-down electrons, and thus $M_S = 1/2$. It is possible to have $M_S > 1/2$, but such states will be excited states. Since there is one unpaired spin-up electron, the quantum number related to the total spin is $S = 1/2$, and the system is a doublet.

The equilibrium geometry was first calculated using the the unrestricted Hartree-Fock method with the 6-31G** basis set. The molecule was found to be planar with the hydrogen atoms placed at the corners of an equilateral triangle and the carbon atom placed in the center of the triangle. The bond length between the carbon atom and each hydrogen atom was calculated to be $d = 2.027$. With this bond length, the energy and squared magnitude of the total spin was calculated with the 6311++G(3df,3pd) basis set. The parenthesis indicate that first row atoms are polarised with three d-functions and one f-function[1] and that the hydrogen atom is polarised with three p-functions and one d-function. This is a rather large basis set with a total of 102 basis functions for the CH$_3$ molecule. The results are listed in table 11.7.

The squared magnitude of the total spin was calculated to be $\langle \mathbf{S}^2 \rangle = 0.7620$, which is close to the exact value $S(S + 1) = 3/4$. Thus we can conclude that the spin contamination is relatively modest in this case.

The so-called spin density

$$\rho^S(\mathbf{r}) = \rho^\alpha(\mathbf{r}) - \rho^\beta(\mathbf{r}), \tag{11.14}$$
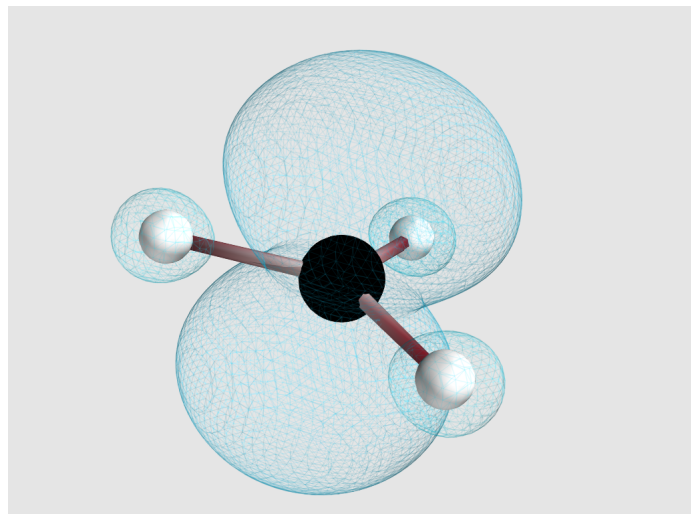
where $\rho^\alpha(\mathbf{r})$ and $\rho^\beta(\mathbf{r})$ are defined in equations (11.12) - (11.13), gives information about the location of the unpaired electrons of the system. Figure 11.11 shows a plot of the spin density for the CH$_3$ molecule calculated with the 6-31G** basis set. All isosurfaces have the same absolute value, the one centered on the carbon atom being positive, and the others being negative.

11.3.2   The O$_2$ molecule

In the previous subsection we made a short reasoning regarding the electrons and which molecular orbitals they occupy in the ground state of the CH$_3$ molecule. This led us to conclude that there should be 5 electrons with spin up and 4 with spin down. The same reasoning for the O$_2$ molecule might suggest that there should be 8 electrons with

---

[1]Note, however, that each d function has six components $d_{xy}, d_{yz}, d_{xz}, d_{xx}, d_{yy}$ and d_{zz}. Similarly, the f-function has 10 components.

Figure 11.11: Contour plot of the spin density of the CH$_3$ radical computed with the 6-31G**
basis set. All isosurfaces have the same absolute value, the one centered on the carbon atom
being positive, and the others being negative.

Table 11.7: Calculated energies (a.u.) and spin for the CH$_3$ radical. The bond length
$d = 2.027$ a.u. was calculated using the UHF-method with the 6-31G** basis set. The energies
were computed with this bond length and the larger 6311++G(3df,3pd) basis set (102 basis
functions).

	UHF	UMP2	UMP3
Energy	-39.577217	-39.766506	-39.785292
$\langle \mathbf{S}^2 \rangle$	0.7620	-	-

Table 11.8: Energies (a.u.) and spin for the O_2 molecule calculated with the
6-311++G(3df,3pd) basis set (90 basis functions). The bond length has been set equal to the
experimental value[a] 2.282 (a.u.)
[a] Filippa *et al* [47]

Determinant	M_s	$\langle \mathbf{S}^2 \rangle$ HF	Energy HF	MP2	MP3
Restricted	0	0	-149.588566	-150.142272	-150.130182
Unrestricted	0	1.0232	-149.648202	-150.152525	-150.152971
	1	2.0487	-149.674954	-150.189863	-150.184227

Experimental energy[a]: -150.3268

spin up as well as 8 electrons with spin down so that $M_S = 0$. However, calculations reveal that this is not the case. Table 11.8 shows the results from calculations performed with restricted as well as unrestricted determinants. The unrestricted calculations were carried out with two different spin configurations: $M_S = 0$ (8 spin-up and 8 spin-down electrons) and $M_S = 1$ (9 spin-up and 7 spin-down electrons). We make the following observations.
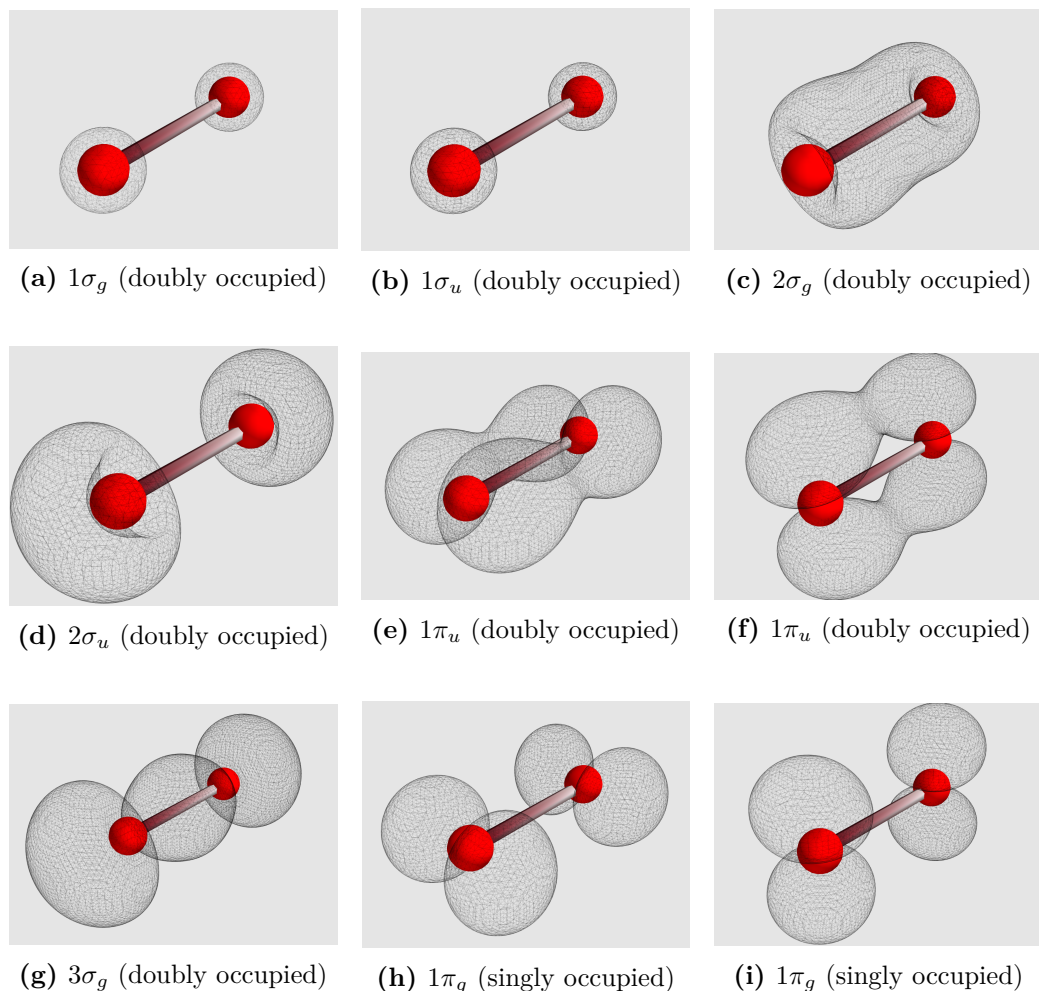
Firstly, we note that the lowest Hartree-Fock energy is obtained when $M_S = 1$. In this electron configuration, there are two unpaired spin-up particles, and the exact state is therefore an eigenstate of the total spin operator $\mathbf{S}^2$ with $S = 1$. Thus the results predict that the ground state of O_2 is a triplet. The calculated total spin is $\langle \mathbf{S}^2 \rangle = 2.0487$ which is not far from the exact value of 2. Hence, the determinant is only mildly contaminated with higher spin states.

Secondly, the unrestricted determinant with $M_S = 0$ yields a lower and therefore also more accurate Hartree-Fock energy than the restricted determinant. However, this determinant does a poor job in describing a singlet state due to severe spin contamination.
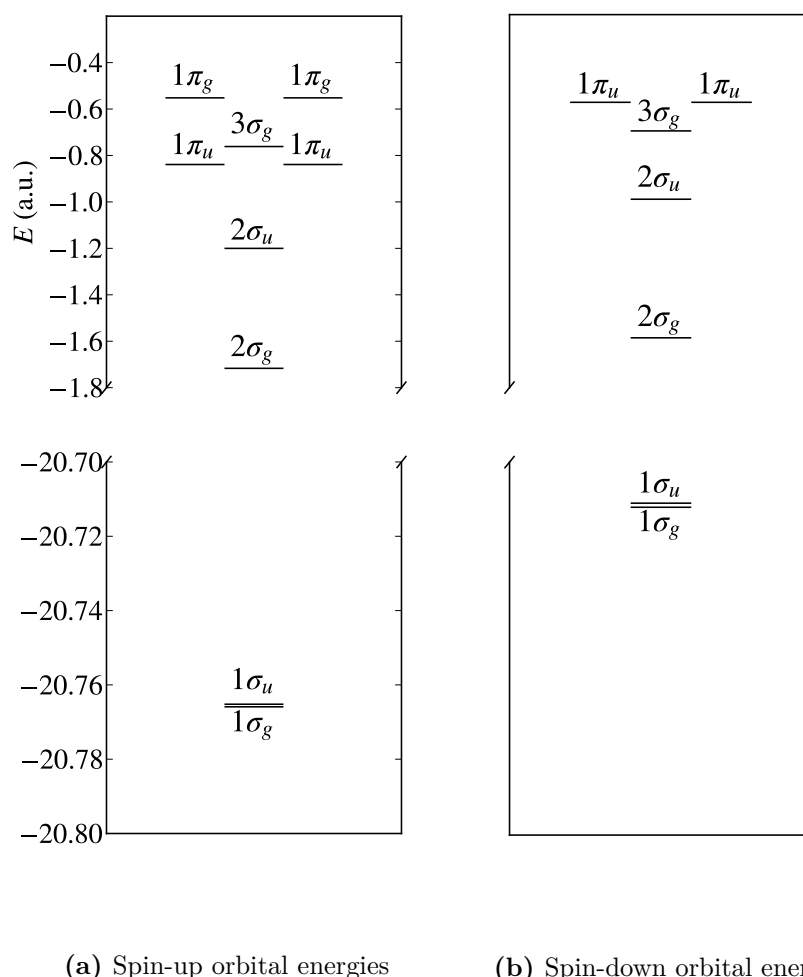
Thirdly, the third order Møller-Plesset corrections increase the energy for two of the determinants, which is somewhat unexpected. However, this type of oscillatory behaviour has also been observed by other authors, see for example Cremer and He [48].

The squared magnitude of the molecular orbitals occupied by the nine spin-up electrons in triplet O_2 are shown in figure 11.12. They are ordered by increasing energy. The spin-down orbitals are similar to the first seven spin-up orbitals.

According to Atkins [49], one can to a first approximation think of the MOs as being formed by AOs in a rather simple way. In this picture, the first MO is thought to be simply the sum of the atomic $1s$ orbitals. It is labeled $1\sigma_g$, where the subscript *g* stands for *gerade*, which is the german word for *even*. It indicates that the orbital is even under inversion of coordinates, $\mathbf{r} \rightarrow -\mathbf{r}$. The second MO is the difference between the the two $1s$ AOs and is therefore named $1\sigma_u$, where *u* stands for *ungerade*, meaning *odd*. Thus the $1\sigma_u$ MO is odd under the inversion of coordiantes. Since the two $1s$ AOs are core, they are considered to be unimportant when forming bonds with other atoms. The two first MOs of figure 11.12 support this; there is no overlap between the AOs which form them. The third and fourth MOs are named $2\sigma_g$ and $2\sigma_u$ and are

(a) $1\sigma_g$ (doubly occupied)   **(b)** $1\sigma_u$ (doubly occupied)   **(c)** $2\sigma_g$ (doubly occupied)

(d) $2\sigma_u$ (doubly occupied)   **(e)** $1\pi_u$ (doubly occupied)   **(f)** $1\pi_u$ (doubly occupied)

(g) $3\sigma_g$ (doubly occupied)   **(h)** $1\pi_g$ (singly occupied)   **(i)** $1\pi_g$ (singly occupied)

Figure 11.12: The molecular orbitals $|\phi_k^\alpha|^2$ occupied by the nine spin-up electrons in triplet O_2. The orbitals are ordered by increasing energy. The spin-down orbitals are similar to the first seven spin-up orbitals. The calculations were performed with the 6-31G* basis set. See the main text for an explaination of the names of the molecular orbitals.

(a) Spin-up orbital energies   (b) Spin-down orbital energies

Figure 11.13: Orbital energies (a.u.) of triplet O_2 obtained from unrestricted Hartree-Fock calculations with the 6-31G* basis set.

formed from the $2s$ AOs in the same way as the first two MOs were formed from the $1s$ AOs. Since the $2s$ orbitals are valence orbitals, they are important when creating bonds. This agrees with the figure; the AOs which form the third and fourth MOs are clearly overlapping, and they do indeed look like something we would get when adding and subtracting two atomic $2s$ orbitals. The remaining MOs are constructed from $2p$ AOs. In particular, the fifth MO is a sum of $2p_y$ AOs, where the x-axis is directed along the line passing through both nuclei. It is therefore named $1\pi_u$, and it is odd since each of the $2p_y$ AOs are odd. Similarly, the sixth MO is a sum of $2p_z$ AOs and is also named $1\pi_u$. Although different in appereence, the seventh MO is actually a sum of $2p_x$ AOs. Its different shape is due to the fact that the AOs from which it is formed meet "head on" in between the nuclei. Since it looks somewhat like an atomic s orbtitial, it has been given the name $3\sigma_g$. Finally, the last two MOs are the even versions of the two $1\pi_u$ MOs mentioned previously.

The orbital energies are shown in figure 11.13. Interestingly, although the seven lowest spin-up MOs are similar to the spin-down MOs, their energy levels are different. This is because the two extra spin-up electrons have an exchange interaction with the other spin-up electrons, but not with the spin-down electrons.

The degeneracy of the two highest spin-up MOs $(1\pi_g)$ gives a heuristic explaination for the fact that the ground state of O_2 is a triplet. The two electrons with highest energy can be placed in separate $1\pi_g$ orbitals and with parallell spins, which is energetically favourable compared to placing them in the same orbital and with opposite spins.

11.4   Dissociation energy of C_2H_6 to $2CH_3$

In this section we study the C-C bond dissociation energy of C_2H_6 (ethane). This is a rather interesting case since experimental values are available, that is, values actually obtained in the lab. In the previous sections, however, experimental values referred to the exact or the most accurate eigenvalues of the Hamiltonian (2.3) which the author could find in the literature.
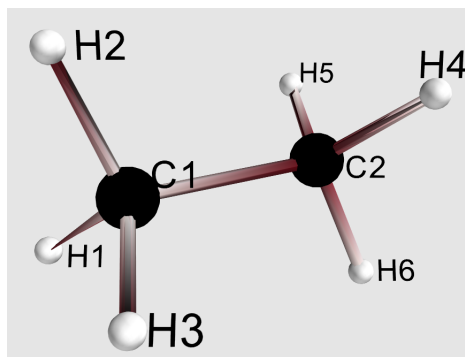
The C-C bond dissociation energy was calculated simply by subtracting the energy of one C_2H_6 molecule from the energy of two CH_3 molecules:

$$E_{\text{diss}} = 2E(\text{CH}_3) - E(\text{C}_2\text{H}_6). \tag{11.15}$$

The energies of the C_2H_6 and CH_3 molecules were calculated with the restricted and unrestricted methods, respectively, and with the 6-31++G** basis set. For the geometry of the CH_3 molecule, we used the bond length found in the previous section, that is $d = 2.027$ a.u. The geometry of C_2H_6 was found by minimising the energy with the STO-3G basis set. The result of the minimisation is summarised in table 11.9 and figure 11.14. As the numbers show, one of the carbon-hydrogen bonds is slightly longer than the others. Also, two of the angles are slightly larger. These variations give an indication of the precision of the minimisation algorithm on this particular molecule. The slight variation of values is due to the fact that the energy is rather insensitive to small perturbations of the geometry near equilibrium.

Table 11.9: Bond lengths (a.u.) and bond angles calculated for the C_2H_6 molecule using the STO-3G basis set. The positions of all atoms were varied freely during minimisation (no symmetries exploited). The atom numbering is defined in figure 11.14.

Bond length		Bond angle	
d(C1-C1)	2.906		
d(C1-H1)	2.502	θ(C2-C1-H1)	110.8°
d(C1-H2)	2.502	θ(C2-C1-H2)	110.5°
d(C1-H3)	2.502	θ(C2-C1-H3)	110.8°
d(C2-H4)	2.502	θ(C1-C2-H4)	110.8°
d(C2-H5)	2.502	θ(C1-C2-H5)	110.5°
d(C2-H5)	2.503	θ(C1-C2-H6)	110.8°

Figure 11.14: Equilibrium geometry of the C_2H_6 molecule calculated with the STO-3G basis set. Bond lengths and angles are listed in table 11.9.

Table 11.10: C-C bond dissociation energy for the C_2H_6 molecule calcultated with the 6-31++G** basis set. The energies of the C_2H_6 and CH_3 molecules were calculated with the restricted and unrestricted methods, respectively. The dissociation energy was calculated according to equation (11.15) without correcting for the motions of the nuclei (see main text). For the CH_3 molecule, the bond length was set equal to $d = 2.027$ a.u., as calculated in the previous section. The geometry of the C_2H_6 molecule is summarised in table 11.9 and figure 11.14. All values below are in a.u., except those in paranthesis, which are in kcal/mol. The experimental bond enthalpy is reported at 90.1 kcal/mol by Blanksby *et al* [50].

Method	Energy			
	C_2H_6	CH_3	$C_2H_6 \rightarrow 2CH_3$	
HF	-79.238754	-39.566788	0.105178	(66.0)
MP2	-79.556482	-39.701444	0.153594	(96.4)
MP3	-79.585725	-39.718857	0.148011	(92.9)

The results of the energy calculations are shown in table 11.10. Although the perturbative terms only give modest corrections to the energy of the molecules, they clearly have a profound impact on the energy *difference*. Furthermore, compared to the experimental bond enthalpy reported at 90.1 kcal/mol by Blanksby *et al* [50], the MP2- and MP3-energies come out quite good, overestimating by 7.0% ad 3.1 %, respectively. The Hartree-Fock energy, however, underestimates the experimental value by 26.7%. This indicates that the correlation energy plays an important role when calculating bond dissociation and reaction energies.

In situations where the correlation energy is the same before and after the reaction taking place, we would expect the Hartree-Fock approximation to yield reasonable results, because then the errors introduced by neglecting the correlation energy would cancel. On the other hand, whenever the correlation energy changes as a result of the reaction, there will be no such cancellation. Since the correlation energy is likely to be larger for the C_2H_6 molecule (greater number of interacting electrons), this can explain the poor performance of the Hartree-Fock method.

It should be noted, though, that the calculations above are not entirely realistic since they do not include the energy due to the vibrations of the nuclei. Such vibrations are present even at absolute zero temperature. This is perhaps most easily realised by considering the fact that, when in the equilibrium configuration, the nuclei are (approximately) trapped in a harmonic oscillator potential, and the lowest energy level of the harmonic oscillator is a positive quantity. The sum of the lowest energies associated with all the vibrational modes of a molecule is called the zero-point vibrational energy (ZPVE) [17]. To some extent, these energies can cancel when calculating dissociation/reaction energies. Nevertheless, they must be included when accurate results are desired.

11.5   Conclusions

In this chapter we have presented and discussed results obtained from calculations on various molecules. The results show that both the restricted and unrestricted methods produce reasonable energies for geometries close to equilibrium. Moreover, the unrestricted solution reduces to the restricted solution for closed shell molecules at equilibrium. However, during bond stretching, the two methods give diverging results; the unrestricted energies behave physically, but the restricted energies do not. Hence, unrestricted methods should be used when studying molecules far from equilibrium.

However, we have seen that also the unrestricted results are flawed; for intermediate bond lengths, the unrestricted Møller-Plesset perturbation theory converges very slowly, giving the potential energy curve a rather strange behaviour in this range. Other authors have attributed this to spin contamination of the unrestricted determinant [31, 38, 39], and our results support this.

Regarding the prediction of equilibrium geometries, the Møller-Plesset results generally bring us closest to the experimental values. However, the results are rather good already at the Hartree-Fock level.

We observed that the correlation energy plays a very important role when computing dissociation/reaction energies; although it gives relatively modest adjustments for

each individual molecule, it has a major impact when calculating energy *differences*.

Chapter 12

Conclusion and future prospects

12.1   Conclusion

The aim of this thesis was to write from scratch an *ab initio* program able to calculate the electronic structure and properties of molecules. To this end, I decided to implement the Hartree-Fock method, both the restricted and the unrestricted version. The main reason for this choice, was the fact that it has the ability to produce quite reasonable results for medium to large sized molecules with moderate computing effort. However, the method is by construction limited in accuracy; when the basis set approaches completeness, the Hartree-Fock energy is bound to overestimate the exact energy. To remedy this, I chose to implement the Møller-Plesset perturbation theory up to third order, based on the restricted as well as the unrestricted Hartree-Fock reference determinants.

The thesis consists of three parts. Part I first reviewed the basics of many-body quantum mechanics necessary for the development of the methods of choice. Therafter, the Hartree-Fock method was derived and discussed in detail. The restricted and unrestricted determinants were defined, and the self-consistent field equations which follow, the Roothan and Pople-Nesbet equations, respectively, were derived. Solving these equations necessitates the computation of the expectation value of the one- as well as two-particle parts of the Hamiltonian with respect to the chosen set of basis functions. For this purpose, the efficient integration scheme due to Boys and McMurchie and Davidson was reviewied. Thereafter, the Møller-Plesset perturbation theory was discussed.

Part II described how the methods of choice was implemented in the C++ programming language. The various classes and their relations were discussed, and some of the more intricate parts of the implementation was described in detail. Furthermore, the code was validated by demonstrating that it reproduces results published by other authors. The program is available in its entirety at https://github.com/henrikei/ HartreeFock.

Part III presented and discussed results produced by the program. The strengths as well as weaknesses of the methods were debated. The results show that both the restricted and unrestricted methods produce reasonable energies for geometries close to equilibrium. Moreover, the unrestricted solution reduces to the restricted solution

for closed shell molecules at equilibrium. However, during bond stretching, the two methods give diverging results; the unrestricted energies behave physically, but the restricted energies do not. Hence, unrestricted methods should be used when studying molecules far from equilibrium.

However, the results show that also the unrestricted results are flawed; for intermediate bond lengths, the unrestricted Møller-Plesset perturbation theory converges very slowly, giving the potential energy curve a rather strange behaviour in this range. Other authors have attributed this to spin contamination of the unrestricted determinant [31, 38, 39], and our results support this. Regarding the prediction of equilibrium geometries, the restricted Møller-Plesset methods yield the best results. However, the results are quite good already at the Hartree-Fock level.

We observed that the correlation energy plays a very important role when computing dissociation/reaction energies; although it gives relatively modest adjustments for each individual molecule, it has a major impact when calculating energy *differences*.

12.2   Future prospects

There are several possibilities for future work:

- Presently, the two-particle integrals used in the Hartree-Fock and Møller-Plesset calculations are stored in a four dimensional array (`field<mat>` in Armadillo). Although this makes the code run fast, it puts a limit on the number of basis functions due to high memory requirements. To be able to analyse large molecules, it is necesseray to calculate the two-particle integrals "on the fly".

- During bond breaking, the unrestricted Møller-Plesset calculations exhibit slow convergence due to spin contamination. To some extent, this can be fixed by implementing Møller-Plesset perturbation theory with spin annihilation [40, 41].

- It is of great interest to implement first and second derivatives of the energy. There are at least three reasons for this:

    1. The second derivatives can be used to calculate the vibrational modes and frequencies [51] needed in order to obtain the zero order vibrational energy (ZPVE), see section 11.4.

    2. The first and second order derivatives make it possible to implement more efficient minimisation algorithms such as for example the Newton-Raphson method.

    3. The first derivatives yield the forces acting on the nuclei, thereby making it possible to study quantum molecular dynamics.

- The code can be used as a first principle source for the parametrisation of molecular dynamics potentials.

Appendices

Appendix A

Spin contamination of the unrestricted determinant

In this appendix we continue the discussion of section 3.3 on how the operators $\mathbf{S}^2$ and S_z act on the restricted and unrestricted determinants. We first show that any Slater determinant is an eigenstate of S_z. Thereafter we show that the restricted closed shell determinant is an eigenstate of $\mathbf{S}^2$. Finally, we argue why the unrestricted determinant is generally not an eigenstate of $\mathbf{S}^2$.

Before continuing, we introduce the so-called raising and lowering operators. For single-particle states, they are defined by

$$
\begin{aligned}
s_+ &= s_x + is_y, \\
s_- &= s_x - is_y.
\end{aligned}
\tag{A.1}
$$

They have the effect of raising and lowering the spin-down and spin-up states

$$
s_+|\alpha\rangle = 0, \qquad s_+|\beta\rangle = |\alpha\rangle, \tag{A.2}
$$
$$
s_-|\alpha\rangle = |\beta\rangle, \qquad s_-|\beta\rangle = 0. \tag{A.3}
$$

Using the commutation relations of equation (3.28), one can show that

$$
\mathbf{s}^2 = s_\pm s_\mp \mp s_z + s_z^2. \tag{A.4}
$$

The many-particle raising and lowering operators are defined by

$$
S_+ = \sum_{i=1}^{N} s_+(i), \tag{A.5}
$$

$$
S_- = \sum_{i=1}^{N} s_-(i), \tag{A.6}
$$

and they satisfy the similar relation

$$
\mathbf{S}^2 = S_\pm S_\mp \mp S_z + S_z^2. \tag{A.7}
$$

We now show that any Slater determinant is an eigenstate of S_z. Explicitly

$$S_z|\psi_1\psi_2\ldots\psi_N\rangle = \frac{1}{2}(N_\alpha - N_\beta)|\psi_1\psi_2\ldots\psi_N\rangle \tag{A.8}$$

where N_α and N_β are the numbers of spin-up and spin-down electrons, respectively, and $N = N_\alpha + N_\beta$. This is easily demonstrated by writing the determinant in terms of the antisymmetrization operator $\mathcal{A}$ of equation (2.26) and using the fact that S_z and $\mathcal{A}$ commutes.

Next, we consider the action of $\mathbf{S}^2$ on the restricted and closed shell determinant

$$|\Psi^{\mathrm{RCS}}\rangle = |\phi_1\phi_2\ldots\phi_{N/2}\bar{\phi}_1\bar{\phi}_2\ldots\bar{\phi}_{N/2}\rangle \tag{A.9}$$

of N particles. Here, we have let the overbar and lack of overbar indicate that the spatial orbitals are accompanied by a $|\beta\rangle$ and $|\alpha\rangle$ spin state, respectively. The superscript RCS has been added to indicate that we are dealing with a restricted closed shell determinant. We want to show that the determinant is an eigenstate of $\mathbf{S}^2$ with eigenvalue 0. We evaluate the action of $\mathbf{S}^2$ on this determinant with the aid of equation (A.7). Note that from equation (A.8) it follows that we need only consider the term $S_- S_+$ since $N^\alpha = N^\beta$. Writing the Slater determinant in terms of the antisymmetrisation operator $\mathcal{A}$ and the Hartree product, and using the fact that $[S_+, \mathcal{A}] = 0$, we can let S_+ act directly on the Hartree product. The action of $s_+(i)$ on $\phi_i(\mathbf{r}_i)$ gives zero, and $s_+(i)\bar{\phi}_i(\mathbf{r}_i) = \phi_i(\mathbf{r}_i)$. However, the last action produces a Slater determinant with two equal columns and therefore also gives zero. We therefore conclude that the restricted closed shell determinant is a pure singlet state.

Finally, consider the unrestricted determinant

$$|\Psi^{\mathrm{UD}}\rangle = |\phi_1^\alpha\phi_2^\alpha\ldots\phi_{N^\alpha}^\alpha\bar{\phi}_1^\beta\bar{\phi}_2^\beta\ldots\bar{\phi}_{N^\beta}^\beta\rangle, \tag{A.10}$$

for a system with N^α particles with spin up and N^β particles with spin down. We now calculate the expectation value $\langle\mathbf{S}^2\rangle$ resulting from this determinant using equation (A.7)

$$\langle\mathbf{S}^2\rangle = \langle\Psi^{\mathrm{UD}}|(S_- S_+ + S_z + S_z^2)|\Psi^{\mathrm{UD}}\rangle \tag{A.11}$$

$$= \langle S_- S_+\rangle + \frac{N^\alpha - N^\beta}{2}\left(\frac{N^\alpha - N^\beta}{2} + 1\right). \tag{A.12}$$

Focusing now on the first term after the last equality sign

$$\langle S_- S_+\rangle = \langle\Psi^{\mathrm{UD}}|S_- S_+ \sqrt{N!}\,\mathcal{A}\,\phi_1^\alpha\phi_2^\alpha\ldots\phi_{N^\alpha}^\alpha\bar{\phi}_1^\beta\bar{\phi}_2^\beta\ldots\bar{\phi}_{N^\beta}^\beta \tag{A.13}$$

$$= \langle\Psi^{\mathrm{UD}}|\sqrt{N!}\,\mathcal{A}\,S_- S_+ \phi_1^\alpha\phi_2^\alpha\ldots\phi_{N^\alpha}^\alpha\bar{\phi}_1^\beta\bar{\phi}_2^\beta\ldots\bar{\phi}_{N^\beta}^\beta \tag{A.14}$$

$$= \langle\Psi^{\mathrm{UD}}|\sqrt{N!}\,\mathcal{A}\,S_- \phi_1^\alpha\phi_2^\alpha\ldots\phi_{N^\alpha}^\alpha\left(\phi_1^\beta\bar{\phi}_2^\beta\ldots\bar{\phi}_{N^\beta}^\beta\right. \tag{A.15}$$

$$\left.+\bar{\phi}_1^\beta\phi_2^\beta\ldots\bar{\phi}_{N^\beta}^\beta + \cdots + \bar{\phi}_1^\beta\bar{\phi}_2^\beta\ldots\phi_{N^\beta}^\beta\right) \tag{A.16}$$

$$= -\sum_{i=1}^{N^\alpha}\left[|\langle\phi_i^\alpha|\phi_1^\beta\rangle|^2 + \langle\phi_i^\alpha|\phi_2^\beta\rangle|^2 + \cdots + |\langle\phi_i^\alpha|\phi_{N^\beta}^\beta\rangle|^2\right] + N^\beta \tag{A.17}$$

$$= -\sum_{i=1}^{N^\alpha}\sum_{j=1}^{N^\beta}|\langle\phi_i^\alpha|\phi_j^\beta\rangle|^2 + N^\beta. \tag{A.18}$$

In equation (A.14) we have used the fact that S_+ and S_- commute with $\mathcal{A}$. Equations (A.15) - (A.16) result from the fact that $s_+(i)\phi_j^\alpha(\mathbf{r}_i) = 0$ and $s_+(i)\bar{\phi}_j^\beta(\mathbf{r}_i) = \phi_j^\beta(\mathbf{r}_i)$, and equation (A.17) is a result of the action of S_-. The final expression for the expectation value is

$$\langle \mathbf{S}^2 \rangle = \frac{N^\alpha - N^\beta}{2}\left(\frac{N^\alpha - N^\beta}{2} + 1\right) + N^\beta - \sum_{i=1}^{N^\alpha}\sum_{j=1}^{N^\beta}|\langle \phi_i^\alpha|\phi_j^\beta\rangle|^2. \tag{A.19}$$

Consider now the eigenvalues of $\mathbf{S}^2$. For a system of N^α spin-up particles and N^β spin-down particles, the exact state is an eigenstate of S_z and $\mathbf{S}^2$ with eigenvales $(N^\alpha - N^\beta)/2$ and $S(S + 1)$, respectively, where S can take the values [17]

$$S \in \left\{\frac{|n^\alpha - n^\beta|}{2}, \frac{|n^\alpha - n^\beta|}{2} + 1, \ldots, \frac{n^\alpha + n^\beta}{2}\right\}, \tag{A.20}$$

where n^α and n^β are the numbers of *unpaired* spin-up and spin-down electrons, respectively. Usually $S = (N^\alpha - N^\beta)/2$ [17]. In the following we assume for convenience that $N^\alpha \geq N^\beta$. We see from equation (A.19) that the correct expection value is obtained if the two last terms of the equation cancel. One way this can happen is if all the spin-down orbitals are paired with spin-up orbitals with identical spatial distributions, because in that case $\langle \phi_i^\alpha|\phi_j^\beta\rangle = \delta_{ij}$, and the sum is reduced to N^β. What we have described is a restricted determinant which is open shell if $N^\alpha \neq N^\beta$ and closed shell otherwise. Such determinants are eigenstates of $\mathbf{S}^2$.

However, often the two last terms do not cancel, and $\langle \mathbf{S}^2 \rangle$ is larger than the often desired value

$$\frac{N^\alpha - N^\beta}{2}\left(\frac{N^\alpha - N^\beta}{2} + 1\right), \tag{A.21}$$

and we say that the determinant is contaminated with higher spin.

Appendix B

Third order perturbation terms

We need to integrate out the spin of the equations in figure 6.2. The diagrams in the figure are often referred to as the particle ladder diagram, hole ladder diagram and loop diagram, respectively. Their contributions are

$$I_{\text{p-ladder}} = \sum_{ijabcd} \frac{\langle ij||ab\rangle\langle ab||cd\rangle\langle cd||ij\rangle}{8\varepsilon_{ij}^{ab}\varepsilon_{ij}^{cd}} \tag{B.1}$$

$$I_{\text{h-ladder}} = \sum_{ijklab} \frac{\langle ij||ab\rangle\langle ab||kl\rangle\langle kl||ij\rangle}{8\varepsilon_{ij}^{ab}\varepsilon_{kl}^{ab}} \tag{B.2}$$

$$I_{\text{loop}} = -\sum_{ijkabc} \frac{\langle ij||ab\rangle\langle kb||ic\rangle\langle ac||kj\rangle}{\varepsilon_{ij}^{ab}\varepsilon_{kj}^{ac}} \tag{B.3}$$

where

$$\varepsilon_{ij}^{ab} = \varepsilon_i + \varepsilon_j - \varepsilon_a - \varepsilon_b, \tag{B.4}$$

and the other denominators are defined similarly. In the following two sections we show how the spin is integrated out in the restricted and unrestricted case, respectively.

B.1 The restricted case (RHF)

B.1.1 Particle ladder diagram

We want to simplify the sum in equation (B.1). As for the second order case (MP2), we split each sum into two: one over spin-up orbitals and one over spin-down orbitals. For example, the sum over hole states is modified in the following way

$$\sum_{i=1}^{N} \psi_i = \sum_{i=1}^{N/2} \phi_i\alpha + \sum_{i=1}^{N/2} \phi_i\beta. \tag{B.5}$$

Doing this blindly will result in a total of $2^{12} = 4096$ sums. However, most of them will vanish since integrals over unequal spin functions are equal to zero. The list of spin combinations which contribute is shown in table B.1. Actually, only half the list is given; the other half is obtained by replacing α by β and vice versa. The contributions

Table B.1: Spin combinations which contribute in the sum (B.1) in the restricted case. The list does not include combinations that can be obtained by replacing α with β and vice versa; this is accounted for by a multiplicative factor of 2 in the sum.

Combination	i	j	a	b	c	d	mult. factor
1	α	α	α	α	α	α	2
2	α	β	α	β	α	β	2
3	α	β	α	β	β	α	2
4	α	β	β	α	α	β	2
5	α	β	β	α	β	α	2

from the two halves are identical, which means that we only need to calculate the first one and multiply by a factor of 2. Adding the five contributions listed, multiplying by 2, and integrating out the spin gives (in the same order as in the table)

$$
\begin{aligned}
I_{\text{p-ladder}} = \sum_{i,j=1}^{N/2} \sum_{\substack{a,b,c,d \\ =N/2+1}}^{M} \frac{1}{4\varepsilon_{ij}^{ab}\varepsilon_{ij}^{cd}} &\Big[\langle ij||ab\rangle\langle ab||cd\rangle\langle cd||ij\rangle \\
&+ \langle ij|g|ab\rangle\langle ab|g|cd\rangle\langle cd|g|ij\rangle + \langle ij|g|ab\rangle\langle ab|g|dc\rangle\langle cd|g|ji\rangle \\
&+ \langle ij|g|ba\rangle\langle ab|g|dc\rangle\langle cd|g|ij\rangle + \langle ij|g|ba\rangle\langle ab|g|cd\rangle\langle cd|g|ji\rangle \Big]
\end{aligned}
\tag{B.6}
$$

where, as before, N is the number of particles, M is the number of basis functions and the explicit summation indices indicate that we are summing over spatial orbitals ϕ instead of spin orbitals ψ. Multiplying out the antisymmetric integrals and collecting equal terms yields

$$
\begin{aligned}
I_{\text{p-ladder}} = \sum_{i,j=1}^{N/2} \sum_{\substack{a,b,c,d \\ =N/2+1}}^{M} \frac{1}{4\varepsilon_{ij}^{ab}\varepsilon_{ij}^{cd}} &\Big[2\langle ij|g|ab\rangle\langle ab|g|cd\rangle\langle cd|g|ij\rangle \\
&+ 2\langle ij|g|ab\rangle\langle ab|g|dc\rangle\langle cd|g|ji\rangle + 2\langle ij|g|ba\rangle\langle ab|g|dc\rangle\langle cd|g|ij\rangle \\
&+ 2\langle ij|g|ba\rangle\langle ab|g|cd\rangle\langle cd|g|ji\rangle - \langle ij|g|ba\rangle\langle ab|g|cd\rangle\langle cd|g|ij\rangle \\
&- \langle ij|g|ab\rangle\langle ab|g|dc\rangle\langle cd|g|ij\rangle - \langle ij|g|ab\rangle\langle ab|g|cd\rangle\langle cd|g|ji\rangle \\
&- \langle ij|g|ba\rangle\langle ab|g|dc\rangle\langle cd|g|ji\rangle \Big].
\end{aligned}
\tag{B.7}
$$

From the fact that the summation indices are dummy and that $\langle pq|g|rs\rangle = \langle qp|g|sr\rangle$, it follows that the first four terms are equal and that the last four terms are so as well. Thus the sum can be written as

$$
I_{\text{p-ladder}} = \sum_{i,j=1}^{N/2} \sum_{\substack{a,b,c,d \\ =N/2+1}}^{M} \frac{\langle ij|g|ab\rangle\langle ab|g|cd\rangle\big(2\langle cd|g|ij\rangle - \langle cd|g|ji\rangle\big)}{\varepsilon_{ij}^{ab}\varepsilon_{ij}^{cd}}.
\tag{B.8}
$$

Table B.2: Spin combinations which contribute in the sum (B.3) in the restricted case. The list does not include combinations that can be obtained by exchanging α with β and vice versa; this is accounted for by a multiplicative factor of 2 in the sum.

Combination	i	j	a	b	k	c	mult. factor
1	α	α	α	α	α	α	2
2	α	β	β	α	α	α	2
3	β	α	α	β	α	α	2
4	β	β	β	β	α	α	2
5	α	β	α	β	α	β	2

B.1.2   Hole ladder diagram

The procedure for integrating out the spin of $I_{\text{h-ladder}}$ mirrors that of $I_{\text{p-ladder}}$. The result is

$$I_{\text{h-ladder}} = \sum_{i,j,k,l=1}^{N/2} \sum_{\substack{a,b \\ =N/2+1}}^{M} \frac{\langle ij|g|ab\rangle\langle ab|g|kl\rangle\big(2\langle kl|g|ij\rangle - \langle kl|g|ji\rangle\big)}{\varepsilon_{ij}^{ab}\varepsilon_{kl}^{ab}}. \tag{B.9}$$

B.1.3   Loop diagram

The five possible combinations of spin functions, excluding the ones obtainable by replacing α with β and vice versa, are shown in table B.2. Adding the five contributions listed and integrating out spin gives (in the same order as in the table)

$$
\begin{aligned}
I_{\text{loop}} = -\,2 \sum_{i,j,k=1}^{N/2} \sum_{\substack{a,b,c \\ =N/2+1}}^{M} \frac{1}{\varepsilon_{ij}^{ab}\varepsilon_{kj}^{ac}} \Big[& \langle ij||ab\rangle\langle kb||ic\rangle\langle ac||kj\rangle + \langle ij|g|ba\rangle\langle kb||ic\rangle\langle ac|g|jk\rangle \\
+\, & \langle ij|g|ba\rangle\langle kb|g|ci\rangle\langle ac||kj\rangle + \langle ij||ab\rangle\langle kb|g|ci\rangle\langle ac|g|jk\rangle \\
+\, & \langle ij|g|ab\rangle\langle kb|g|ic\rangle\langle ac|g|kj\rangle \Big].
\end{aligned}
\tag{B.10}
$$

If we multiply out the antisymmetric integrals, this can be written as

$$
\begin{aligned}
I_{\text{loop}} = -\,2 \sum_{i,j,k=1}^{N/2} \sum_{\substack{a,b,c \\ =N/2+1}}^{M} \frac{1}{\varepsilon_{ij}^{ab}\varepsilon_{kj}^{ac}} \Big[& \langle ij|g|ab\rangle\langle kb|g|ic\rangle\Big(2\langle ac|g|kj\rangle - \langle ac|g|jk\rangle\Big) \\
+\, & \langle ij|g|ab\rangle\langle kb|g|ci\rangle\Big(2\langle ac|g|jk\rangle - \langle ac|g|kj\rangle\Big) \\
+\, & \langle ij|g|ba\rangle\langle kb|g|ic\rangle\Big(2\langle ac|g|jk\rangle - \langle ac|g|kj\rangle\Big) \\
+\, & \langle ij|g|ba\rangle\langle kb|g|ci\rangle\Big(2\langle ac|g|kj\rangle - 4\langle ac|g|jk\rangle\Big) \Big]
\end{aligned}
\tag{B.11}
$$

Table B.3: Spin combinations which contribute in the sum (B.1) in the unrestricted case. The list does not include combinations that can be obtained by permuting the indices $i \leftrightarrow j$, $a \leftrightarrow b$ and $c \leftrightarrow d$; this is accounted for by a multiplicative factor of 2 in the sum.

Combination	i	j	a	b	c	d	mult. factor
1	α	α	α	α	α	α	1
2	α	β	α	β	α	β	2
3	α	β	α	β	β	α	2
4	α	β	β	α	α	β	2
5	α	β	β	α	β	α	2
6	β	β	β	β	β	β	1

B.2   The unrestricted case

In the unrestricted case we must distinguish between sums over spin-up orbitals and sums over spin-down orbitals. This means that most of the simplifications which exploited the symmetry between spin-up and spin-down orbitals are no longer applicable, and the resulting expressions are quite a bit more involved.

B.2.1   Particle ladder diagram

We need to integrate out the spin of equation (B.1). The different spin combinations which must be considered are given in table B.3. As stated above, there is no longer a symmetry between the spin-up and spin-down orbitals, which means that they must be handled separately. However, the list of spin combinations is still reduced, but in this case due to the symmetry $\langle pq||rs \rangle = \langle qp||sr \rangle$. The list does therefore not include contributions which can be obtained by permuting the indices $i \leftrightarrow j$, $a \leftrightarrow b$ and $c \leftrightarrow d$. In the following we will use the notation

$$|\phi_i^\alpha\rangle = |i^\alpha\rangle \tag{B.12}$$

for brevity. Adding all contributions and collecting equal terms gives

$$
\begin{aligned}
I_{\text{p-ladder}} &= \sum_{i,j=1}^{N^\alpha} \sum_{\substack{a,b,c,d \\ =N^\alpha+1}}^{M} \frac{\langle i^\alpha j^\alpha||a^\alpha b^\alpha\rangle\langle a^\alpha b^\alpha||c^\alpha d^\alpha\rangle\langle c^\alpha d^\alpha||i^\alpha j^\alpha\rangle}{8(\varepsilon_i^\alpha + \varepsilon_j^\alpha - \varepsilon_a^\alpha - \varepsilon_b^\alpha)(\varepsilon_i^\alpha + \varepsilon_j^\alpha - \varepsilon_c^\alpha - \varepsilon_d^\alpha)} \\[2ex]
&+ \sum_{i,j=1}^{N^\beta} \sum_{\substack{a,b,c,d \\ =N^\beta+1}}^{M} \frac{\langle i^\beta j^\beta||a^\beta b^\beta\rangle\langle a^\beta b^\beta||c^\beta d^\beta\rangle\langle c^\beta d^\beta||i^\beta j^\beta\rangle}{8(\varepsilon_i^\beta + \varepsilon_j^\beta - \varepsilon_a^\beta - \varepsilon_b^\beta)(\varepsilon_i^\beta + \varepsilon_j^\beta - \varepsilon_c^\beta - \varepsilon_d^\beta)} \\[2ex]
&+ \sum_{i=1}^{N^\alpha} \sum_{j=1}^{N^\beta} \sum_{\substack{a,c \\ =1+N^\alpha}}^{M} \sum_{\substack{b,d \\ =1+N^\beta}}^{M} \frac{\langle i^\alpha j^\beta|g|a^\alpha b^\beta\rangle\langle a^\alpha b^\beta|g|c^\alpha d^\beta\rangle\langle c^\alpha d^\beta|g|i^\alpha j^\beta\rangle}{(\varepsilon_i^\alpha + \varepsilon_j^\beta - \varepsilon_a^\alpha - \varepsilon_b^\beta)(\varepsilon_i^\alpha + \varepsilon_j^\beta - \varepsilon_c^\alpha - \varepsilon_d^\beta)}.
\end{aligned}
\tag{B.13}
$$

Table B.4: Spin combinations which contribute in the sum (B.3) in the unrestricted case.

Combination	i	j	a	b	k	c	mult. factor
1	α	α	α	α	α	α	1
2	β	α	α	β	α	α	1
3	α	β	β	α	α	α	1
4	β	β	β	β	α	α	1
5	α	β	α	β	α	β	1
6	β	β	β	β	β	β	1
7	α	β	β	α	β	β	1
8	β	α	α	β	β	β	1
9	α	α	α	α	β	β	1
10	β	α	β	α	β	α	1

B.2.2   Hole ladder diagram

The contribution from the hole ladder diagram is derived in the same way as the contribution from the particle ladder diagram. The result is

$$
\begin{aligned}
I_{\text{p-ladder}} =& \sum_{i,j,k,l=1}^{N^\alpha} \sum_{\substack{a,b \\ =N^\alpha+1}}^{M} \frac{\langle i^\alpha j^\alpha || a^\alpha b^\alpha \rangle \langle a^\alpha b^\alpha || k^\alpha l^\alpha \rangle \langle k^\alpha l^\alpha || i^\alpha j^\alpha \rangle}{8(\varepsilon_i^\alpha + \varepsilon_j^\alpha - \varepsilon_a^\alpha - \varepsilon_b^\alpha)(\varepsilon_k^\alpha + \varepsilon_l^\alpha - \varepsilon_a^\alpha - \varepsilon_b^\alpha)} \\
&+ \sum_{i,j,k,l=1}^{N^\beta} \sum_{\substack{a,b \\ =N^\beta+1}}^{M} \frac{\langle i^\beta j^\beta || a^\beta b^\beta \rangle \langle a^\beta b^\beta || k^\beta l^\beta \rangle \langle k^\beta l^\beta || i^\beta j^\beta \rangle}{8(\varepsilon_i^\beta + \varepsilon_j^\beta - \varepsilon_a^\beta - \varepsilon_b^\beta)(\varepsilon_k^\beta + \varepsilon_l^\beta - \varepsilon_a^\beta - \varepsilon_n^\beta)} \\
&+ \sum_{i,k=1}^{N^\alpha} \sum_{j,l=1}^{N^\beta} \sum_{a=1+N^\alpha}^{M} \sum_{b=1+N^\beta}^{M} \frac{\langle i^\alpha j^\beta |g| a^\alpha b^\beta \rangle \langle a^\alpha b^\beta |g| k^\alpha l^\beta \rangle \langle k^\alpha l^\beta |g| i^\alpha j^\beta \rangle}{(\varepsilon_i^\alpha + \varepsilon_j^\beta - \varepsilon_a^\alpha - \varepsilon_b^\beta)(\varepsilon_k^\alpha + \varepsilon_l^\beta - \varepsilon_a^\alpha - \varepsilon_b^\beta)}.
\end{aligned}
\tag{B.14}
$$

B.2.3   Loop diagram

In this case there are a total of ten different spin combinations to consider (the symmtries from the ladder diagrams are no longer valid here), see table B.4. These result in a total of ten sums. Writing out the sums explicitly:

$$
\begin{aligned}
I_{\text{loop}} = {}&- \sum_{i,j,k=1}^{N^{\alpha}} \sum_{\substack{a,b,c \\ =N^{\alpha}+1}}^{M} \frac{\langle i^{\alpha}j^{\alpha}||a^{\alpha}b^{\alpha}\rangle\langle k^{\alpha}b^{\alpha}||i^{\alpha}c^{\alpha}\rangle\langle a^{\alpha}c^{\alpha}||k^{\alpha}j^{\alpha}\rangle}{(\varepsilon_i^{\alpha}+\varepsilon_j^{\alpha}-\varepsilon_a^{\alpha}-\varepsilon_b^{\alpha})(\varepsilon_k^{\alpha}+\varepsilon_j^{\alpha}-\varepsilon_a^{\alpha}-\varepsilon_c^{\alpha})} \\
&- \sum_{j,k=1}^{N^{\alpha}} \sum_{i=1}^{N^{\beta}} \sum_{\substack{a,c \\ =N^{\alpha}+1}}^{M} \sum_{b=N^{\beta}+1}^{M} \frac{\langle i^{\beta}j^{\alpha}|g|b^{\beta}a^{\alpha}\rangle\langle k^{\alpha}b^{\beta}|g|c^{\alpha}i^{\beta}\rangle\langle a^{\alpha}c^{\alpha}||k^{\alpha}j^{\alpha}\rangle}{(\varepsilon_i^{\beta}+\varepsilon_j^{\alpha}-\varepsilon_a^{\alpha}-\varepsilon_b^{\beta})(\varepsilon_k^{\alpha}+\varepsilon_j^{\alpha}-\varepsilon_a^{\alpha}-\varepsilon_c^{\alpha})} \\
&- \sum_{i,k=1}^{N^{\alpha}} \sum_{j=1}^{N^{\beta}} \sum_{\substack{b,c \\ =N^{\alpha}+1}}^{M} \sum_{a=N^{\beta}+1}^{M} \frac{\langle i^{\alpha}j^{\beta}|g|b^{\alpha}a^{\beta}\rangle\langle k^{\alpha}b^{\alpha}||i^{\alpha}c^{\alpha}\rangle\langle a^{\beta}c^{\alpha}|g|j^{\beta}k^{\alpha}\rangle}{(\varepsilon_i^{\alpha}+\varepsilon_j^{\beta}-\varepsilon_a^{\beta}-\varepsilon_b^{\alpha})(\varepsilon_k^{\alpha}+\varepsilon_j^{\beta}-\varepsilon_a^{\beta}-\varepsilon_c^{\alpha})} \\
&- \sum_{k=1}^{N^{\alpha}} \sum_{i,j=1}^{N^{\beta}} \sum_{c=N^{\alpha}+1}^{M} \sum_{\substack{a,b \\ =N^{\beta}+1}}^{M} \frac{\langle i^{\beta}j^{\beta}||a^{\beta}b^{\beta}\rangle\langle k^{\alpha}b^{\beta}|g|c^{\alpha}i^{\beta}\rangle\langle a^{\beta}c^{\alpha}|g|j^{\beta}k^{\alpha}\rangle}{(\varepsilon_i^{\beta}+\varepsilon_j^{\beta}-\varepsilon_a^{\beta}-\varepsilon_b^{\beta})(\varepsilon_k^{\alpha}+\varepsilon_j^{\beta}-\varepsilon_a^{\beta}-\varepsilon_c^{\alpha})} \\
&- \sum_{i,k=1}^{N^{\alpha}} \sum_{j=1}^{N^{\beta}} \sum_{a=N^{\alpha}+1}^{M} \sum_{\substack{b,c \\ =N^{\beta}+1}}^{M} \frac{\langle i^{\alpha}j^{\beta}|g|a^{\alpha}b^{\beta}\rangle\langle k^{\alpha}b^{\beta}|g|i^{\alpha}c^{\beta}\rangle\langle a^{\alpha}c^{\beta}|g|k^{\alpha}j^{\beta}\rangle}{(\varepsilon_i^{\alpha}+\varepsilon_j^{\beta}-\varepsilon_a^{\alpha}-\varepsilon_b^{\beta})(\varepsilon_k^{\alpha}+\varepsilon_j^{\beta}-\varepsilon_a^{\alpha}-\varepsilon_c^{\beta})} \\
&- \sum_{i,j,k=1}^{N^{\beta}} \sum_{\substack{a,b,c \\ =N^{\beta}+1}}^{M} \frac{\langle i^{\beta}j^{\beta}||a^{\beta}b^{\beta}\rangle\langle k^{\beta}b^{\beta}||i^{\beta}c^{\beta}\rangle\langle a^{\beta}c^{\beta}||k^{\beta}j^{\beta}\rangle}{(\varepsilon_i^{\beta}+\varepsilon_j^{\beta}-\varepsilon_a^{\beta}-\varepsilon_b^{\beta})(\varepsilon_k^{\beta}+\varepsilon_j^{\beta}-\varepsilon_a^{\beta}-\varepsilon_c^{\beta})} \\
&- \sum_{i=1}^{N^{\alpha}} \sum_{j,k=1}^{N^{\beta}} \sum_{b=N^{\alpha}+1}^{M} \sum_{\substack{a,c \\ =N^{\beta}+1}}^{M} \frac{\langle i^{\alpha}j^{\beta}|g|b^{\alpha}a^{\beta}\rangle\langle k^{\beta}b^{\alpha}|g|c^{\beta}i^{\alpha}\rangle\langle a^{\beta}c^{\beta}||k^{\beta}j^{\beta}\rangle}{(\varepsilon_i^{\alpha}+\varepsilon_j^{\beta}-\varepsilon_a^{\beta}-\varepsilon_b^{\alpha})(\varepsilon_k^{\beta}+\varepsilon_j^{\beta}-\varepsilon_a^{\beta}-\varepsilon_c^{\beta})} \\
&- \sum_{j=1}^{N^{\alpha}} \sum_{i,k=1}^{N^{\beta}} \sum_{a=N^{\alpha}+1}^{M} \sum_{\substack{b,c \\ =N^{\beta}+1}}^{M} \frac{\langle i^{\beta}j^{\alpha}|g|b^{\beta}a^{\alpha}\rangle\langle k^{\beta}b^{\beta}||i^{\beta}c^{\beta}\rangle\langle a^{\alpha}c^{\beta}|g|j^{\alpha}k^{\beta}\rangle}{(\varepsilon_i^{\beta}+\varepsilon_j^{\alpha}-\varepsilon_a^{\alpha}-\varepsilon_b^{\beta})(\varepsilon_k^{\beta}+\varepsilon_j^{\alpha}-\varepsilon_a^{\alpha}-\varepsilon_c^{\beta})} \\
&- \sum_{i,j=1}^{N^{\alpha}} \sum_{k=1}^{N^{\beta}} \sum_{\substack{a,b \\ =N^{\alpha}+1}}^{M} \sum_{c=N^{\beta}+1}^{M} \frac{\langle i^{\alpha}j^{\alpha}||a^{\alpha}b^{\alpha}\rangle\langle k^{\beta}b^{\alpha}|g|c^{\beta}i^{\alpha}\rangle\langle a^{\alpha}c^{\beta}|g|j^{\alpha}k^{\beta}\rangle}{(\varepsilon_i^{\alpha}+\varepsilon_j^{\alpha}-\varepsilon_a^{\alpha}-\varepsilon_b^{\alpha})(\varepsilon_k^{\beta}+\varepsilon_j^{\alpha}-\varepsilon_a^{\alpha}-\varepsilon_c^{\beta})} \\
&- \sum_{j=1}^{N^{\alpha}} \sum_{i,k=1}^{N^{\beta}} \sum_{\substack{b,c \\ =N^{\alpha}+1}}^{M} \sum_{a=N^{\beta}+1}^{M} \frac{\langle i^{\beta}j^{\alpha}|g|a^{\beta}b^{\alpha}\rangle\langle k^{\beta}b^{\alpha}|g|i^{\beta}c^{\alpha}\rangle\langle a^{\beta}c^{\alpha}|g|k^{\beta}j^{\alpha}\rangle}{(\varepsilon_i^{\beta}+\varepsilon_j^{\alpha}-\varepsilon_a^{\beta}-\varepsilon_b^{\alpha})(\varepsilon_k^{\beta}+\varepsilon_j^{\alpha}-\varepsilon_a^{\beta}-\varepsilon_c^{\alpha})}
\end{aligned}
$$

(B.15)

Bibliography

[1] Svenn-Arne Dragly. Bridging quantum mechanics and molecular dynamics with artificial neural networks. Master's thesis, University of Oslo, 2014.

[2] Milad H. Mobarhan. Ab initio molecular dynamics, a virtual laboratory. Master's thesis, University of Oslo, 2014.

[3] A. Szabo and N.S. Ostlund. *Modern Quantum Chemistry: Introduction to Advanced Electronic Structure Theory.* Dover Books on Chemistry Series. Dover Publications, 1996.

[4] E.K.U. Gross, E. Runge, and O. Heinonen. *Many-particle theory.* A. Hilger, 1991.

[5] I. Shavitt and R.J. Bartlett. *Many-Body Methods in Chemistry and Physics: MBPT and Coupled-Cluster Theory.* Cambridge Molecular Science. Cambridge University Press, 2009.

[6] M. Born and R. Oppenheimer. Zur Quantentheorie der Molekeln. *Ann. Phys.*, 389:457, 1927.

[7] W. Pauli. The connection between spin and statistics. *Phys. Rev.*, 58:716, 1940.

[8] G.C. Wick. The evaluation of the collision matrix. *Phys. Rev.*, 80:268, 1950.

[9] D. R. Hartree. The wave mechanics of an atom with a non-coulomb central field. part i. theory and methods. *Math. Proc. Camb. Phil. Soc.*, 24:89, 1928.

[10] V. Fock. Näherungsmetode zur lösung des quantenmechanischen mehrkörperproblems. *Z. Phys*, 61:126, 1930.

[11] J. Thijssen. *Computational Physics.* Cambridge University Press, 2007.

[12] M.L. Boas. *Mathematical Methods in the Physical Sciences.* Wiley, 2005.

[13] D.J. Griffiths. *Introduction to Quantum Mechanics.* Pearson Education, Limited, 2013.

[14] R. Shankar. *Principles of Quantum Mechanics.* Springer London, Limited, 2012.

[15] C. C. J. Roothaan. New developments in molecular orbital theory. *Rev. Mod. Phys.*, 23:69, 1951.

[16] J. A. Pople and R. K. Nesbet. Self-consistent orbitals for radicals. *J. Chem. Phys.*, 22:571, 1954.

[17] C.J. Cramer. *Essentials of Computational Chemistry: Theories and Models.* Wiley, 2002.

[18] W. J. Hehre, R. F. Stewart, and J. A. Pople. Self-consistent molecular-orbital methods. i. use of gaussian expansions of slater-type atomic orbitals. *J. Chem. Phys.*, 51:2657, 1969.

[19] T. Helgaker, P. Jørgensen, and J. Olsen. *Molecular electronic-structure theory.* Wiley, 2000.

[20] T. Živković and Z. B. Maksić. Explicit formulas for molecular integrals over hermite-gaussian functions. *J. Chem. Phys*, 49:3083, 1968.

[21] L. E. McMurchie and E. R. Davidson. One- and two-electron integrals over cartesian gaussian functions. *J. Comput. Phys.*, 26:218, 1978.

[22] David P. Tew, Wim Klopper, and Trygve Helgaker. Electron correlation: The many-body problem at the heart of chemistry. *J. Comput. Chem.*, 28:1307, 2007.

[23] Christoffer Hirth. Studies of quantum dots: Ab initio coupled-cluster analysis using opencl and gpu programming. Master's thesis, University of Oslo, 2012.

[24] Jørgen Høgberget. Quantum monte-carlo studies of generalized many-body systems. Master's thesis, University of Oslo, 2013.

[25] John Rayleigh. *The theory of sound.* Dover, New York, 1945.

[26] E. Schrödinger. Quantisierung als eigenwertproblem. *Ann. Phys.*, 385:437, 1926.

[27] C. Møller and M.S. Plesset. Note on an approximation treatment for many-electron systems. *Phys. Rev.*, 46:618, 1934.

[28] John A. Nelder and R. Mead. A simplex method for function minimization. *Comput. J.*, 7:308, 1965.

[29] Armadillo website. http://arma.sourceforge.net/.

[30] Basis set exchange: A community database for computational sciences. https://bse.pnl.gov/bse/portal.

[31] Peter M. W. Gill, John A. Pople, Leo Radom, and Ross H. Nobes. Why does unrestricted mo/ller–plesset perturbation theory converge so slowly for spin-contaminated wave functions? *J. Chem. Phys.*, 89:7307, 1988.

[32] Alexander I. Boldyrev and Jack Simons. Theoretical search for large rydberg molecules: Nh3ch3, nh2(ch3)2, nh(ch3)3, and n(ch3)4. *J. Chem. Phys.*, 97:6621, 1992.

[33] Nwchem website. http://www.nwchem-sw.org/index.php/Release62:MP2.

[34] J. M. Schulman and D. N. Kaufman. Application of many-body perturbation theory to the hydrogen molecule. *J. Chem. Phys.*, 53:477, 1970.

[35] J.W. Moskowitz and M. H. Kalos. A new look at correlations in atomic and molecular systems. i. application of fermion variational monte carlo method. *Int. J. Quant. Chem.*, XX:1107, 1981.

[36] P. C. Hariharan and J. A. Pople. The influence of polarization functions on molecular orbital hydrogenation energies. *Theoret. Chim. Acta*, 28:213, 1973.

[37] Antara Dutta and C. David Sherrill. Full configuration interaction potential energy curves for breaking bonds to hydrogen: An assessment of single-reference correlation methods. *J. Chem. Phys.*, 118:1610, 2003.

[38] R. J. Bartlett. Many-body perturbation theory and coupled cluster theory for electron correlation in molecules. *Ann. Rev. Phys. Chem.*, 32:359, 1981.

[39] Petr Čársky and Ivan Hubač. Restricted hartree-fock and unrestricted hartree-fock as reference states in many-body perturbation theory: a critical comparison of the two approaches. *Theoretica chimica acta*, 80:407, 1991.

[40] H. Bernhard Schlegel. Potential energy curves using unrestricted møller–plesset perturbation theory with spin annihilation. *J. Chem. Phys.*, 84:4530, 1986.

[41] Peter J. Knowles and Nicholas C. Handy. Projected unrestricted møller–plesset second-order energies. *J. Chem. Phys.*, 88:6991, 1988.

[42] T. Koopmans. Über die Zuordnung von Wellenfunktionen und Eigenwerten zu den Einzelnen Elektronen Eines Atoms. *Physica*, 1:104, 1934.

[43] B. J. Rosenberg, W. C. Ermler, and I. Shavitt. Ab initio scf and ci studies on the ground state of the water molecule. ii. potential energy and property surfaces. *J. Chem. Phys.*, 65:4072, 1976.

[44] W. Meyer. Pno–ci studies of electron correlation effects. i. configuration expansion by means of nonorthogonal orbitals, and application to the ground state and ionized states of methane. *J. Chem. Phys.*, 58:1017, 1973.

[45] A. Rauk, L. C. Allen, and E. Clementi. Electronic structure and inversion barrier of ammonia. *J. Chem. Phys.*, 52:4133, 1970.

[46] P. E. Cade and W. J. Huo. Electronic structure of diatomic molecules. vi.a. hartree—fock wavefunctions and energy quantities for the ground states of the first-row hydrides, ah. *J. Chem. Phys.*, 47:614, 1967.

[47] Claudia Filippi and C. J. Umrigar. Multiconfiguration wave functions for quantum monte carlo calculations of first-row diatomic molecules. *J. Chem. Phys.*, 105:213, 1996.

[48] Dieter Cremer and Zhi He. Sixth-order møller−plesset perturbation theoryon the convergence of the mpn series. *J. Phys. Chem.*, 100:6173, 1996.

[49] Peter W. Atkins and Ronald S. Friedman. *Molecular Quantum Mechanics.* Oxford University Press, 5 edition, 2010.

[50] Stephen J. Blanksby and G. Barney Ellison. Bond dissociation energies of organic molecules. *Acc. Chem. Res.*, 36:255, 2003.

[51] Errol G. Lewars. *Computational Chemistry: Introduction to the Theory and Applications of Molecular and Quantum Mechanics.* Springer, second edition, 2011.